

Effects of β -hydroxybutyrate in ischemic stroke

Dissertation

zur Erlangung des Doktorgrades

der Naturwissenschaften

Vorgelegt beim Fachbereich 14

Biochemie, Chemie und Pharmazie

der Johann Wolfgang Goethe-Universität

in Frankfurt am Main

Von

Alina Barbara Lehto

aus Fairfax County, VA (USA)

(D30)

Vom Fachbereich (14) Biochemie, Chemie und Pharmazie der
Johann Wolfgang Goethe-Universität als Dissertation angenommen.

Dekan: Prof. Dr. Clemens Glaubitz

Gutachter: Prof. Dr. Jochen Klein

Datum der Disputation: 21.10.2022



To Conny and Mike

Thank you for your unconditional love and support

Table of Contents

ZUSAMMENFASSUNG	1
1. INTRODUCTION	7
1.1 STROKE	7
1.1.1 HEMORRHAGIC STROKE	7
1.1.2 ISCHEMIC STROKE	7
1.1.3 RISK FACTORS.....	9
1.1.4 PATHOBIOLOGY FOLLOWING ISCHEMIC STROKE	9
1.1.5. MCAO MOUSE MODEL.....	14
1.2. ACUTE INTERVENTIONS AND NEUROPROTECTANTS	17
1.2.1 ACUTE INTERVENTIONS.....	17
1.2.2 NEUROPROTECTION AGENTS	17
1.2.3 NEUROPROTECTANTS AND RECANALIZATION.....	19
1.3. KETONE BODIES AND THE KETOGENIC DIET	20
1.3.1 KETONE BODIES	20
1.3.2 KETOGENIC DIET	21
1.3.3 KETOGENIC DIET IN ISCHEMIC AND TRAUMATIC BRAIN INJURY	22
1.3.4 POSSIBLE MECHANISMS OF ACTION.....	22
1.3 MITOCHONDRIA	25
1.3.1 STRUCTURE.....	25
1.3.2 MITOCHONDRIAL ENERGY METABOLISM	26
1.4. QUESTIONS OF THE THESIS	28
<u>2. MATERIALS AND METHODS</u>	<u>30</u>
2.1 LABORATORY ANIMALS	30
2.2 DIETS	30
2.3 MICRODIALYSIS	31
2.3.1 MATERIALS.....	31
2.3.2 MANUFACTURE OF MICRODIALYSIS PROBES.....	32
2.3.3 MANUFACTURE OF PERFUSION TUBES	34
2.3.4 SOLUTION FOR PERFUSION	34
2.3.5 IN VITRO-RECOVERY	34
2.3.6 FUNCTIONALITY CHECK	35
2.3.7 IMPLANTATION OF MICRODIALYSIS PROBES IN MICE	35
2.3.8 MICRODIALYSIS EXPERIMENT	36
2.4 TRANSIENT MIDDLE CEREBRAL ARTERY OCCLUSION (MCAO)	37
2.4.1 MATERIALS.....	38
2.4.2 MCAO SURGERY	38
2.4.3 SHAM SURGERY.....	39
2.4.4 POST-SURGICAL TREATMENT.....	39
2.5. TREATMENTS	40
2.5.1 TREATMENT WITH β -HYDROXYBUTYRATE	40
2.5.2 CONTROL GROUP.....	40
2.6 BEHAVIORAL STUDIES	40
2.6.1 CORNER TEST.....	41
2.6.2 ROTAROD.....	42
2.6.3 CHIMNEY TEST	43
2.7 MITOCHONDRIAL RESPIRATION	44
2.7.1 INSTRUMENTS AND MATERIALS	44

2.7.2 BASICS	45
2.7.3 PREPARATION	49
2.7.4 EXPERIMENTAL PROCEDURE	52
2.8 DETERMINATION OF CITRATE SYNTHASE ACTIVITY	54
2.8.1 INSTRUMENTS AND MATERIALS	54
2.8.2 PRINCIPLE.....	56
2.8.3 EXPERIMENTAL PROCEDURE.....	57
2.9 PHOTOMETRICAL ANALYSIS OF METABOLIC INTERMEDIATES.....	58
2.9.1 INSTRUMENTS AND MATERIALS	58
2.9.2 PRINCIPLE.....	58
2.10 TTC STAINING.....	61
2.10.1 INSTRUMENTS AND MATERIALS	61
2.10.2 PRINCIPLE.....	62
2.10.3 EXPERIMENTAL PROCEDURE.....	62
3. STATISTICAL ANALYSIS	63

4. RESULTS..... 64

4.1 MICRODIALYSIS	64
4.1.1 IN VITRO-RECOVERY	64
4.1.2 CHANGE OF METABOLITE CONCENTRATIONS AFTER ADMINISTRATION OF 30 MG/KG β -HYDROXYBUTYRATE.....	64
4.2. <i>IN VITRO</i> STIMULATION OF MITOCHONDRIAL RESPIRATION WITH β-HYDROXYBUTYRATE	66
4.3 REPRODUCIBILITY OF TRANSIENT MIDDLE CEREBRAL ARTERY OCCLUSION	68
4.4 RESPIRATION 60 MINUTES AFTER REPERFUSION.....	69
4.4.1 MITOCHONDRIAL ACTIVITY	69
4.5 RESPIRATION 24 HOURS AFTER REPERFUSION	74
4.5.1 MITOCHONDRIAL ACTIVITY	74
4.5.2 PLASMA METABOLITES.....	77
4.5.3 BEHAVIORAL TESTS.....	79
4.5.4 TTC STAININGS	81
4.6. RESPIRATION 72 HOURS AFTER REPERFUSION	81
4.6.1 WEIGHT LOSS.....	81
4.6.2 MITOCHONDRIAL RESPIRATION	82
4.6.3 PLASMA METABOLITES.....	85
4.6.4 BEHAVIORAL TESTS.....	87
4.6.5 TTC STAINING	89
4.7. RESPIRATION 7 DAYS AFTER REPERFUSION	90
4.7.1 WEIGHT DEVELOPMENT	90
4.7.2 MITOCHONDRIAL RESPIRATION	91
4.7.3 PLASMA METABOLITES.....	93
4.7.4 BEHAVIORAL TESTS.....	94

5. DISCUSSION

5.1 DISCUSSION OF METHODS	96
5.1.1 MICRODIALYSIS	96
5.1.2 INTRALUMINAL SUTURE MIDDLE CEREBRAL ARTERY OCCLUSION (MCAO) MODEL	98

5.1.3 OTHER MCAO MODELS.....	100
5.1.4 MEASUREMENT OF MITOCHONDRIAL RESPIRATION WITH THE OROBOROS OXYGRAPH.....	102
5.1.5 MEASUREMENT OF MITOCHONDRIAL RESPIRATION IN REGARD TO HYPOXIA	103
5.1.6 NEUROLOGICAL OUTCOME	104
5.2. DISCUSSION OF RESULTS	105
5.2.1 WEIGHT DEVELOPMENT	105
5.2.2 IN VITRO STIMULATION OF MITOCHONDRIA WITH VARIOUS COMPOUNDS	105
5.2.3 CITRATE SYNTHASE NORMALIZATION	106
5.2.4 MITOCHONDRIAL RESPIRATION: EARLY EVENTS	106
5.2.5 MITOCHONDRIAL RESPIRATION: LATER EVENTS	108
5.2.6 METABOLITES	109
5.2.7 BEHAVIORAL TESTS.....	110
<u>6. CONCLUSION.....</u>	<u>111</u>
<u>LIST OF REFERENCES.....</u>	<u>113</u>
<u>PUBLICATIONS.....</u>	<u>132</u>

List of Abbreviations

ACC	Arteria carotis communis
ACE	Arteria carotis externa
Acetyl-CoA	Acetyl coenzyme A
Ach	Acetylcholine
ACI	Arteria carotis interna
aCSF	Artificial cerebrospinal fluid
<i>ad libitum</i>	Free access to food and water
Ama	Antimycin A
AMPA	α -amino-3-hydroxy-5-methyl-4-isoxazolepropionic acid
AP	Anterior/Posterior
ApoB	Apolipoprotein B
ATP	Adenosine triphosphate
BHB	β -hydroxybutyrate
CD-1	Mouse strain
CoQ	Coenzyme Q
CS	Citrate synthase
Cyt C	Cytochrome C
DALY	Disability adjusted life years
DTNB	5,5'-dithiobis-(2-nitrobenzoic acid) (Ellman's reagent)
DV	Dorsoventral
ETS	Electron transfer system
FADH ₂	Flavine adenine dinucleotide
GABA	γ -aminobutyric acid
GC-MS	Gas chromatography-mass spectrometry
GOD	Glucose oxidase
HDL	High density lipoprotein
Hg	[mm] of mercury
i.p.	intraperitoneal
i.v.	intravenous
L	Lateral
LDH	Lactate dehydrogenase
LDL	Low density lipoprotein
LH	Left hemisphere
LI	Laterality index
LOD	Lactate oxidase
MCA	Middle cerebral artery
MCAO	Middle cerebral artery occlusion
MCT	Monocarboxylate transporter
MD	Microdialysis
MIR0	Mitochondrial respiratory medium
NF- κ B	Nuclear factor- κ B
NMDA	N-methyl-d-aspartic acid
NO	Nitric oxide
NOS	Nitric oxide synthase
OGD	Oxygen glucose deprivation
Omy	Oligomycin
OXPPOS	Oxidative phosphorylation
PBS	Phosphate buffered saline
POD	Peroxidase

PPAR- α	Peroxisome proliferator-activator receptor α
PTFE	Polytetrafluoroethylene (Teflon)
PyrOD	Pyruvate oxidase
RH	Right hemisphere
ROS	Reactive oxygen species
ROX	Residual oxygen consumption
rpm	Rotations per minute
rt-PA	recombinant tissue plasminogen activator
S.E.M.	Standard error of the mean
SDH	Succinate dehydrogenase
SUIT	Substrate-uncoupler-inhibitor titration
TCA	Tricarboxylic acid [cycle]
TMPD	N,N,N',N'-tetramethyl-p-phenylenediamine
TNF- α	Tumor necrosis factor α
TTC	Triphenyl tetrazolium chloride
UCP	Uncoupling protein

Zusammenfassung

Der Schlaganfall ist eine der weltweit häufigsten Todesursachen – aufgrund des steigenden Alters der Weltbevölkerung, stieg die Inzidenz in den letzten Jahrzehnten. Ein Schlaganfall kann hämorrhagischer oder ischämischer Natur sein. Der hämorrhagische Schlaganfall tritt seltener auf, führt allerdings in bis zu 80% der Fälle zum Tod des Patienten. Der ischämische Schlaganfall hingegen tritt seltener auf, betrifft häufig ältere Menschen und ist eine häufige Ursache für Behinderung und eingeschränkte Lebensqualität. Behinderungen als Folge eines Schlaganfalls schließen unter anderem kognitive und motorische Einschränkungen, Blaseninkontinenz und Depressionen ein. Trotz intensiver Forschung in den vergangenen Jahrzehnten gibt es bis heute neben der endovaskulären Thrombektomie, einem mechanischen Verfahren zur Entfernung des Thrombus, nur eine zugelassene pharmakologische Intervention zur Behandlung des ischämischen Schlaganfalls, nämlich den rekombinanten gewebspezifischen Plasminogenaktivator (rt-PA). Beide Therapieoptionen verfügen über ein geringes Zeitfenster von unter 4,5 Stunden und bedürfen einer strengen Indikationsstellung, da bei fälschlicher Anwendung Komplikationen, beispielsweise Gefäßrupturen, systemische oder subarachnoidale Blutungen drohen. Weitere Interventionsmöglichkeiten, die in der Vergangenheit erforscht wurden, wiesen die Problematik auf, dass sie in Tiermodellen funktionierten, aber im Menschen nicht die gewünschten Effekte zeigten. Dies kann zum einen daran liegen, dass sich Tiermodelle nicht 1:1 auf den Menschen übertragen lassen. Zum anderen kann es daran liegen, dass viele der erforschten Substanzen als Neuroprotektiva in einem kleinstmöglichen Zeitfenster gegeben werden müssen; im Experiment werden sie oft vor der Auslösung des Schlaganfalls verabreicht. Das ist in der klinischen Situation aufgrund der strengen Indikationsstellung des Schlaganfalls häufig nicht möglich. Es bedarf also dringend einer untoxischen pharmakologischen Intervention, die unabhängig von der Art des Schlaganfalls, beispielsweise bereits im Krankenwagen auf dem Weg ins Krankenhaus verabreicht werden kann. Ein Ansatz, der bereits von diesem Arbeitskreis verfolgt wurde und in Mäusen vielversprechende Ergebnisse gezeigt hat, ist die ketogene Diät. Ketonkörper stellen im z.B. Fastenzustand, bei kohlenhydratarmer Diät, oder bei langer und intensiver körperlicher Betätigung eine Quelle für Acetyl-CoA dar. Sie dienen als alternative Energiequelle für das Gehirn. Die drei Ketonkörper, die endogen von der Leber gebildet werden, sind Acetoacetat, Aceton und β -Hydroxybutyrat (BHB). In vorangegangenen Experimenten dieses Arbeitskreises wurden Mäuse fettreich und kohlenhydratarm ernährt, sodass sie eine Ketose entwickelten. Im Vergleich zu normal ernährten Tieren schnitten ketogen ernährte Mäuse nach 90-minütiger transientscher Ischämie in Verhaltensversuchen, die 24 Stunden nach Reperfusion durchgeführt wurden, besser ab als die normal ernährten Tiere. Da eine durch ketogene Diät hervorgerufene Ketose ebenfalls keiner klinischen Situation entspricht, die kurzfristig herbeigeführt werden kann, ist ein praktikablerer Ansatz

die Verabreichung des Ketonkörpers BHB unmittelbar nach Reperfusion nach 90-minütiger transientscher Ischämie. Obwohl BHB bereits im Schlaganfall und anderen neurodegenerativen Erkrankungen untersucht wurde, ist sein Wirkmechanismus bis heute weitgehend unbekannt. Es gibt Hinweise darauf, dass BHB einen positiven Einfluss auf die mitochondriale Atmung hat. Außerdem gilt es als nachgewiesen, dass BHB die Blut-Hirn-Schranke mittels Monocarboxylat-Transporter überwindet.

In der vorliegenden Arbeit wurde zunächst untersucht, ob BHB als einmalige Dosis von 30 mg/kg Körpergewicht die Blut-Hirn-Schranke überwindet, wie lange es im Extrazellularraum nachweisbar ist, und ob die Verabreichung einer einmaligen Dosis metabolische Veränderungen im Striatum zur Folge hat. Die BHB Konzentrationen im Striatum stiegen nach intraperitonealer Injektion innerhalb der ersten 30 Minuten etwa auf den doppelten Wert (von 2 auf 4 μM). Die Stoffwechselmetabolite Glukose, Laktat und Pyruvat waren nach BHB-Gabe unbeeinflusst.

Im Anschluss wurde der Einfluss von BHB auf isolierte Hirnmitochondrien untersucht. Zunächst wurde gemessen, ob BHB die Respiration in isolierten Hirnmitochondrien aus nichtischämischen Gehirnen *in vitro* stimuliert. BHB war in der Lage, die mitochondriale Atmung zu stimulieren. Als Vergleichssubstanzen wurden Pyruvat und Succinat gewählt. Succinat ist das Komplex II Substrat und zeigte als Einzelgabe die stärkste Stimulation der mitochondrialen Atmung. Pyruvat, welches eine ADP-unabhängige Atmung („*leak respiration*“) stimuliert, zeigte die schwächste Wirkung, wirkte aber sehr viel stärker, wenn gleichzeitig Malat zugestzt wurde.

In der zentralen Versuchsreihe der vorliegenden Arbeit wurde bei Mäusen mittels Fadenmodell ein ischämischer Schlaganfall ausgelöst, der 90 Minuten beibehalten wurde.

Hierzu erhalten die Tiere eine Injektion mit Buprenorphin, bevor sie 15 Minuten später mittels Isofluran narkotisiert werden. Anschließend werden die Mäuse auf dem Rücken fixiert und am Halsbereich wird ein ca. 1 cm langer Schnitt vorgenommen. Die *Arteria carotis communis* (ACC) wird freigelegt, und die Äste der darüber abzweigenden *Arteria carotis externa* (ACE) und *Arteria carotis interna* (ACI) werden abgebunden. Mit einer Mikroschere wird ein Schnitt an der ACE vorgenommen und ein steriler silikonbeschichteter Faden wird eingeführt. Danach wird die ACE vollständig abgetrennt, die Ligation der ACI wird gelöst und der Faden wird in die ACI umgeleitet, die zur mittleren Zerebralarterie führt. Der silikonbeschichtete Faden wird nun vorsichtig nach oben geschoben, bis ca. 1 cm des Fadens aus der abgeschnittenen Arterie herausstehen. Anschließend wird der Faden fixiert, das Tier wird zugenäht und aufwachen gelassen.

Nach 90 Minuten wird das Tier erneut narkotisiert, der Faden wird entfernt und somit eine Reperfusion der verschlossenen mittleren Zerebralarterie herbeigeführt. Unmittelbar nach Reperfusion wurde einer Gruppe BHB in einer Dosis von 30 mg/kg verabreicht, eine Vergleichsgruppe erhielt 0,9% Kochsalzlösung. Anschließend wurden die Hirnmitochondrien der ischämischen rechten

Hemisphäre mit denen der nicht-ischämischen linken Hemisphäre mittels respirometrischer Messung im Oxygraphen vermessen. Bei der respirometrischen Messung von Mitochondrien kann durch Zugabe komplexspezifischer Substrate, Entkoppler und Inhibitoren („SUIT-Protokoll“) die isolierte Atmung der einzelnen mitochondrialen Komplexe gemessen werden. Die Experimente wurden entweder 60 Minuten, 24 Stunden, 72 Stunden oder 7 Tage nach Reperfusion durchgeführt. Die Ergebnisse der respirometrischen Messungen wurden auf Citratsynthase und Proteingehalt normiert. Die Citratsynthase erfüllt den ersten und geschwindigkeitsbestimmenden Schritt im Citratzyklus und wird als Normierung für intakte Mitochondrien genutzt. Zusätzlich wurde die Auswirkung der Verabreichung von BHB auf die motorischen Fähigkeiten der Tiere nach 24 Stunden, 72 Stunden und 7 Tagen nach Reperfusion untersucht. Hierfür wurde eine Reihe von Verhaltensversuchen durchgeführt.

Die Verhaltensversuche beinhalteten den Corner-Test, den Chimney Test und den Rotarod Test.

Der Corner-Test wird durchgeführt, um unilaterale Bewegungsmuster der Tiere zu untersuchen. Eine Maus, die aufgrund einer gelähmten Körperhälfte in ihrer Bewegung einseitig eingeschränkt ist und in eine Ecke mit einem steilen Winkel von 30° gesetzt wird, bewegt sich höchstwahrscheinlich in nur eine Richtung. Dahingegen fallen die Bewegungen einer körperlich nicht eingeschränkten Maus in beide Richtungen zufällig aus. Nach einer Gesamtzahl von 10 Drehungen wurde die Anzahl der Rechtsdrehungen von Linksdrehungen subtrahiert und so ein präferierte Richtung festgestellt. Ein Wert von -10 bedeutet, dass die Maus sich ausschließlich rechts gedreht hat – ein Wert von +10 bedeutet, dass das Tier sich ausschließlich links gedreht hat.

Mittels Chimney-Tests wird die motorische Koordination der Tiere untersucht. Hierzu wird eine 20 cm lange Röhre mit 4 cm Innendurchmesser zunächst waagrecht gehalten, damit die Maus hineinlaufen kann. Im Anschluss wird die Röhre senkrecht aufgestellt, so dass das Tier rückwärts hinausklettern muss und die dafür benötigte Zeit wird notiert. Ein uneingeschränktes Tier benötigt in der Regel um die 2 Sekunden.

Der Rotarod-Test ist ebenfalls dazu vorgesehen, die motorische Koordination der Tiere zu überprüfen. Die Tiere werden auf eine rotierende Walze gesetzt, die innerhalb von 60 Sekunden von 5 auf 40 Rotationen pro Minute beschleunigt. Ein motorisch uneingeschränktes Tier kann diesen Test nach 3-tägigem Training problemlos absolvieren.

Um etwaige metabolische Veränderungen zu erfassen, wurde durch Rumpfbloodentnahme nach Dekapitation das Plasma der Tiere nach 24 Stunden, 72 Stunden und 7 Tagen nach Reperfusion auf Veränderungen der Metaboliten Glukose, Laktat und Pyruvat untersucht.

Die Vermessung der Mitochondrien mittels Oxygraph zeigte 60 Minuten nach Reperfusion erwartungsgemäß in beiden Behandlungsgruppen eine starke Beeinträchtigung aller Komplexe der

Atmungskette in den ischämischen rechten Hemisphären. Am stärksten von der Ischämie betroffen war Komplex I (ca. 50% Respiration verglichen zur linken Hemisphäre). Die Behandlung mit BHB zeigte zu diesem Zeitpunkt keine Verbesserung der mitochondrialen Respiration. 24 Stunden nach Respiration war eine deutliche Verbesserung der Komplex I Atmung in mit BHB behandelten Tieren sichtbar. Die Komplex I Atmung wies in der linken und rechten Hemisphäre keine signifikanten Unterschiede auf, wohingegen die rechte Hemisphäre in Tieren, die mit Kochsalz behandelt wurden, stark eingeschränkt war (um ca. 40% reduziert verglichen zur linken Hemisphäre). Auch für Komplex II und OxPhos wurde ein positiver Effekt in der BHB Gruppe beobachtet.

In den Verhaltensversuchen schnitten die Tiere, in denen ein Schlaganfall induziert wurde, grundsätzlich schlechter ab als scheinoperierte Tiere. Die Tiere, die mit BHB behandelt wurden, wiesen allerdings weitaus heterogenere Bewegungsmuster im Corner Test auf. Auch im Chimney-Test schnitten sie signifikant besser ab als mit Kochsalz behandelte Tiere. Im Rotarod-Test schnitten sowohl die Kochsalz- als auch die BHB-Gruppe deutlich schlechter ab als scheinoperierte Tiere. Zwischen Kochsalz- und BHB-Gruppe konnten keine signifikanten Unterschiede in diesem Test festgestellt werden. Die Metabolitenspiegel zeigten im Vergleich zu scheinoperierten Tieren keine Unregelmäßigkeiten.

72 Stunden nach Reperfusion war noch immer ein positiver Effekt auf Komplex I, Komplex II und OxPhos zu beobachten, allerdings nicht mehr so deutlich wie 24 Stunden nach Reperfusion. Auch in den Verhaltensversuchen verringerten sich die Unterschiede zwischen BHB und Kochsalz-Gruppe. 24 Stunden nach Reperfusion waren im Corner-Test die Drehungen der BHB Tiere weitgehend wahllos in beide Richtungen. Nach 72 Stunden hingegen waren in beiden Gruppen hauptsächlich einseitige Drehungen zu beobachten. Auch im Rotarod-Test waren weiterhin keine signifikanten Unterschiede zwischen Kochsalz- und BHB-Gruppe sichtbar. Lediglich im Chimney-Test, der mehr Kraft erfordert als die anderen beiden Tests, war weiterhin ein Effekt von BHB sichtbar.

7 Tage nach Reperfusion war der positive Effekt von BHB auf die Respiration der mitochondrialen Komplexe nicht mehr statistisch zu erfassen. Ein Trend ist dennoch weiterhin sichtbar. Auch in den Verhaltensversuchen gab es keine statistisch signifikanten Unterschiede mehr zwischen Kochsalzgruppe und BHB Gruppe.

Da Normierung auf Aktivität der Citratsynthase sämtliche Effekte des Schlaganfalls neutralisierte, beziehen sich die oben genannten Ergebnisse aus den respirometrischen Messungen auf Proteingehalt. Normierung auf Citratsynthase ist im Fall der vorliegenden Arbeit weniger aussagekräftig, da sie auf die Menge an funktionierenden Mitochondrien normiert und nicht-funktionale Masse nicht berücksichtigt. So war die Aktivität der Citratsynthase aus rechten ischämischen Hemisphären erwartungsgemäß halb so hoch wie in den linken nicht-ischämischen

Hemisphären, was den Effekt, den der Schlaganfall zur Folge hat, ausgleicht. Dennoch war die Aktivität der Citratsynthase (in den rechten Hemisphären) in der BHB Gruppe 24 Stunden nach Reperfusion signifikant höher als in der Kochsalz Gruppe. Dies ist ein Indikator dafür, dass es 24 Stunden nach Reperfusion noch mehr funktionale Mitochondrien in den ischämischen Hemisphären BHB-behandelter Tiere gibt und dass BHB als einmalige Gabe einen verzögernden Effekt auf die Folgeprozesse des Schlaganfalls hat. Außerdem verloren die Tiere unabhängig von der Behandlung innerhalb der ersten 72 Stunden nach Reperfusion massiv an Gewicht. Die Gewichtsabnahme stagnierte nach 72 Stunden und nach 7 Tagen war ein Trend zur langsamen Gewichtszunahme sichtbar. Die Konzentrationen von Glukose, Laktat und Pyruvat blieben über den beobachteten Zeitraum weitgehend stabil.

Die vorliegende Arbeit lässt folgende Aussagen über die neuroprotektiven Eigenschaften des Ketonkörpers BHB zu. BHB überwindet die Blut-Hirn-Schranke, was durch einen extrazellulären Konzentrationsanstieg von BHB nach intraperitonealer Injektion gezeigt werden konnte. Dieser Anstieg ist - vermutlich aufgrund der BHB-Aufnahme durch andere Organe - allerdings nur zweifach. Der Effekt einer einmaligen BHB-Gabe, verabreicht unmittelbar nach Reperfusion, nach 90-minütiger transients zerebraler Ischämie wurde untersucht. 24 Stunden nach Reperfusion zeigten die Verhaltenstests einen positiven Effekt der einmaligen BHB-Gabe. Interessanterweise hatten weder eine geringe Dosis von 10 mg/kg, noch eine hohe Dosis von 100 mg/kg Körpergewicht einen Einfluss auf die neurologischen Funktionen der Tiere. Es scheint dementsprechend, dass die Dosierung eine wichtige Rolle für den positiven Effekt von BHB auf den Ausgang des Schlaganfalls spielt. Der Grund, weshalb eine höhere Dosis BHB ineffektiv war, ist unbekannt. Die Toxizität von BHB gilt allgemein als gering. In der vorliegenden Arbeit konnte gezeigt werden, dass BHB, verabreicht als Einmaldosis unmittelbar nach Reperfusion, einen positiven Effekt sowohl auf die mitochondriale Atmung als auch auf die motorischen Funktionen von Mäusen hat. Dieser Effekt ist allerdings nur auf bis zu 72 Stunden nach Reperfusion signifikant. Die Effekte verblassten nach 72 Stunden und waren 7 Tage nach Reperfusion nicht länger detektierbar. In Mitochondrien scheint der Effekt von BHB spezifisch für Komplex I sein. Allerdings konnte vorübergehend ebenfalls eine verbesserte Komplex II Atmung beobachtet werden. Der exakte Wirkmechanismus von BHB im Mitochondrium ist allerdings weiterhin unbekannt. Aufgrund der *in vitro* erzielten Ergebnisse ist eine direkte Stimulation der Atmung, möglicherweise nach vorheriger metabolischer Umwandlung des BHB, wahrscheinlicher als Effekte auf Epigenetik oder oxidativen Stress, die ebenfalls beschrieben wurden.

Die möglichen günstigen Effekte einer verlängerten und dauerhaften Gabe von BHB nach ischämischem Schlaganfall sollten in Zukunft untersucht werden. Da die therapeutischen Möglichkeiten zur Behandlung des Schlaganfalls bis heute sehr begrenzt sind, sollte der Effekt von

BHB, insbesondere in Hinblick auf seine geringe Toxizität, als Substanz für klinische Studien in Erwägung gezogen werden. Zukünftige Studien sollten zumindest den Effekt von BHB im Schlaganfall in anderen Tiermodellen untersuchen, zum Beispiel in Affen oder Hunden, um auszuschließen, dass ein Effekt ausschließlich in Nagetieren zu beobachten ist.

1. Introduction

1.1 Stroke

As of today, stroke is the second leading cause of death and disability worldwide, with incidence rising, due to increasing age of the world population (Feigin et al. 2015). In 2016, there were 80.1 million prevalent cases of stroke, causing 5.5 million deaths and 116.4 million DALYs (disease-adjusted life years – one DALY representing the loss of one year in full health) worldwide (Johnson et al. 2019). In Germany alone there were approximately 243.000 prevalent stroke cases, accounting for 58.000 deaths and 900.000 DALYs (Johnson et al. 2019). Disability following stroke is the third common cause for long-term care dependency (Cowman et al. 2010). Stroke can be either of ischemic or of hemorrhagic nature. Whereas ischemic stroke is more common, hemorrhagic stroke accounts for more deaths and disability, especially in countries with lower income with mortality rates of up to 80% (Feigin et al. 2017). Ischemic stroke, predominantly occurring in the elderly, leaves several patients unable to live an independent life. Disabilities following stroke include for example cognitive deficits, bladder incontinence, depression and social disability (Kannel 1979). Despite extensive research in the past decades, recombinant tissue plasminogen activator (rt-PA) remains the only effective pharmacological intervention in the treatment of ischemic stroke to this day. Besides, endovascular thrombectomy has become a proven therapy for acute ischemic stroke. Both therapy options have a narrow time frame and require strict diagnosis.

1.1.1 Hemorrhagic Stroke

Hemorrhagic stroke is caused by rupture of blood vessels in the brain, which again are caused by coagulation disorders or arteriovenous malformations (Rymer 2011). Those anomalies often have a genetic basis (Broderick et al 2007). Acute or chronic load, such as hypertension, traumatic brain injury, or the use of cocaine can lead to rupture of a compromised blood vessel. Hemorrhagic stroke accounts for 10- 15% of all strokes with mortality rates up to 80% (Feigin et al. 2017). As hemorrhagic stroke is not the object of this work, it is only mentioned for the sake of completeness.

1.1.2 Ischemic Stroke

Ischemic stroke makes up for approximately 85% of all strokes (Musuka et al. 2015). It is mostly embolic and caused by rupture of arteriosclerotic plaques in the extracranial cervical carotid or vertebral artery, followed by thrombus formation (Musuka et al. 2015). The thrombus is then carried into the intracranial blood vessels, where it occludes one of the terminal arteries with the

consequence of interrupted perfusion of the affected artery (Kuriakose and Xiao 2020). The brain tissue that depends on glucose and oxygen from the occluded artery becomes ischemic, leading to severe stress and finally necrosis (Broughton et al. 2009). The artery most susceptible to ischemic stroke is the middle cerebral artery – it accounts for approximately 50% of stroke-related disability (Ng et al. 2007).

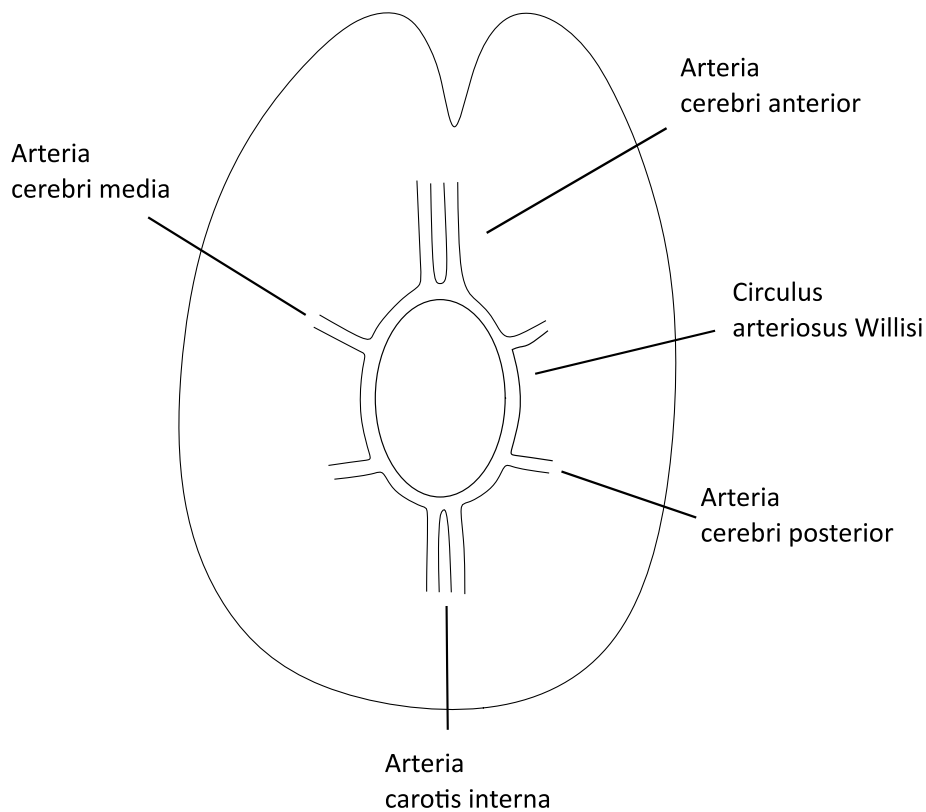


Figure 1: Cerebral arteries of the human brain

1.1.3 Risk factors

The Framingham study (1994) as well as INTERSTROKE (2010) have identified different risk factors for ischemic stroke.

- Increased age (70% of stroke patients > 65 years)
- Hypertension (>160/90 mm Hg)
- Cigarette smoking (risk increases with number of cigarettes smoked per day)
- High waist-to-hip ratio
- Consumption of > 30 alcoholic drinks per month (whereas 1-30 drinks per month are associated with reduced risk of ischemic stroke)
- Dietary habits (increased consumption of red meats, fried and salty foods)
- Psychosocial stress and depression
- Lack of exercise
- Atrial fibrillation
- Increased ApoB concentration
- High non-HDL/HDL cholesterol ratio

1.1.4 Pathobiology following ischemic stroke

Dirnagl et al. (1999) describe four major pathological mechanisms into which ischemic brain injury can be subdivided – excitotoxicity, peri-infarct depolarization, inflammation, and programmed cell death (schematically shown in fig. 3). They occur over time after stroke onset and spread from the core region towards penumbra. Whereas the core of stroke (fig. 2) is fatally damaged within minutes after onset of ischemia, the penumbra – the region between healthy brain tissue and core, with restricted perfusion – remains metabolically active. If left untreated over the course of time, the penumbra eventually becomes apoptotic and necrotic as well, due to excitotoxicity and secondary damages. Since the core is irretrievably damaged upon onset of stroke, effort revolves around finding therapeutic options to rescue as much as possible of the penumbra.

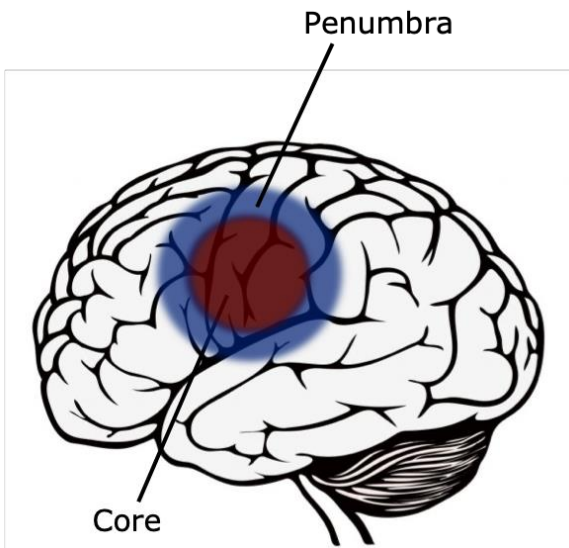


Figure 2: Illustration of ischemic core and surrounding penumbra.

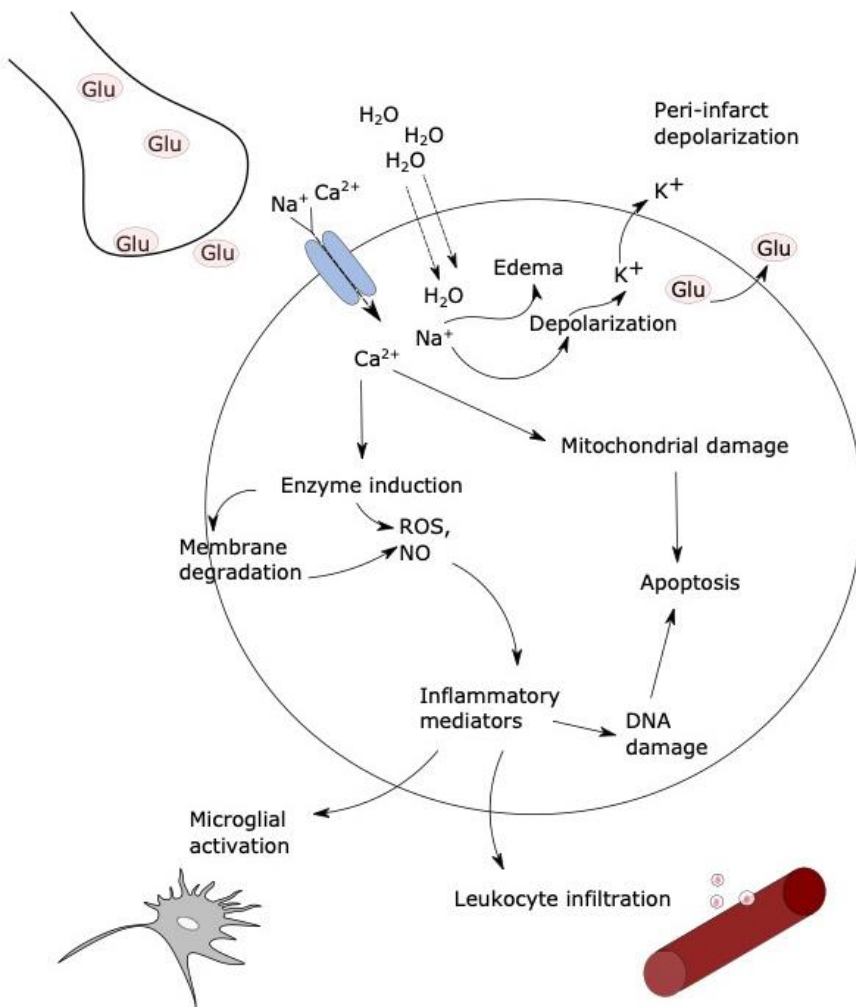


Figure 3: Illustration of pathobiological mechanisms during stroke. Based on Dirnagl et al. (1999).

Excitotoxicity

The brain relies on oxygen and glucose, which are delivered via blood. It generates energy mainly through oxidative phosphorylation. Due to inhibited blood flow in the occluded cerebral artery, oxygen and glucose become scarce, leading to impaired metabolic dynamics. As a result, ion gradients can no longer be upheld, the membrane potential of neurons and glial cells collapses, and the cells depolarize (Martin et al. 1994). The consequence is a massive influx of Ca^{2+} (Nicholson et al. 1977), which, in combination with cellular depolarization, leads to release of large amounts of excitatory amino acids (Shimada et al. 1993; Lai et al. 2014; Belrose et al. 2012). The aggregation of predominantly glutamate is further exacerbated due to impeded glutamate reuptake and leads to over-activation of glutamate receptors. As glutamate receptors are stimulated in a massive manner, the influx of ions intensifies – Ca^{2+} influx is aggravated by activation of NMDA-receptors, Na^+ and Cl^- flow into the cells due to AMPA-receptor stimulation (Park et al. 1989). Furthermore, water is transported into cells passively along with Na^+ and Cl^- . Cellular Brain edema increases intracranial pressure, impairing the perfusion of brain tissue surrounding the core region. Strongly elevated Ca^{2+} levels promote cytoplasmatic and nuclear processes, such as activation of proteolytic enzymes, which, among others, degrade proteins of the cytoskeleton and extracellular matrix proteins (Furukawa et al. 1996). Reactive oxygen species (ROS) generation is driven by activation of phospholipases and cyclooxygenases (Adibhatla and Hatcher 2008). ROS then cause oxidative damage by lipid peroxidation and membrane damage. Moreover, ROS induce inflammation and apoptosis. Highly reactive peroxy-nitrite, which is formed from nitric oxide by the enzyme nitric-oxide-synthase (Ca^{2+} -dependent), promotes further tissue damage (Iadecola 1997; Beckman and Koppenol 1996). Increased NO generation, on the other hand, has protective properties, by ameliorating microcirculation in the tissue. The abundant ROS disrupt the mitochondrial inner membrane and damage proteins needed for transport of electrons, H^+ efflux and ATP generation. Consequently, the mitochondrial membrane begins to leak, mitochondria swell, cytochrome c is released, which triggers apoptosis (Fujimura et al. 1998; Moskowitz et al. 2010).

Altogether, excitotoxic mechanisms lead to necrosis (acute), apoptosis (delayed), and signaling pathways downstream trigger the expression of pro-inflammatory genes, causing post-ischemic inflammation (fig. 4).

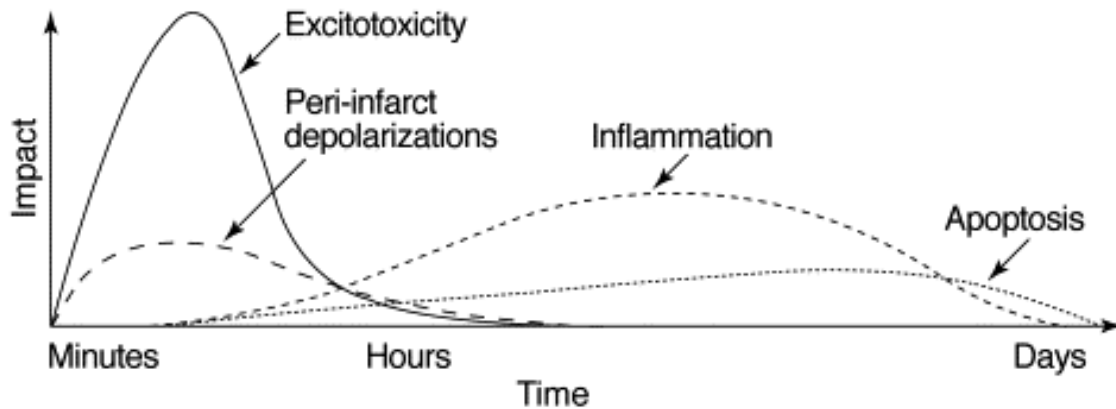


Figure 4: Chronology of pathobiological processes. Excitotoxicity starts early on and causes further events like peri-infarct depolarizations and neuroinflammation, which exacerbates and accelerates destruction of neuronal tissue. Adopted from Dirnagl et al. (1999).

Peri-infarct depolarization

Ischemic glial cells and neurons depolarize because of energy failure, succumbing ion gradients and release of glutamate. Whereas cells in the core region cannot repolarize, neurons and glia in the penumbra region repolarize under energy consumption. Once repolarized, they can depolarize again, exacerbating the extracellular accumulation of K^+ and glutamate. This phenomenon is termed peri-infarct depolarizations and they have been found in numerous animal models of ischemic stroke but have not yet been proven to occur in humans (Hossmann 1996). In animal models they occur several times per hour for six to eight hours after onset of stroke and infarct size correlates with the number of depolarizations (Mies et al. 1993; Strong et al. 2007).

Neuroinflammation

Inflammation is caused by expression of several pro-inflammatory genes, such as $\text{NF}\kappa\text{B}$ and hypoxia inducible factor 1 (O'Neill and Kaltschmidt 1997; Ruscher et al. 1998). Expression of these genes is triggered by hypoxia, elevated Ca^{2+} -levels which activate intracellular signaling systems and abundant amounts of ROS. Mediators of inflammation are produced by damaged brain cells, leading to migration of neutrophils, macrophages and monocytes into the ischemic brain (Rothwell and Hopkins 1995; Zhang et al. 2019). Furthermore, astrocytes become hypertrophic and microglia are activated (decline of processes, adapt ameboid morphology) (Moskowitz et al. 2010). Microglial reaction is in progress in the ischemic brain 24 hours after onset of stroke, especially in the penumbra (Caplan et al. 1997a).

The role of post-ischemic inflammation in the ischemic brain is supported by a series of research results. For instance, cerebral damage after ischemic stroke is reduced when neutrophilic infiltration

is prevented, or when adhesion molecules or their receptors are blocked. Cerebral damage following ischemic stroke is also reduced when interleukin-1 (IL-1), a pivotal inflammatory mediator, is blocked, or when there is no activity of interferon regulatory factor 1 (IRF-1). IRF-1 is a transcription factor that coordinates the expression of genes associated with inflammation (Connolly et al. 1996; Loddick and Rothwell 1996; Iadecola et al. 1999; Alexander et al. 2003). There are various mechanisms through which post-ischemic inflammation may be involved in ischemic damage. While neutrophils exacerbate the extent of ischemia by causing microvascular obstruction, toxic mediators, released by active inflammatory cells and damaged neurons, have critical effects (Del Zoppo et al. 1991). Rodent MCAO models, like human stroke patients, show infiltrating neutrophils that produce inducible NOS (iNOS), which in turn generates toxic amounts of NO (Forster et al. 1999). Furthermore, ischemic neurons express cyclooxygenase 2, which contributes to ischemic injury by generating superoxide and prostanoids (Nogawa et al. 1997). Additionally, ischemic neurons generate TNF α , a cytokine that further aggravates damage following ischemia (Bokhari et al. 2014). Neurotoxins, NO, ROS and prostanoids are also generated by activated microglia. Moreover, neuroinflammation may be associated with apoptosis as antibodies that target adhesion molecules ameliorate apoptosis and post-ischemic inflammation (Caplan et al. 1997b; Bruce et al. 1996).

Programmed cell death

Once brain cells have been exposed to massive amounts of Ca²⁺ or ROS, suffered from excessive activation of glutamate receptors or mitochondrial and DNA damage, they go into apoptosis or necrosis. Whether the cell dies by necrosis or apoptosis depends on cell type, stage in life cycle and intensity of stimulus causing the cell to die (Dirnagl et al. 1999; Leist and Nicotera 1998; Broughton et al. 2009). While necrosis primarily occurs after permanent artery occlusion, apoptosis follows milder damage, predominantly in the penumbra. Apoptosis is promoted by activated caspases, in particular by caspases 1 and 3 (Hara et al. 1997; Namura et al. 1998; D'Amelio et al. 2010; Zhang et al. 2003). They are activated by an apoptosome complex, which was previously activated by cytochrome c, released by mitochondria. Where brain injury was mild, more cells die delayed and by caspase-dependent mechanisms (apoptosis). For instance, after mild occlusion of the middle cerebral artery for 30 minutes, cytochrome c release and caspase activity can be observed at 6 and 9 hours, respectively, after reperfusion. Apoptosis becomes visible between 24 and 72 hours after middle cerebral artery occlusion (MCAO) (Endres et al. 1998). Caspase activity can be further delayed by administration of caspase inhibitors, attenuating the amount of dead brain tissue and the neurological deficit (Hara et al. 1997). Interestingly, the combination of caspase inhibitors with MK801, a NMDA-

receptor-antagonist, was shown to be higher effective, even many hours after mild transient stroke (Yakovlev et al. 1997).

1.1.5. MCAO mouse model

There are various experimental models to mimic human stroke. Due to the complexity of stroke surgeries and strict laws on animal experiments, *in-vitro* models are a less complicated choice. *In-vitro*, ischemia is caused by gassing of cell culture with carbogen (95% N₂, 5% CO₂) and transition to a glucose-free culture medium. This method is termed *oxygen-glucose-deprivation* (OGD) and it is described in detail by Kiewert et al. (2008).

In vivo there are different approaches to experimental stroke. The models can be divided into permanent and transient occlusion of a cerebral artery (Mao et al. 2000). In permanent stroke models, occlusion is upheld until the end of the experiment, whereas reperfusion is allowed after a certain time in transient stroke models. Transient occlusions are usually upheld between 30 minutes and 3 hours (Mao et al. 2000; Conn 2006).

The advantage of transient stroke models is that it leads to a large penumbra (Howells et al. 2010). As described before, the penumbra is the peripheral area of ischemic tissue after ischemic stroke, in which cells are initially only mildly damaged. An ideal neuroprotective agent would stabilize neuronal cells and prevent programmed cell death. The core region of stroke, as mentioned before, is irretrievably damaged upon onset of stroke. For this reason, research for interventions or neuroprotectants revolves around rescuing tissue in the penumbra region (Hillis and Baron 2015).

One stroke model is performed on the open brain. A cerebral artery, mostly the middle cerebral artery, is exposed through a craniectomy and occluded with a suture or clip (Crowell et al. 1981; O'Brien and Waltz 1973). In this case, reperfusion can be allowed after a certain time. If the artery is occluded through obliteration, ischemia becomes permanent (Tamura et al. 1981; Colak et al. 2011). The advantage of the permanent occlusion model through obliteration is high reproducibility (Howells et al. 2010).

In another model, the artery is occluded by means of a nylon filament which is placed in the carotid artery and advanced into the origin of the middle cerebral artery (*middle cerebral artery occlusion, MCAO*). The middle cerebral artery (MCA) is a terminal artery that supplies the striatum. The core region after MCAO accordingly is the striatum with the penumbra region ranging to hippocampus and cortex (Kiewert et al. 2010).

This model was first described by Koizumi et al. (1986). Then, the filament was inserted directly via the carotid artery. Surgically, this means that the filament occluded the middle cerebral artery while leaving the common carotid artery ligated. Consequently, the result was hemi cranial ischemia rather

than ischemia located strictly in the striatum. The model was further refined by Longa et al. (1989), using the external carotid artery as auxiliary artery for inserting the filament (fig. 5). The method is described in detail in section 2.4.2. (MCAO surgery).

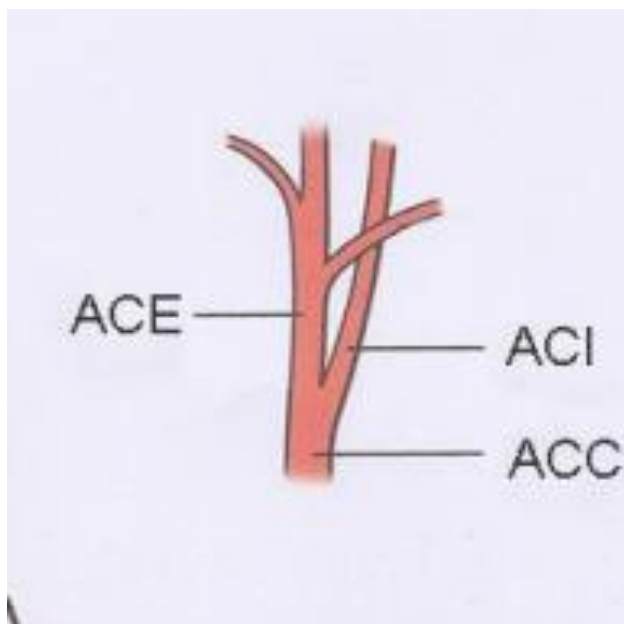


Figure 5: Ramification of the common carotid artery (ACC) in external carotid artery (ACE) and internal carotid artery (ACI). Modified from Schenk and Smith: Dissection Guide & Atlas to the Rat.

This refined method allows to reopen the ACC and restore blood flow in all arteries except in the MCA. Accordingly, the region of stroke is more precise and located only in the striatum. The advantage of the MCAO model is that reperfusion is enabled by simply retracting the filament. Surgery is minimally invasive on the carotid artery at the neck instead of opening the skull and operating on the open brain.

An overview of the MCAO models with experimental instructions was published by O'Neill and Clemens (2001). Advantages and disadvantages of the models mentioned above were discussed by Howells et al. (2010), Liu and McCullough (2011), Laing et al. (1993), Dittmar et al. (2003), (Kuraoka et al. 2009) and Weinachter et al. (1990).

The filament itself is substantial for a successful surgery. The suture is usually made of nylon or polyamide. Composition and size of the filament head determine the extent of stroke. The filament must not have sharp edges in order not to injure endothelium when being moved within the arteries because this could cause uncontrolled clot formation. Entirely silicone coated sutures occlude a longer area of the artery circle of the brain, whereas filaments with a small silicone head occlude the MCA terminally (fig. 6). In this case, however, the filament must be placed accurately at the MCA's origin in order to occlude it. This is achieved by on-line monitoring by Laser Doppler. Coated filaments can be

placed easier and strokes induced with these filaments show better reproducibility (Schmid-Elsaesser et al. 1998). An example of a coated filament is shown in image 1.

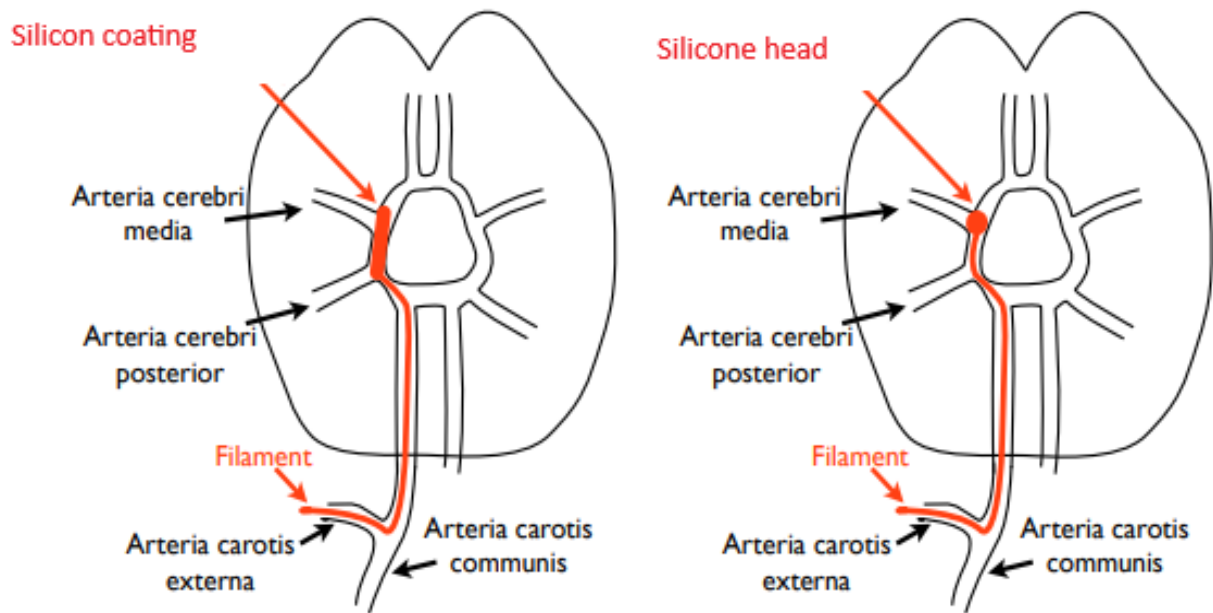


Figure 6: Schematic image of middle cerebral artery occlusion. Comparison of occlusion with silicone coated filament (left) and filament with silicone head (right). Figure modified from Tina Schwarzkopf (2015).

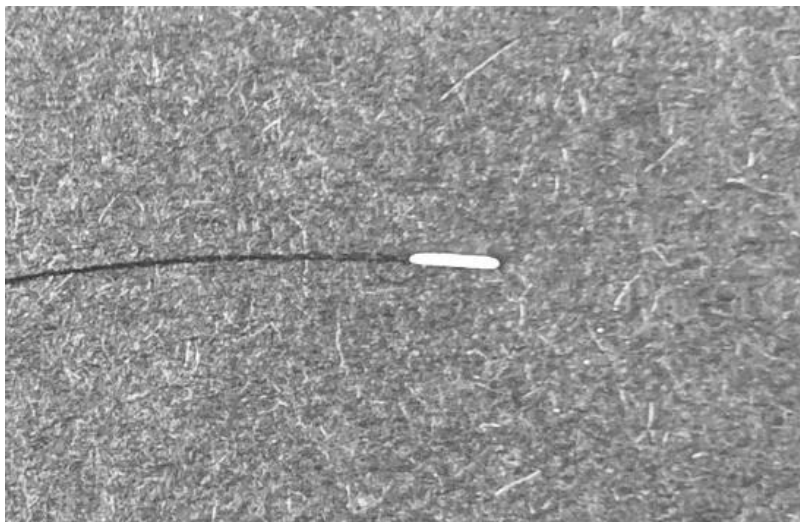


Image 1: Silicon coated nylon filament by Doccol (MA, USA); 2-3 mm length, 0.25 ± 0.02 mm diameter.

Poly-L-lysine coated filaments seem to be of advantage when inducing stroke in older and multimorbid animals.

The third stroke model that is commonly used in animal experiments is most similar to stroke as it occurs in humans. The clot model uses an artificial blood clot which is placed in the MCA through the circle of Willis. This model was first described in dogs by (HILL et al. 1955) and further developed in rats by Kudo et al. (1982). Initially the clots were injected in the ACC. However, the resulting strokes were variable in extent and location of infarction. For this reason, the model was further refined regarding clot size and location of injection, which led to improved reproducibility (Dinapoli et al. 2006; Wang et al. 2001; Toomey et al. 2002). Controllability is best if the clots are injected directly into the MCA via catheter (Zhang et al. 1997a). This, however, does not resolve the issue of spontaneous clot formation and the variability of time until reperfusion after administration of rt-PA (Niessen et al. 2002).

1.2. Acute Interventions and Neuroprotectants

1.2.1 Acute Interventions

As mentioned before, there are two approved therapy options to restore cerebral blood flow, pharmacologically and mechanically. Pharmacological intervention, thrombolysis, is carried out by i.v. injection of the recombinant tissue plasminogen activators (rt-PA) Alteplase or Tenecteplase maximally 4.5 hours after onset of stroke, although a “door-to-needle” time of ≤ 60 minutes is associated with lower mortality and an overall better outcome (Fonarow et al. 2011). On the other hand, the administration of rt-PA bears a considerable risk of complications, such as intracranial hemorrhage or major systemic hemorrhage, requiring close monitoring of patients after thrombolysis (Miller et al. 2011). Mechanical thrombectomy includes either blood clot removal using a stent retriever or rt-PA delivery through a catheter (Smith et al. 2008). Success rates of intravenous rt-PA and mechanical thrombectomy lie at approximately 21% and 48%, respectively, whereas the success rate of combined thrombectomy with rt-PA lies around 60% (Bhatia et al. 2010; Smith et al. 2008). However, due to time constraints, less than 5% of patients receive this therapy.

1.2.2 Neuroprotection Agents

A fairly current review of Hakim (2012) discusses the “future of thrombolysis therapy”. It focusses on an improved administration of rt-PA. This should be done quicker, requiring development of optimized neurological screening methods.

As of today, one of the challenges in stroke research lies in protecting the penumbra region which is only mildly damaged immediately after stroke to prevent cells from going into apoptosis. The property

of a compound to do so is termed “neuroprotection”. A neuroprotection agent protects brain cells of damaging effects through pharmacological or biochemical intervention. This way disease progression is delayed and quality of life can be improved (Shoulson 1998). Newly developed neuroprotective compounds must be able to penetrate the brain and unfold their action in the infarcted area until thrombolysis has been successful. In acute situations the drug must be administrable by emergency doctors regardless of CT scan results. Otherwise, the drug must be suited for daily use by patients of high risk.

There are more than a thousand animal studies in which neuroprotection agents were investigated regarding ameliorating effects of ischemic brain injury. Whereas many studies were promising in animal models, most studies failed when tested in a 4-6-hour timeframe from onset of stroke in humans. Among the agents that have made it into clinical trials are calcium channel blockers, glutamate antagonists (NMDA and AMPA), GABA agonists, antioxidants and/or free radical scavengers, NOS-transduction down-regulators, hemodilution agents, magnesium therapy and hypothermia. Many agents, however, only act when given before stroke. This does not reflect the clinical situation. The most promising compounds will be briefly discussed in this chapter.

Calcium channel blockers

Nimodipine can penetrate the blood-brain barrier. It blocks L-type calcium channels which prevents the influx of calcium into neurons, causing vasodilation (Kazda and Towart 1982, Scriabine et al. 1989). Clinically it is used to treat acute vasospasms (Ducros 2012). Unfortunately, it did not show a superior therapeutic effect compared to placebo in clinical trials for treatment of acute ischemic stroke (Zhang et al. 2012; Horn et al. 2001).

Glutamate antagonists

MK-801 (dizocilpine) and CNS-1102 (aptiganel), both non-competitive NMDA-receptor blockers, bind with high affinity and cause long-lasting blockade. *In vitro* as well as *in vivo* they significantly improved the effects of stroke (Ginsberg 1995; Minematsu et al. 1993). Both compounds failed in clinical trials due to severe dosage-dependent adverse effects like nausea, vomiting, hallucinations, paranoia, and catatonia (Albers et al. 2001; Kovacic and Somanathan 2010).

NMDA-receptor glycine-site antagonist

Gavestinel is also a NMDA-receptor antagonist, but with a different binding site than the two compounds mentioned above which reduced psychiatric side effects. Because no benefit could be shown for the treatment of stroke, gavestinel failed in clinical trials (Lees et al. 2000).

Antioxidants

Antioxidants are supposed to reduce the formation of reactive oxygen species (ROS) in the core region of stroke. Compounds that have made it into preclinical or clinical trials are NXY-059, tirilazad, ebselen and edaravon. All compounds failed due to lack of benefit (Ginsberg 2008).

NO signal transduction downregulators

The compound lubeluzol down-regulates the path of nitric oxide synthesis (Lesage et al. 1996). A Cochrane meta-analysis of five studies including 3510 patients could not determine reduced mortality after stroke under treatment with lubeluzol. On the contrary, an increase of arrhythmias (QT prolongation) was observed (Gandolfo et al. 2002).

Antibodies

Enlimomab is a murine antibody that targets the intracellular adhesion molecule ICAM-1 and thereby reduces leukocyte adhesion. However, the ASTIN clinical trial determined insufficient efficacy (Krams et al. 2003).

1.2.3 Neuroprotectants and recanalization

A further approach to treatment of ischemic stroke was concomitant administration of a thrombolysis agent and neuroprotectants. In the FAST-MAG study, the administration of intravenous magnesium sulfate, a known neuroprotective in preclinical stroke models, was investigated in patients with suspected stroke within 2 hours after symptom onset. The intervention showed no beneficial effect with respect to disability outcomes at 90 days (Saver et al. 2015). Ebselen, administered together with a low dose of rt-PA, enhanced the neuroprotective effects of rt-PA in rabbits. (Lapchak and Zivin 2003). However, this combination was not tested in a clinical setting.

1.3. Ketone bodies and the ketogenic diet

The ketogenic diet is among investigated preventive options with promising results. In this diet, glucose is mostly substituted by fat (≤ 50 g carbohydrates per day, $\geq 70\%$ of calories from fat) (Ludwig 2020). It will be discussed in this following chapter.

1.3.1 Ketone bodies

Ketone bodies include three distinct $C_{3/4}$ bodies, β -hydroxybutyrate, acetoacetate and acetone (fig. 7).

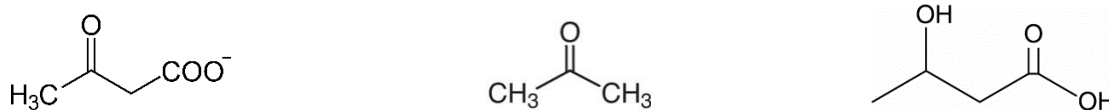


Figure 7: Acetoacetate, acetone and β -hydroxybutyrate

They serve as a source of energy when glucose, the main source of energy for the brain, becomes scarce. This occurs, among others, during intense physical activity or fasting, in low-carb diets, or metabolic diseases like diabetes. Under those circumstances, the organism develops ketonemia and ketone bodies become the primary source for energy (Fukao et al. 2004). Ketogenesis primarily takes place in liver mitochondria and uses acetyl-CoA, which is obtained through β -oxidation of fatty acids, as starting molecule (fig. 8).

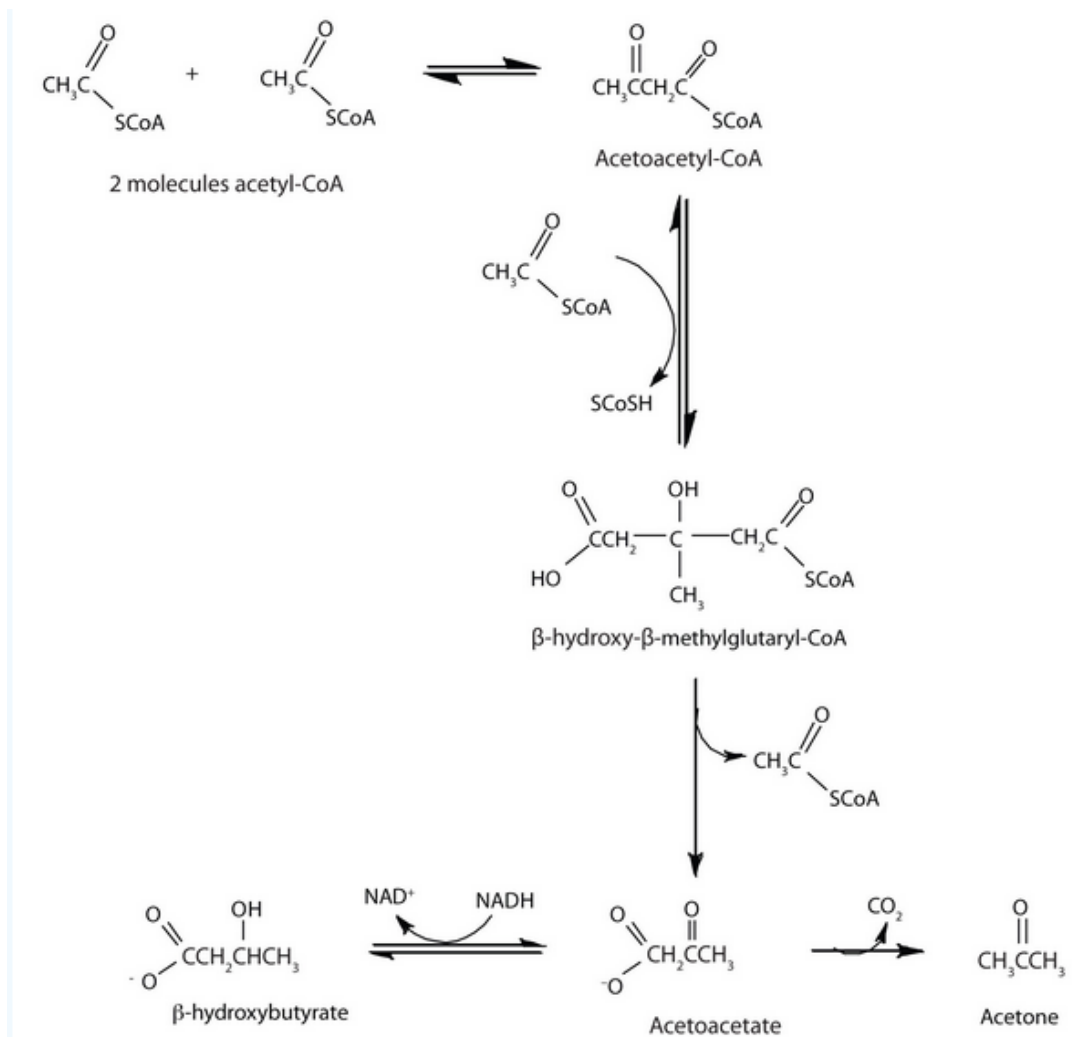


Figure 8: Formation of the three ketone bodies β -hydroxybutyrate, acetoacetate and acetone. Source: Anon, 2019.. Available at: <https://chem.libretexts.org/@go/page/129921> [Accessed March 18, 2022].

Acetone is formed by spontaneous decarboxylation of acetoacetate and cannot be used as a source for energy generation. It is eliminated pulmonary (Chandel 2015). Due to a missing enzyme, the β -ketoacyl-CoA transferase, hepatocytes themselves cannot metabolize ketone bodies. Via MCT1/2 they enter the blood and are so distributed to extrahepatic tissue (e.g. the brain), where they are absorbed by means of, again, MCT1/2. Once in extrahepatic cells, BHB and acetoacetate are transported into the mitochondrial matrix. The mitochondrial β -hydroxybutyrate dehydrogenase then converts BHB to acetoacetate. A CoA-group is transferred onto acetoacetate and afterwards acetoacetyl-CoA is cleaved thiolitically to two molecules of acetyl-Coa. Acetyl-CoA is then fed into the citric acid cycle.

1.3.2 Ketogenic diet

Ketogenic diet, high in fat, moderate in proteins and low in carbohydrates was first established in 1920 and is to this day used for treatment of epilepsy in children (Martin et al. 2016). Preclinical data also

suggests beneficial effects of ketosis in experimental models of neurodegenerative disease such as Alzheimer's, Parkinson's, Huntington's disease and spinal injuries (van der Auwera et al. 2005; Cheng et al. 2009; Ruskin et al. 2011; Streijger et al. 2013).

1.3.3 Ketogenic diet in ischemic and traumatic brain injury

As discussed before, excitotoxicity, oxidative stress and apoptosis are three of the major pathobiological processes in stroke. Some *in-vitro* data points out ameliorating effects of ketosis regarding ischemic stroke. Maalouf et al. (2007) observed that ketone bodies are able to reduce glutamate-induced damages in neuronal membranes and decrease ROS concentrations as well as ROS formation *in vitro* in isolated neurons. Besides that, the presence of ketone bodies in ischemic tissue led to decreased amounts of apoptotic biomarkers (Maalouf et al. 2007; Gasior et al. 2006). In rats, Prins et al. (2005) found the ketogenic diet to reduce the volume of cortical edema 7 days after controlled traumatic brain injury. However, beneficial effects could only be shown in younger animals, although availability of ketone bodies was alike in all age groups in the experiment. The authors assume that animals at younger developmental stages may be able to utilize ketone bodies more efficiently (Rafiki et al. 2003; Vannucci and Simpson 2003; Pierre and Pellerin 2005). In a different study, rats were fasted for 48 hours prior to ischemic stroke (duration 30 minutes by four-vessel occlusion), leading to similar ketosis as ketogenic diet. Here, fasting showed protective effects against neuronal loss in hippocampus, neocortex and striatum and reduction of mortality and post-ischemic seizures (Marie et al. 1990). In conclusion, the ketogenic diet and fasted state have neuroprotective properties in ischemic, as well as traumatic brain injury. Furthermore, Yamada et al. (2005) showed that rats who were fed a ketogenic diet are resistant to loss of cortical neurons when suffering from insulin-induced hypoglycemia.

1.3.4 Possible mechanisms of action

The mechanism by which ketosis takes effect in ischemic or traumatic brain injury remains unknown, but β -hydroxybutyrate (BHB) is thought to be involved. It may be used as an alternative source for energy to attenuate ATP depletion caused by stroke. Beneficial effects of BHB administration in models of hypoxic or ischemic conditions could be shown in the past in regard to brain damage and neuronal functions (Cherian et al. 1994; Dardzinski et al. 2000; Suzuki et al. 2001; Smith et al. 2005). The same neuroprotective effect was observed for the other ketone bodies acetone and acetoacetate, as they can also be used for energy generation (García and Massieu 2001; Massieu et al. 2001; Noh et al. 2006). It is noteworthy that, after traumatic brain injury, neuronal uptake of BHB is increased in

rats that received a ketogenic diet compared to standard chow (Prins et al. 2004). This suggests that ketosis may drive the uptake of β -hydroxybutyrate by the brain.

Effects on energy metabolism

Ketone bodies that are generated while consuming a ketogenic diet or fasting can be used as an alternative energy source in conditions of metabolic stress. It is possible that the brain can use β -hydroxybutyrate more efficiently for energy supply per unit of oxygen than glucose (Veech et al. 2001). Bough et al. (2006) were able to show that the ketogenic diet leads to coordinated upregulation of hippocampal genes encoding mitochondrial and energy metabolism enzymes. The dentate-hilus region of the hippocampus of rats fed a ketogenic diet was examined by electron microscope and showed an increase of mitochondrial profiles, located in dendrites or axon terminals, by 46% compared to rats fed a standard diet. This indicates that the ketogenic diet stimulates mitochondrial biogenesis. The increased number of mitochondria is further substantiated by an elevated phosphocreatine: creatine ratio in hippocampal tissue which suggests higher cellular energy reserves (Bough et al. 2006).

Altogether, when receiving a ketogenic diet, there are two factors that may increase the resilience of neurons to metabolic stress – a greater number of mitochondria themselves and fuel of higher energy efficiency. These factors, in combination, may be an explanation as for why neurons that underlie ketosis have a higher resistance to metabolic changes.

Effects on glutamate-mediated toxicity

Another possible mechanism of action of the ketogenic diet may be the disruption of glutamate-mediated toxicity, one of the major pathobiological mechanisms following ischemic or traumatic brain injury. However, there is only limited evidence to prove this hypothesis. Noh et al. (2006) observed neuroprotective effects of acetoacetate against glutamate-mediated toxicity *in vitro* in hippocampal neuron cells. Interestingly, the same was found for immortalized hippocampal cells lacking ionotropic glutamate receptors. Furthermore, acetoacetate was shown to reduce the formation of early cellular markers that indicate glutamate-induced apoptosis and necrosis (Noh et al. 2006).

Effects on γ -aminobutyric acid systems

There is some research that suggests that the ketogenic diet unfolds its neuroprotective effect through increase of γ -aminobutyric acid (GABA) levels, causing GABA-mediated inhibition (Yudkoff et al. 2001).

Ketone bodies were also shown to enhance GABA concentrations in synaptosomes of rat brains (Erecińska et al. 1996). No elevation of GABA levels could be shown in rats upon receipt of a ketogenic diet (Al-Mudallal et al. 1996).

Antioxidant mechanisms

Neuroprotection of the ketogenic diet may also be caused by direct or indirect antioxidative effects. Ziegler et al. (2003) found the ketogenic diet to induce the activity of glutathione peroxidase in rat hippocampi. The glutathione peroxidase is an enzyme that prevents lipid peroxidation through reduction of lipid hydroperoxide to the corresponding alcohol. Moreover, the ketogenic diet leads to increased production of mitochondrial uncoupling proteins (UCP) (Sullivan et al. 2004). The dentate gyri of mice showed increased expression of UCP2, UCP4, and UCP5 after being fed a ketogenic diet and mitochondrial respiration in this group was higher than in mice that received the standard diet. Uncoupling proteins contribute to ROS formation reduction by dissipating the mitochondrial membrane potential. UCP production is thought to be increased by fatty acids (Freeman et al. 2006). In epilepsy patients, levels of arachidonate correlated with seizure control. However, it could not be confirmed that arachidonate induces UCP expression (Fraser et al. 2003).

Effects on programmed cell death

It is possible that the ketogenic diet serves as protectant against different forms of apoptosis. A protective effect could be shown against apoptosis in mice, triggered by kainate, an excitotoxin and glutamate receptor agonist (Noh et al. 2003). Another possible reduction of apoptosis may be via increased generation of calbindin, as found in mice that received a ketogenic diet (Noh et al. 2005a). Due to its capacity to buffer intracellular calcium, a mediator of cell death, calbindin is thought to have neuroprotective properties (Bellido et al. 2000). Moreover, ketogenic diet may suppress the accumulation of clusterin, another pro-apoptotic protein, which is driven by kainic acid (Noh et al. 2005b; Jones 2002).

Anti-inflammatory effects

It has been shown abundantly in the past that inflammation is part of the pathophysiological mechanisms in neurodegenerative diseases (Akiyama 2000; Praticò and Trojanowski 2000; Chamorro and Hallenbeck 2006). In this context, it is noteworthy to point out effects of ketosis on neuroinflammation (Palmlblad et al. 1991; Stamp et al. 2005). Thus, rats that were fasted intermittently showed increased levels of interferon- γ in the hippocampus, which was shown to have

a protective effect against excitotoxicity-associated cell death (Lee et al. 2006). Furthermore, the high amounts of fatty acids may induce anti-inflammatory reactions, such as peroxisome proliferator-activated receptor α (PPAR- α), which has an inhibitory effect on transcription of nuclear factor- κ B (NF- κ B) and activation protein-1 (Cullingford 2004).

Carbohydrate restriction as a protective mechanism

The neuroprotective effects of restriction of carbohydrates were investigated by using 2-deoxy-d-glucose, a glucose analog that is not broken down by glycolysis. Administration of 2-deoxy-d-glucose for 7 days showed neuroprotective effects against hippocampal damage, as well as functional neurological deficits induced by kainate. Besides, 2-deoxy-d-glucose showed beneficial effects against glutamate- and oxidative stress-induced neuronal cell death *in vitro* (Lee et al. 1999).

Caloric restriction has also been associated with a changed status of epigenetic mechanisms, DNA methylation, and histone modification, in gene loci that play a role in aging (Hass et al. 1993). *In vivo*, as well as *in vitro*, caloric restriction has shown to postpone aging (Li et al. 2011).

1.3 Mitochondria

Mitochondria are the energy generating compartments of a cell. It is widely accepted that they were acquired through symbiosis of archaeons as host and α -proteobacteria as primordial mitochondria early in the earth's history, known as endosymbiont theory. According to this theory, both organisms were co-dependent on each other for various nutrients, which remains accurate as of today. Mitochondria and the surrounding cell still depend on each other for metabolites. Today, all eukaryotic cells, with few exceptions, have mitochondria and rely on them for homeostasis and energy supply – malfunctioning mitochondria lead to disease (Chandel 2015).

1.3.1 Structure

A mitochondrion is an oval-shaped organelle, consisting of an outer and inner membrane with an intermembrane space in between (fig. 9). The inner membrane is folded and forms cristae. The space within the inner membrane is the matrix. Although nuclear DNA bears the information for most of the mitochondrial proteins (approximately 3000), mitochondria themselves have their own circular DNA. It is inherited maternally and encodes 37 genes, of which 13 protein products are crucial for oxidative phosphorylation.

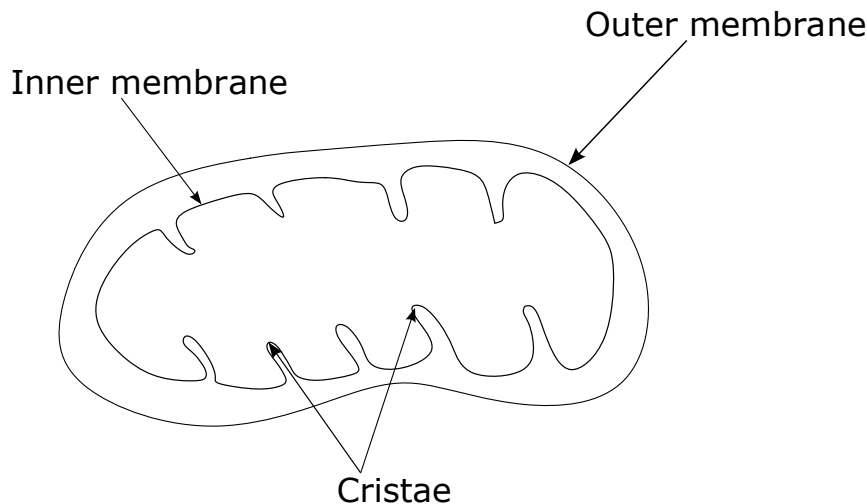


Figure 9: Schematic structure of a mitochondrion

1.3.2 Mitochondrial energy metabolism

Glucose is the primary energy source for the brain. It is broken down to pyruvate in the cytosol (mainly in glial cells), lactate is taken up by neurons, and transported into the mitochondrial matrix via the pyruvate shuttle and oxidized to acetyl-CoA. Other sources for pyruvate are glycolysis, ketone bodies (fatty acid-) or amino acid degradation. Glycolysis, fatty acid oxidation and TCA cycle yield the reducing equivalents nicotinamide-adenine-dinucleotide (NADH) and flavin-adenine-dinucleotide (FADH₂) which are fed into oxidative phosphorylation (OXPHOS) to reduce oxygen to water. The principle of OXPHOS is an establishment of a proton gradient along the inner mitochondrial membrane. The resulting energy is used for ATP generation (fig. 10).

Oxidative phosphorylation

NADH and FADH₂, which are formed in the course of the citric acid cycle, must be regenerated to NAD and FAD in order for the citric acid cycle to continue. The electron transfer system (ETS) includes complexes I-IV. Complex I, NADH dehydrogenase, consisting of 46 subunits, is the largest of the four complexes. It oxidizes NADH to NAD⁺ and the two electrons that are released are transferred onto the electron carrier coenzyme Q (ubiquinone). Simultaneously, four protons are pumped out of the matrix into the intermembrane space. Complex II (succinate dehydrogenase, SDH) is involved in the citric acid cycle as succinate dehydrogenase (SDH). It consists of four subunits. In the citric acid cycle the SDH subunit A oxidizes succinate to fumarate while reducing FAD to FADH₂. The electrons from FADH₂ are transferred onto subunits SDH-B, -C, and -D and delivered to ubiquinone. Ubiquinone passes the electrons from complex I and II on to complex III (ubiquinol-cytochrome c-oxidoreductase; cytochrome reductase) and is thereby converted to ubiquinol (QH₂). Complex III, consisting of 11

subunits, passes one electron to cytochrome c. Complex IV, the cytochrome-c oxidase, catalyzes the oxidation of cytochrome c and transfers the four electrons from cytochrome c to molecular oxygen. Hereby, two molecules of H₂O are formed. As it has the highest reduction potential, oxygen is the terminal electron acceptor in the ETS. Complexes I, III and IV are proton pumps that pump protons against positive voltage $\Delta\Psi$ from matrix into intermembrane space during electron transfer. This creates an electrochemical potential of a small chemical gradient (ΔpH) and a large electrical gradient, the membrane potential. The electrochemical proton gradient is used by complex V (ATP synthase) for ATP generation (oxidative phosphorylation). The codependency of oxidative phosphorylation and the citric acid cycle is shown in figure 10.

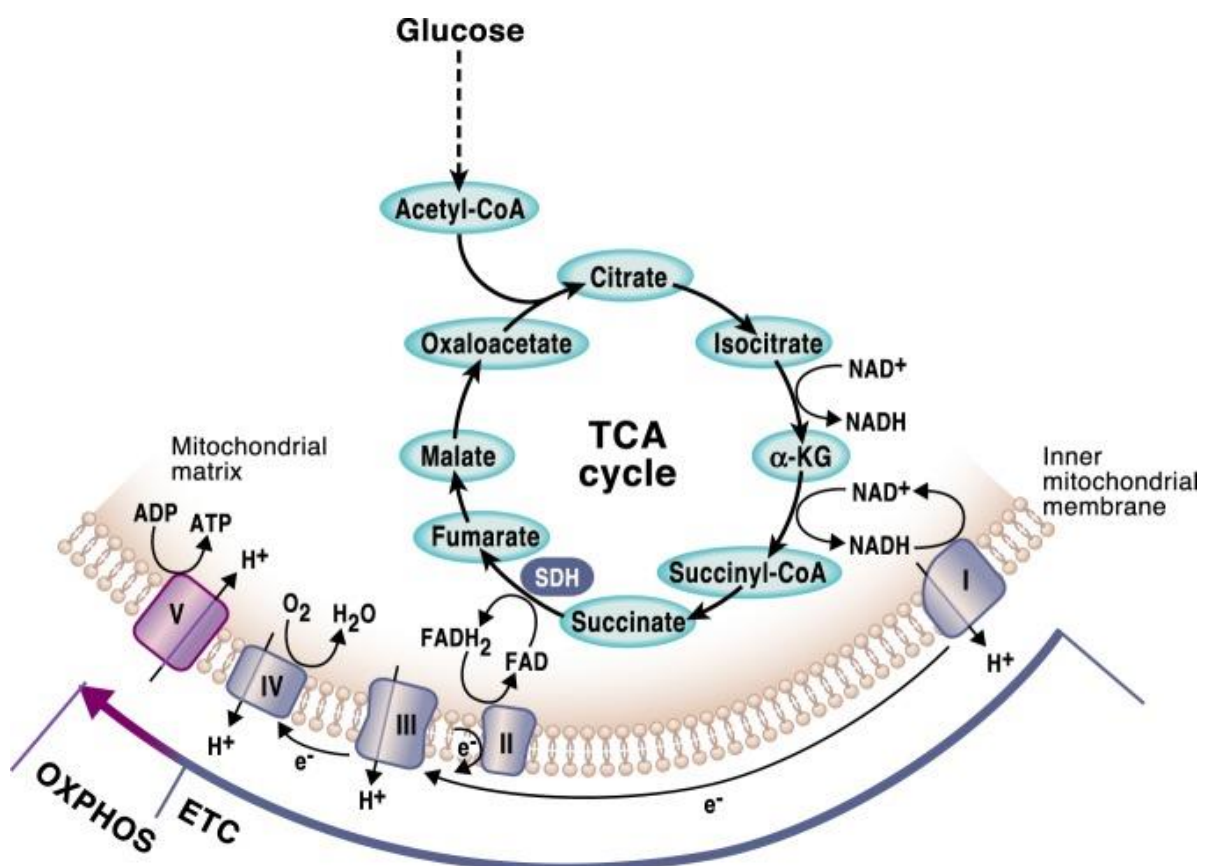


Figure 10: The citric acid cycle and oxidative phosphorylation are closely intertwined. Reactions of the TCA cycle yield NADH and FADH₂, which are required to maintain the mitochondrial respiratory chain. Complexes I and II regenerate NAD⁺ and FAD, which are required for functioning of the TCA cycle with its oxidative properties. Figure adopted from Martínez-Reyes and Chandel (2020).

Oxidation of 1 molecule NADH generates 10 protons (4 H⁺ each from complex I and III, and 2 H⁺ from complex IV) (Gnaiger 2020). Oxidation of FADH₂ yields 6 protons since it is not oxidized via complex I. Respiration of complex IV coupled to ATP generation by complex V is termed coupled respiration. Partly, however, protons in the intermembrane space can leak back through the inner membrane

instead of going by complex V (*leaking*). In absence of ADP, this proton leak reduces the proton gradient to establish electron transfer via ETS. Thus, oxygen consumption is reduced. Oxygen consumption by complex IV that is not coupled to ATP generation, but caused by proton leak, is termed uncoupled respiration. Consequently, mitochondrial oxygen consumption is a combination of coupled and uncoupled respiration (Chandel 2015). The function of each complex will be further explained in section 2.7.2. in *Materials and Methods*.

1.4. Questions of the thesis

Due to the lack of therapeutic options for the treatment of ischemic stroke and promising results in stroke research from the ketogenic diet, the question arose if BHB, given acutely as a single compound instead of being formed during ketogenesis, can have beneficial effects. In this thesis, the following questions were investigated.

Question 1: Does BHB, given exogenously reach the brain, i.e., cross the blood-brain barrier, and to what extent?

BHB is known to be able to cross the blood-brain barrier through monocarboxylate transporters. However, the kinetics (time course) of BHB entering the brain remains unknown. It was also unknown whether BHB, given acutely, changes the levels of other energy metabolites (glucose, lactate) in the brain. Therefore, a series of microdialysis experiments was performed, in which mice received a single dose of BHB and microdialysate was collected from the extracellular space of the hippocampus.

Question 2: Can isolated mitochondria utilize BHB for respiration?

The mechanism of action of BHB, to this day, is not fully understood. Some data suggest a mitochondrial mechanism of action via complex I stimulation. For this reason, in a set of experiments, BHB was added to isolated mitochondria in various concentrations and the resulting respiration was compared to the respiration caused by other complex I and complex II substrates.

Question 3: Does the administration of BHB after transient ischemia have an effect on motor functions and behavior of mice?

Prior work of this lab found the ketogenic diet to significantly improve the neurological functions of mice after transient cerebral ischemia. This finding raises the question as to whether BHB as a single dose has the same effect. Furthermore, it is unclear how long potential beneficial effects can be measured in the animals. Therefore, mice will be investigated for motor functions and behavior 24 hours, 72 hours, and 7 days after reperfusion.

Question 4: Does the administration of BHB as a single dose post ischemia affect brain mitochondria and their respiration ?

Some data suggest a mitochondrial mechanism of action of BHB, but no data exist as to how brain mitochondria react to it after transient ischemia. This question was the main scope of the present work. In this large series of experiments, mice underwent 90 minutes of transient cerebral ischemia, then the mitochondria of the impaired (ischemic) right hemisphere and the unimpaired left hemisphere were isolated and their oxygen consumption measured. Time points for measurement were 60 minutes, 24 hours, 72 hours, and 7 days after reperfusion.

Question 5: Does transient cerebral ischemia with subsequent administration of a single dose of BHB affect plasma metabolites?

Prior work of this lab found plasma metabolites to be changed after transient ischemia in mice that have been fed mice a fat-rich and carbohydrate-low diet. This finding raises the question whether this is also observable in animals that receive a single dose of BHB after 90-minute transient ischemia. Again, time points of analysis will be 24 hours, 72 hours, and 7 days after reperfusion.

2. Materials and Methods

2.1 Laboratory Animals

All experiments were performed with CD-1 mice, obtained from Charles River. The mice were 4-12 weeks old and weighed 28-40 grams. All animals were housed in the animal farm run by the Institute for Pharmacology and Clinical Pharmacy of the Goethe University Frankfurt at Campus Riedberg. Housing conditions were in line with the requirements of the GV-Solas (Gesellschaft für Versuchstierkunde, animal committee). In accordance with GV-Solas guidelines, the animals were kept at a room temperature of 20-22 °C, humidity of 40-60%, food and water *ad libitum* at a 12-hour light-dark cycle. The cages contained bedding, cellulose and tubes or rodent cottages for environmental enrichment. Each cage housed no more than six animals. All experiments were approved by the local authority (Regierungspräsidium Darmstadt) and performed in accordance with the local committee's and ARRIVE guidelines.

CD-1 mice

The CD-1 mouse is an outbred wild-type breed from Charles River (Sulzfeld, Germany). They derive from a non-inbred stock in the laboratory of Dr. de Coulon, Centre Anticancereux Romand, Lausanne, Switzerland and were adopted by Charles River in 1959.

2.2 Diets

The animals were fed the standard chow, Altromin 1324, produced by the company "Altromin Spezialfutter GmbH & Co" (Lage, Germany). After having undergone stroke, the animals received the liquid diet "ClearH2O® Recovery", produced by the company "ClearH2O" (Westbrook, Maine, USA). The composition of each diet is specified in the table below.

Table 1: Composition of diets used in experiments.

	Altromin 1324	ClearH2O® Recovery
Calories [kcal/100g]	338,6	110,9
Carbohydrates [%]	61	23,2
Protein [%]	24	0,6
Fat [%]	15	1,9

2.3 Microdialysis

2.3.1 Materials

Table 2: Materials for microdialysis probe manufacture.

Material	Manufacturer
Epoxy glue	SunChrom GmbH, Fiedrichsdorf, D
Fused silica ID 40 µm OD 105 µm	Ziemer-Chromatographie, Mannheim, D
Polysulfone membrane (haemodialysis filter FX Cor Diax 600)	Fresenius Medical Care AG & Co. KGaA, Bad Homburg, D
Cyanacrylate glue (Pattex® superglue plastic)	Henkel AG&Co. KGaA, Düsseldorf, D
TEFLON tubing 1.6 x 0.35 mm	SunChrom® GmbH, Friedberg, D
Scalpel (Feather® Surgical Blade No. 10)	pfm medical ag, cologne, D
30 G x 11" (0.3 x 25 mm) cannula Sterican® Z	B.Braun Melsungen AG, Melsungen, D
25 G x 11/2" (0.5 x 40 mm) cannula 100 Sterican®	B.Braun Melsungen AG, Melsungen, D
Fine pen (Stabilo point 88 fine 0.4)	Schwan-STABILO Schwanhäußer GmbH & Co. KG, D
Hot glue (Glue sticks ULTRA Power x 11 mm)	Steinel® GmbH, Herzebrock-Clarholz, D
Sandpaper P60 230 x 280	Robert Bosch GmbH, Gerlingen-Schillerhöhe, D

Microdialysis is a minimally invasive sampling method for extracellular spaces. It is used to collect small, water-soluble compounds, such as energy metabolites, neurotransmitters, or small pharmaceutical compounds. In this work, microdialysis was used to investigate extracellular glucose, lactate, and pyruvate concentrations. This technique was originally developed by Delgado et al. (1972) and further improved in the following decades (Lindfors et al. 1989; Lönnroth et al. 1989; Lönnroth et al. 1987). The probes can be implanted into various tissues and are afterwards perfused with fluids of similar composition as the surrounding interstitial fluid, though lacking the compounds of interest. This leads to a concentration gradient between interstitial fluid and perfusion fluid. Due to passive diffusion through a semi-permeable membrane, molecules from the surrounding tissue are collected. A compound's ability to pass the semi permeable membrane depends on its hydrophilicity or lipophilicity and size. The probes used in the experiments in this work had a molecular cut-off of 30 kDa. Cut-off is defined as the molecular weight [Da] at which 80% of the molecules are unable to pass the semi permeable membrane.

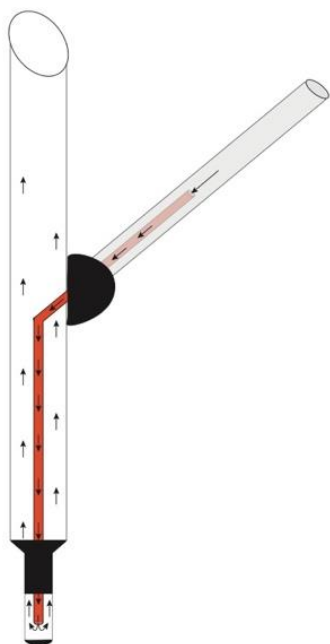


Figure 11: Schematic illustration of a microdialysis probe.

The concentration gradient is maintained by continuous perfusion with fresh aCSF, at a flow rate of 2 μL per minute. Through an outlet tip the dialysate can be collected at fixed time points and concentration changes of one or more analytes can be monitored over a course of time in the living animal. The molecular cut-off for large compounds is an advantage in so far, as the collected dialysate is very pure, thus requiring no further purification before chemical analysis.

2.3.2 Manufacture of microdialysis probes

The probes require three days to be manufactured and ready to use. Rat probes were also built for a short series of experiments. The materials are identical with those described below – only the dimensions differ.

Day 1

PTFE tubes are cut into 2.5 cm pieces. The end that will later serve as outlet is cut into an angle of about 45 degrees. Afterwards, the PTFE tubing is roughened with sandpaper to increase the adherence of the epoxy glue. Next, the fused silica is carefully cut into 2.25 cm pieces. For inserting the fused silica into the PTFE tube, a 30 G cannula is used to puncture the PTFE tubing. The fused silica is then inserted into the PTFE tubing with the cannula as guidance. After removing the cannula, the fused silica is brought into position where 5 mm protrude from the flat end. The fused silica is fixated in place using a drop of gelatinous cyanoacrylate glue at the puncture site. It is then left to harden overnight.

Day 2

Once the glue has dried, the polysulfone membrane is pulled over the fused silica with 5.5 mm protruding. Furthermore, syringes of 25G needles are cut into 1 cm long metal sleeve pieces. With a fine pen, the membrane is marked to define an exchange length of 2 mm from the end of the membrane. Next, the epoxy glue is prepared. Therefore, 30 parts of the yellow hardener must be mixed with 70 parts of the black epoxy glue. A small drop of epoxy glue (excessive amounts may clog the capillary) is used to seal the tip of the membrane using a fine needle. The joint between microdialysis membrane and PTFE tubing is also sealed with epoxy glue, using the same fine needle as before. Then the epoxy glue is applied to the membrane up until the marking point, leaving 2 mm of microdialysis membrane available for diffusion. The metal sleeve is pulled over the protruding fused silica and fixated with epoxy glue. The epoxy glue must be left to harden for at least 24 hours.

Day 3

For further stability of the probes, hot glue is applied around the bifurcation of the probes. Again, the glue must be left to harden, which, with hot glue, takes only a few minutes.

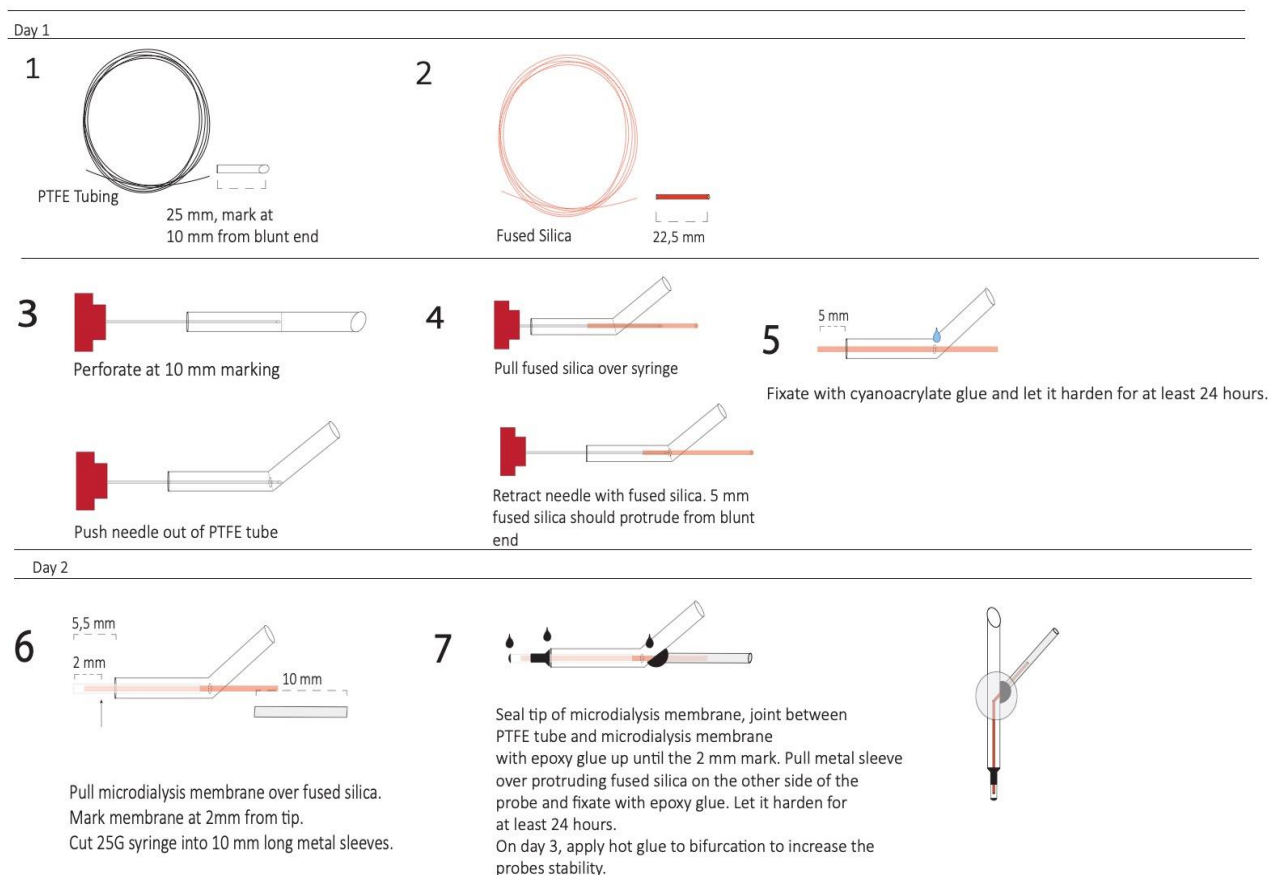


Figure 12: Schematic display of manufacture of microdialysis probes.

2.3.3 Manufacture of perfusion tubes

In order to connect the Hamilton syringe with the microdialysis probe, another tube is required as an adapter. Therefore, an 80 cm long PE tube (inner diameter: 0,28 mm, outer diameter 0,61 mm) is stuck into a 7 mm long piece of TYGON LMT-55 tube (inner diameter 0,38 mm, wall thickness 0,91 mm) roughened with an activator and glued together with cyanoacrylate glue.

2.3.4 Solution for perfusion

One hour before starting and throughout an experiment, the probes are continuously flushed with artificial cerebrospinal fluid (aCSF) at a constant flow rate. The composition is listed in the following table (table 3).

Table 3 Composition of perfusion solution.

Compound	Concentration [mM]
NaCl	147
KCl	2.7
MgCl ₂ x 6 H ₂ O	1.2
CaCl ₂ x 2 H ₂ O	1.2

Perfusion solution is prepared as bulk of 2 L, aliquoted into 50 mL falcons and stored at -20 °C until needed.

2.3.5 In vitro-recovery

The *in vitro*-recovery is needed for the determination of absolute concentrations in the cerebrospinal fluid and assessment of reproducibility of the manufacturing process. For determining the recovery, the probe is perfused with a solution that contains substances in known concentrations. The dialysate is then measured and the quotient from measured concentration and true concentration equals the recovery rate. Glucose, pyruvate and lactate were measured by means of the Iscus™, acetylcholine and choline by means of high-performance liquid chromatography (HPLC).

Equation 1: Calculation of Recovery Rate.

$$\text{Recovery rate [\%]} = \frac{c(\text{Microdialysate})}{c(\text{Recovery Solution})} \times 100$$

Table 4: Standard solution for recovery.

Compound	Concentration [μM]	Manufacturer
Acetylcholine perchlorate	0.1	Sigma-Aldrich, Taufkirchen, D
Choline chloride	10	Sigma-Aldrich, Taufkirchen, D
Glucose	1.000	Sigma-Aldrich, Taufkirchen, D
Sodium- lactate	400	Sigma-Aldrich, Taufkirchen, D
Sodium pyruvate	20	Sigma-Aldrich, Taufkirchen, D

2.3.6 Functionality check

Before implanting a probe, it must be checked for functionality, to ensure it is not damaged (clogged or torn, for example). The probes are perfused with aCSF at a flow rate of 1-2 μ L/min. Once the dialysate appears in the outlet tube, it may be implanted or stored in aCSF for up to 7 days. The aCSF prevents the membrane from drying out. All non-functioning probes are discarded.

2.3.7 Implantation of microdialysis probes in mice

Aim of the surgery is to implant a microdialysis probe into the core region of stroke, the left striatum, of the mouse brain (coordinates in table 5). Mice are sedated with isoflurane 5% in a plexiglass box. After approximately 2 minutes, the mice are transferred into and fixated in the stereotactic device. To prevent hypothermia, the animals are kept on a heating pad (set to 37 °C) at all times. Narcosis is maintained at 1-2% isoflurane through a plastic mask. Bepanthen® eye cream is applied to prevent desiccation of the eyes. After ensuring the mouse is irresponsive to a pinch between the toes of a hind leg (“interdigital reflex”) and thus in deep narcosis, the head is fixed between two pins. The fur covering the skull is then disinfected with an alcohol pad. Afterwards, an approximately 1 cm long sagittal cut is made to expose the skull. The thin skin covering the cranial bone is removed using a pointy Dumont forceps. The skull must be dry to expose the bregma, which is then marked with a felt-tip. A broken-off 25G syringe is clamped in the stereotactic device, brought into position above the bregma and the coordinates are noted. From bregma, the left striatum is reached by moving the stereotaxic instrument +0.5 mm into anterior and +2.2 mm into lateral direction (coordinates taken from Ungerstedt 1971). Again, the position is carefully marked with a fine felt-tip. A small hole is drilled at the new marking point. The dura mater is carefully punctured with a sterile syringe. Bleeding is arrested by filling the drill hole with a piece of twirled tissue. In the meantime, the cranial bone is roughened with a 1:1 mixture of a biphasic activator. The piece of twirled tissue also prevents activator

fluid from leaking into the drill hole. After allowing the activator to dry for two minutes, the probe is carefully clamped into the stereotaxic device and brought into position above the drill hole. The tissue is removed, and the probe is lowered into the hole. Once resistance increases, the probe has reached the brain tissue. From here, the probe is lowered -3.8 mm ventrally. With the probe still clamped in, light-activated dental cement (Permacem®) is applied onto the cranial bone and scalp to fixate the probe and close the wound. The light intensity of the surgery light is increased, and the dental cement is allowed to harden for a few minutes. Then, the probe can be released from the stereotaxic device. The mouse is taken out of the stereotaxic device, weighed, and brought into the microdialysis cage.

Table 5 Coordinates of left striatum from bregma.

Anterior/Posterior	Lateral/Contralateral	Dorsoventral
+ 0,5 mm	+ 2,2 mm	- 3,8mm

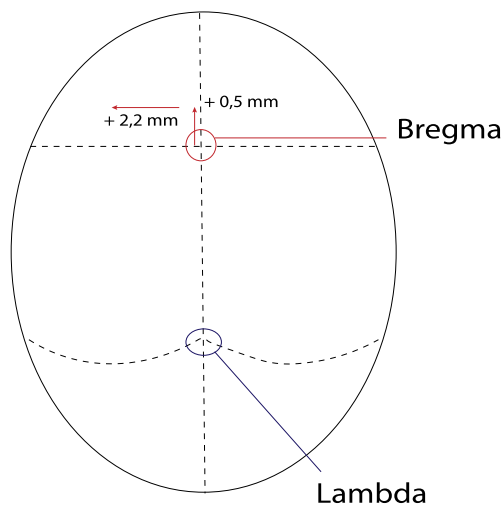


Figure 13 Implantation region in left striatum. View on mouse skull with coordinates

2.3.8 Microdialysis experiment

All microdialysis experiments are started at least 18 hours after probe implantation to let tissue damaged during the procedure heal and ensure restored integrity of the blood-brain (Benveniste and Diemer 1987) Pumps and Hamilton syringes are tested for functionality. The syringes are then filled with 1 mL of aCSF and connected to the inlet tube. The tubes are purged with aCSF at a flow rate of 10 μ L/min until liquid shows up bubble-free at the other end. The tube is then connected to the metal

sleeve inlet of the microdialysis probe. For collection of microdialysate, a 10 μL ultratip is attached to the outlet of the probe with a 3 mm long PTFE tube as connector. The flow rate is set to 2 $\mu\text{L}/\text{min}$ and the experiment is started after 30 minutes of equilibration (dialysate in the meantime is continuously discarded).

Application of β -hydroxybutyrate

Samples were collected every 10 minutes. Two samples were drawn before injection (30 minutes before). At 0 minutes, sodium β -hydroxybutyrate, dissolved in 0.9% saline solution, was applied by intraperitoneal injection. Sampling was continued until 120 minutes after injection. 15 μL of collected dialysate were pipetted into a micro inlet for borosilicate glass vials. These samples were later derivatized and were supposed to be analyzed using gas chromatography. The remaining 5 μL were transferred into microvials for analysis by CMA/Isco metabolite analyzer. All samples were kept on ice during the experiment and stored at $-80\text{ }^{\circ}\text{C}$ until further analysis.

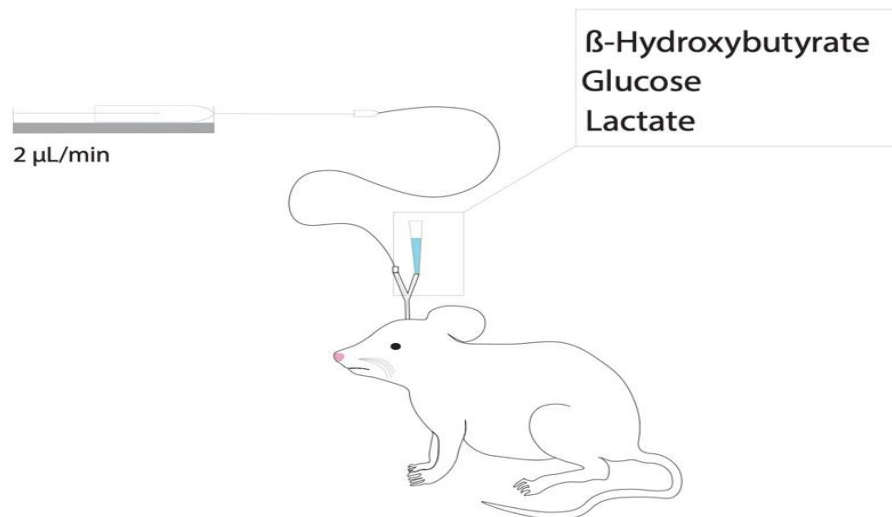


Figure 14: Illustration of microdialysis.

2.4 Transient Middle Cerebral Artery Occlusion (MCAO)

In this work, the most common stroke in humans, i.e., stroke caused by occlusion of the middle cerebral artery (MCA, *A. cerebri media*) was imitated in mice. Due to its anatomical properties, the MCA is most susceptible to infarctions in the brain (Rubiera et al. 2006; Navarro-Orozco and Sánchez-Manso 2022). Mice, having a similar anatomy of the brain arteries, are a suitable model for imitation of stroke in humans (Fluri et al. 2015). Stroke was induced according to Longa et al. (1989). This model uses a silicon-covered filament which is inserted into the carotid artery and pushed to the origin of

the MCA, blocking blood circulation for a certain time (90 minutes in this work). Later removal of the suture allows blood flow, imitating reperfusion after transient stroke. The transient model is preferable because permanent occlusion is far more harmful to the animals and would have caused substantially higher mortality rates in the experiments (Ström et al. 2013).

2.4.1 Materials

Material	Manufacturer
Bepanthen Augen- und Nasensalbe	Bayer, Leverkusen, D
Dumont Forceps	FST, Heidelberg, D
Electro Cauterie	Bovie, Clearwater, USA
Fiber Optic Light Guide	Optech Microscope Services Ltd, Oxfordshire, UK
Fine Scissors	FST, Heidelberg, D
Flow Meter for Anesthesia Pump	Porter Instruments, Hatfield, USA
Homeothermic blanket with flexible probe	Harvard Apparatus, Holliston, USA
Laser Doppler	Moore Instruments, Devon, USA
Silicone covered Monofilament Ø0,25 mm	Doccol, Redlands, USA
Silk Suture Thread, non-sterile	FST, Heidelberg, D
Spring Scissors 2mm	FST, Heidelberg, D
Tissue Forceps	FST, Heidelberg, D
Vetflo™ Vaporizer Anesthesia System	Kent Scientific Corporation, Torrington, USA
Wound Suture Clip & Applying Forceps	FST, Heidelberg, D

2.4.2 MCAO surgery

The animal is weighed immediately before undergoing surgery. It is then anesthetized with isoflurane 5% in a plexiglass box. After approximately two minutes it is taken out of the box and transferred onto the heating pad (preheated to 37 °C) which is covered with surgical drapes. Narcosis is maintained at 1.5-2% through a plastic mask. The mouse is given an intraperitoneal injection of 0.1 mg/kg buprenorphine and Bepanthen eye cream is applied to prevent desiccation of the eyes. Once the mouse is in deep narcosis, ensured by testing the interdigital reflex, the mouse is placed on the surgery pad lying on its belly. The scalp is cut open to expose the bregma and with the stereotactic device, the position of the striatum is located. The location is marked, and cerebral blood flow is measured by means of the Laser-Doppler. The mouse is then placed backside down on the surgery pad and the paws are fixated with Velcro® to expose the chest and neck. The fur is disinfected and shortened. A

sagittal incision of about 1.5 cm is made at the neck, the subcutaneous fat and sternocephalic muscle are pulled apart and all is retracted with sterile clips. From this point on, every part of the procedure is done using an operating microscope. Beneath the retracted tissue lies the trachea which is also carefully moved to the right side. Moving of the trachea exposes the common carotid artery. It is carefully dissected with Dumont forceps and reversibly ligated with a silk suture. The artery is further prepared upward, exposing the larynx, until the external carotid artery (ECA) is exposed. The internal carotid artery (ICA) is below the ECA and cannot be seen directly. ECA and ICA are also ligated. At this step, the tissue must be prepared very cautiously to not damage the vagus nerve. Once all branches of the carotid artery are ligated, a small cut is made into the external carotid artery with very fine spring scissors and a silicon-covered monofilament (0.25 mm diameter) is placed in the ECA. It is fixated with a silk suture. Next, the reversible ligation of the ICA is undone, the ECA is cut through entirely and the upper stump is cauterized. The now loose ECA stump containing the filament is turned 180 degrees, so the filament can be pushed upwards into the ICA. The filament is carefully and slowly pushed up until approximately 1 cm of filament is left outside the ECA. The silk suture is pulled tighter to keep the filament in place. Then the reversible ligation of the CCA is undone and blood flow is allowed. The wound retractors are removed, and the wound is closed with a wound clip. Cerebral blood flow is measured with the Laser-Doppler to ensure that filament is blocking the MCA. Blood flow should be reduced by at least 80%.

In a small, single housing cage, the mouse is allowed to wake up and move around freely for 90 minutes. After 90 minutes, the mouse is sedated once again, the wound is reopened, CCA ligated and the suture removed, thus allowing reperfusion of the MCA. The ECA stump is then cauterized. The wound is closed with two wound clips. Cerebral blood flow is measured once again to prove reperfusion and should be >60% of the original blood flow. At the end of the experiment (60 minutes, 24 hours, 72 hours, or 7 days after reperfusion) the animal is sedated with isoflurane and then euthanized.

2.4.3 Sham Surgery

Sham surgeries are performed identically, except that the suture is not inserted in the artery.

2.4.4 Post-surgical treatment

Mice were given 1 mL lactated Ringer's solution i.p. immediately after reperfusion to compensate for fluid and energy loss while undergoing surgery and inability to chew after having suffered from stroke. The i.p. injection of lactated Ringer's solution was repeated the next three days. After surgery the animals were kept under red light to restore body temperature that may have been lost during the

procedure. Throughout the experiment, all animals were kept in single housing cages. Buprenorphine (0.1 mg/kg i.p.) was administered twice a day until three days after stroke. Recovery, i.e., weight development, eating behavior, wound healing, general behavior, overall condition, and neurological condition were recorded on score sheets at least twice a day.

2.5. Treatments

2.5.1 Treatment with β -hydroxybutyrate

After reperfusion the treatment group was treated with a sodium β -hydroxybutyrate solution. The vehicle for the 4.5 mg/mL solution was 0.9% saline solution. The animals received a single sodium β -hydroxybutyrate dosage of 30 mg/kg bodyweight immediately after reperfusion.

2.5.2 Control group

The control group received 0.2 mL of 0.9% saline solution once immediately after reperfusion.

2.6 Behavioral studies

The behavioral studies were performed to assess the animals' motoric abilities before and after stroke, as well as the influence of the treatment with β -hydroxybutyrate. The tests employed in this work were designed for stroke research as they enable the evaluation of impaired motion under the influence of hemiparesis (Bouët et al. 2007). Preliminarily, the extent of stroke can also be evaluated visually – general symptoms are unkempt fur, swelling of the right eye, right bound posture, and unilateral movement to the right.

Each mouse was trained to do the behavioral tests for three days prior to MCAO.

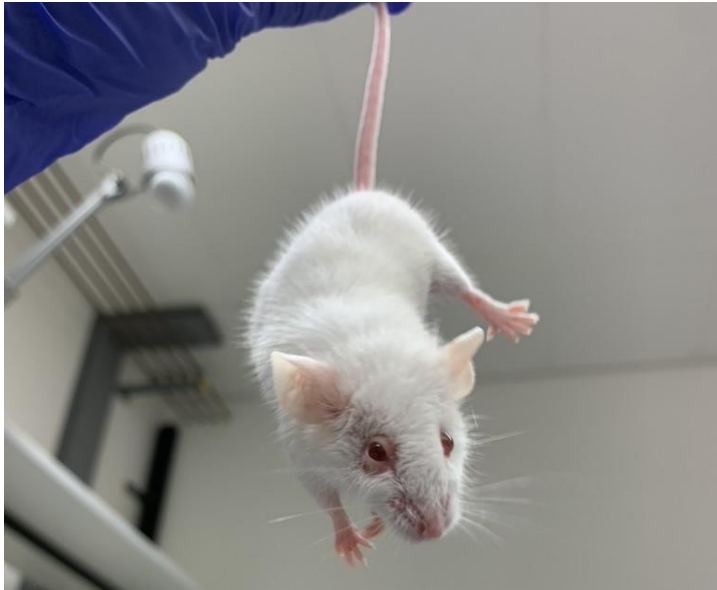


Image 2: Mouse after 90 minutes MCAO.

2.6.1 Corner Test

The corner test is an experiment for measuring the extent of the unilateral movement. If an impaired mouse is put into a narrow corner (30°), it is most likely to turn unilaterally to the right, whereas an unimpaired mouse will turn to both sides randomly. The mouse was allowed to do 10 turns. The turns to the left and right were noted, and the laterality index was calculated modified from Bouet et al. 2007. If the animal did not move at all, the experiment was stopped. In the present work, right turns were deducted from left turns after a total of 10 turns.

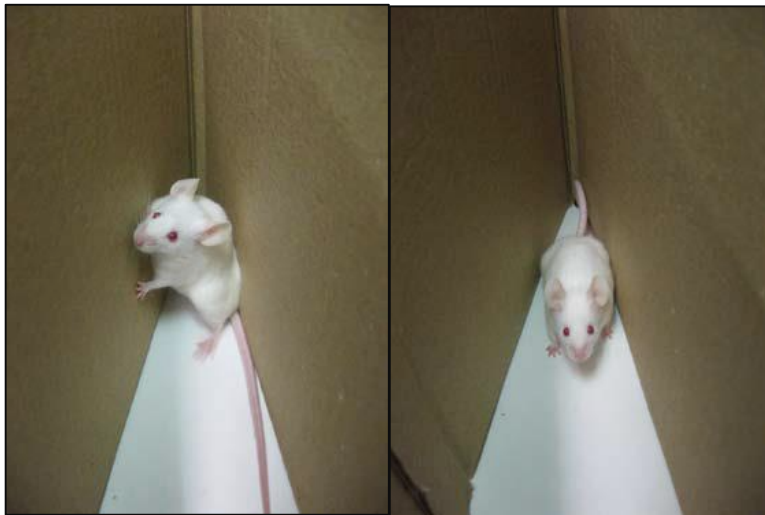
For unimpaired animals, the expected value is 0 since they move equally in both directions. If an animal turns unilaterally to the left, it results in a value of 10. Unilateral turns to the right equal a value of -10.



1. Corner test setup

2. Mouse moves into corner

3. Mouse stands up



4. Turn to left

5. Turn complete

Image 3: Corner test. Images modified from Tina Schwarzkopf (2015)

2.6.2 Rotarod

In the Rotarod experiment, the mouse is placed on a rotating axle on which it is supposed to walk (image 4). At the beginning the Rotarod spins at 5 rpm and it continuously accelerates to 40 rpm in the following 60 seconds. The time in which the animal walked on the spinning axle without falling off was noted. In this time, the mouse was allowed once to turn around and walk backwards for a few seconds before turning back into the right direction. If it turned more than once or clenched to the axle and thus started rotating, the experiment was stopped and did not count.



Image 4: Mice on rotarod.

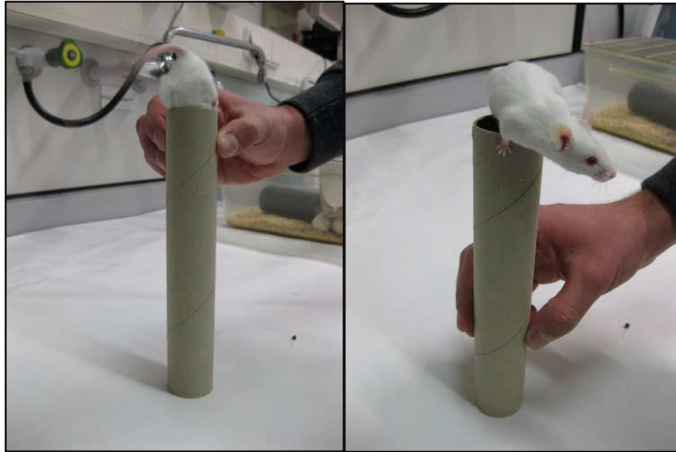
2.6.3 Chimney Test

In the chimney test the mouse walks into a tube of 20 cm length and 4 cm width. Once it reaches the end, the tube is tipped 90 degrees to stand on the table vertically. Motorically impaired animals have difficulties crawling backwards up to the top of the tube. The experiment was stopped if an animal did not reach the top of the tube within 60 seconds.



1. Mouse crawls into tube

2. Tube must be set upright



3. Mouse crawls out backwards, time is recorded.

Image 5: Chimney test setup. Modified from Tina Schwarzkopf (2015)

2.7 Mitochondrial Respiration

2.7.1 Instruments and materials

Table 6: Oxygraph instruments and chemical compounds for the oxygraph.

Instrument	Manufacturer
Oroboros Oxygraph O2k	Oroboros instruments, Innsbruck, AT
Potter homogenisator Typ Potter S	B.Braun, Melsungen, D
Milli-Q Academic Water Filter System	Merck Millipore, Darmstadt, D
Beckman Microfuge R	Beckmann & Coulter GmbH, Krefeld, D
Surgical tools	Fine Science Tools, Heidelberg, D
Water bath GFL	Thermolab, Ulm, D
Compound	Manufacturer
HEPES (2-[4-(2-Hydroxyethyl)-1-piperazinyl]-ethansulfon)	Merck (Sigma Aldrich), Darmstadt, D
DTNB (5,5'-dithiobis-(2-nitrobenzoesäure)	Merck (Sigma Aldrich), Darmstadt, D
ADP (Adenosindiphosphat)	Merck (Sigma Aldrich), Darmstadt, D
Antimycin A	Merck (Sigma Aldrich), Darmstadt, D
BioRad reagent A+B	Merck (Sigma Aldrich), Darmstadt, D
BSA (bovine serum albumin)	Merck (Sigma Aldrich), Darmstadt, D
CaCl ₂ x 2 H ₂ O	Merck (Sigma Aldrich), Darmstadt, D
FCCP (Fluoro-carbonyl-cyanide-p-trifluoromethoxy-phenylhydrazone)	Merck (Sigma Aldrich), Darmstadt, D

Citrate synthase	Merck (Sigma Aldrich), Darmstadt, D
Cytochrom C	Merck (Sigma Aldrich), Darmstadt, D
Ethanol > 99%	Merck, Darmstadt, D
EGTA (Ethylenglycol-bis(2-aminoethylether)-N,N,N',N'-tetraacetic acid)	Merck (Sigma Aldrich), Darmstadt, D
Glucose x H ₂ O	Merck (Sigma Aldrich), Darmstadt, D
Monopotassium phosphate	Merck, Darmstadt, D
Potassium lactobionate	Merck (Sigma Aldrich), Darmstadt, D
Water-bath GFL	Thermolab, Prèverenges, CH
TMPD (N'-N'-N'-N'-Tetramethyl-p-phenyldiamine-dihydrochlorid)	Merck (Sigma Aldrich), Darmstadt, D
Sodium ascorbate	Merck (Sigma Aldrich), Darmstadt, D
Sodium azide	Merck (Sigma Aldrich), Darmstadt, D
Sodium chloride	Merck (Sigma Aldrich), Darmstadt, D
Sodium malate	Merck (Sigma Aldrich), Darmstadt, D
Sodium pyruvate	Merck (Sigma Aldrich), Darmstadt, D
Sodium succinate	Merck (Sigma Aldrich), Darmstadt, D
Oligomycin	Merck (Sigma Aldrich), Darmstadt, D
Sodium oxaloacetate	Merck (Sigma Aldrich), Darmstadt, D
Protease inhibitor cocktail complete	Roche, Basel, CH
Rotenone	Merck (Sigma Aldrich), Darmstadt, D
Sucrose (Saccharose)	Merck, Darmstadt, D
Hydrochloric acid 37%	Merck, Darmstadt, D
Taurine	Merck (Sigma Aldrich), Darmstadt, D

2.7.2 Basics

In the cell, energy is generated through glycolysis in the cytosol, where glucose is broken down to pyruvate. Pyruvate is then transported into the mitochondrial matrix, where it is transformed to acetyl-CoA via oxidative decarboxylation. Acetyl-CoA is the starting compound of the citric acid cycle. Alternatively, acetyl-CoA can be generated through degradation of fatty acids (β -oxidation). The citric acid cycle takes place within the mitochondrial matrix and yields NADH + H⁺, as well as FADH₂, which are fed into the mitochondrial respiration chain. This leads to generation of ATP via proton motive force. The function of each complex (I-V) of the respiration chain is shortly explained below and schematically shown in figure 15.

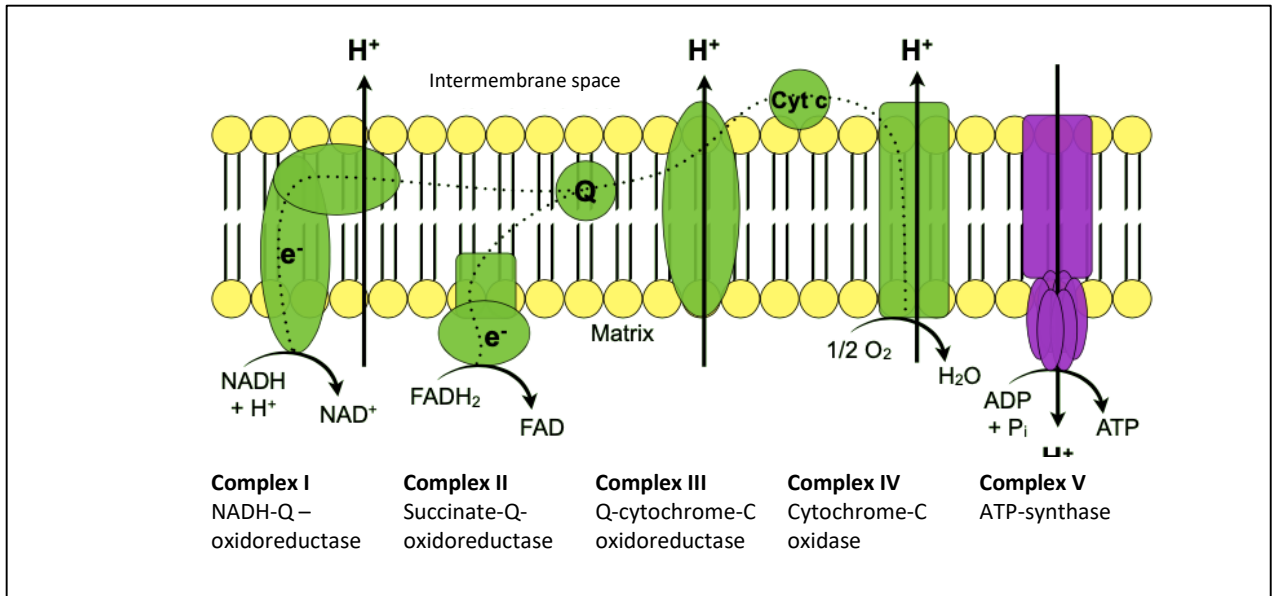
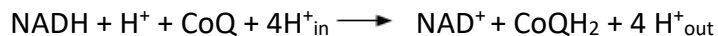


Figure 15: Mitochondrial respiratory chain. Figure modified from Tina Schwarzkopf (2015)

Complex I

Complex I, as all other complexes, is located within the inner mitochondrial membrane, which separates mitochondrial matrix and intermembrane space. Complex I reactions of mitochondrial respiration are catalyzed by NADH-Q-oxidoreductase. It transfers two electrons from $\text{NADH} + \text{H}^+$ to coenzyme Q (CoQ). Via Q, electrons are transported to cytochrome c oxidoreductase (complex III). Besides, complex I transports four protons into the intermembrane space against the gradient.



Complex II

The enzyme that catalyzes complex II reactions, succinate-Q-reductase, reduces succinate to fumarate. Thereby, one electron is transferred from FADH_2 to coenzyme Q, which again feeds electrons into complex III.

Complex III

The electrons yielded from complex I and complex II are fed into the cytochrome-c oxidoreductase, complex III, and emitted to cytochrome C (cyt C) in the intermembrane space. Simultaneously, four protons are pumped into the intermembrane space.

Complex IV

The cytochrome-c oxidase (complex IV) takes up cytochrome C (cyt C) from the intermembrane space and oxidizes it. Conversely, the reaction from O₂ to H₂O is catalyzed. Thus, electrons are scavenged, and another two protons are pumped into the intermembrane space.

Complex V

The ATP-synthase (complex V) catalyzes the phosphorylation of ADP to ATP.

In this work, mitochondrial respiration was analyzed through stimulation and inhibition of the complexes I to IV, thus determining the impact of each complex on respirational activity. For this type of analysis mitochondria must be free of other cell components and dependent on externally added substrates. This is reached through the centrifugation protocol described in section 2.7.3. Mitochondrial respiration is measured in isolated mitochondria. Substrates and inhibitors are added in abundance to prevent effects caused by shortness of agents. The Oxygraph-2k system (Oroboros Instruments, Innsbruck, Austria) has two inert chambers in which oxygen consumption is measured over the course of time and after addition of substrates, uncouplers and inhibitors. The protocol by which substrates, uncouplers and inhibitors are added goes by the name "SUIT protocol".

Table 7: Summary of all substrates, uncouplers and inhibitors, as well as their function.

Substrate	Function	Effect
Pyruvate and malate	Substrate complex I	Stimulation of complex I
ADP	Substrate ATP synthase	Maximum coupled respiration with ATP generation under electron flow via complex I
Succinate	Substrate complex II	Maximum coupled respiration with ATP generation under electron flow via complex I and complex II
Cytochrome C	Substitution of possible cytochrome C loss through membrane damage, quality control for mitochondrial membrane integrity.	Maximum coupled respiration with ATP generation under electron flow via complex I and II and under substitution of possibly lost cytochrome C.
FCCP	Uncoupler	Complexes I to IV work at maximum capacity.
Rotenone	Inhibitor complex I	Uncoupled complex II respiration becomes visible.

Oligomycin	Inhibition ATP synthase	The remaining leak respiration is caused by 1) compensation of proton leakage at maximum membrane potential and 2) leakage of electrons and protons, causing the generation of ROS
Antimycin	Inhibition of complex III	The remaining respiration is caused by ROS and proton leakage.
TMPD	Artificial electron donor	Maximum (fictive) complex IV respiration
Ascorbate	Regeneration of TMPD	
Sodium azide	Inhibition of complex IV	Measured respiration is caused by autoxidation of the electron donor.

Respiratory steady states

For a better understanding of the experimental procedure and its results, the different respiratory steady states (fig. 17) are explained in the following paragraph.

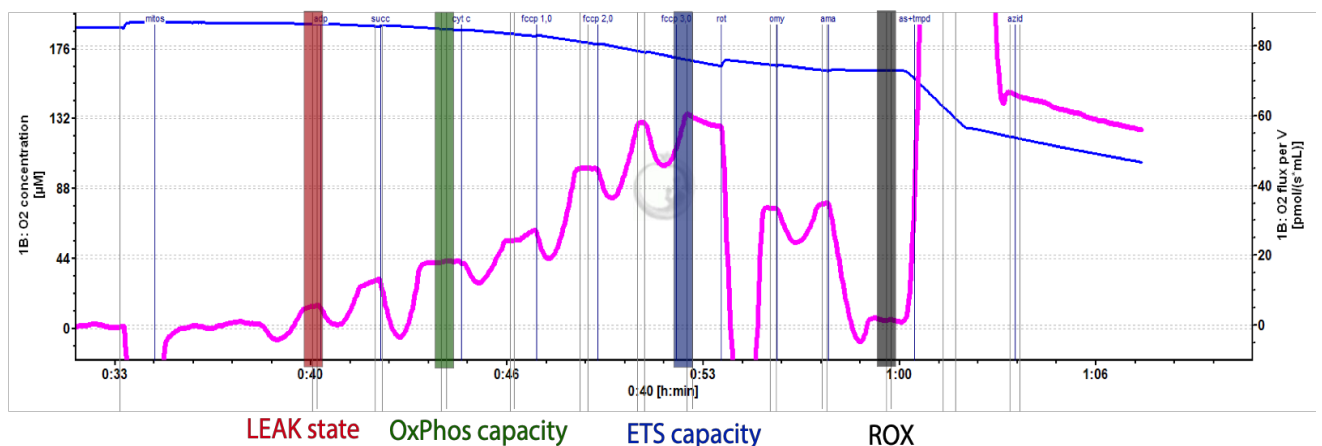


Figure 16: Respiratory states of mitochondria.

LEAK states

Leak respiration is a term for oxygen consumption without contributing to ATP generation, leading to heat production. It is a type of respiration that has compensating functions for the loss of protons or electrons in the course of ROS production. Mitochondrial leak respiration occurs either in presence of substrates and absence of ADP, in presence of ATP, or after inhibition of phosphorylating enzymes (Gnaiger et al. 2020).

OxPhos capacity

OxPhos capacity is measured through addition of complex I-linked substrates, ADP, and succinate. It is the maximum respiratory capacity of mitochondria, activated by sufficient concentrations of ADP,

inorganic phosphate and oxygen. Oxidative phosphorylation is coupled to flux of protons, pumped out of the matrix by complexes I, II and IV. The force established by proton flux drives ADP phosphorylation. OxPhos capacity, when measured, is usually corrected for residual oxygen consumption (ROX), when all activity of oxidative phosphorylation is inhibited, which is in this work reached through addition of rotenone and antimycin A (Gnaiger et al. 2020).

ETS Capacity

ETS capacity is measured by uncoupling the phosphorylation system from proton flux. Therefore, the protonophor FCCP is added to the isolated mitochondria. Respiration is thus uncoupled from the intrinsic proton flux, as there are limitless amounts of protons available.

ROX

As mentioned above, residual oxygen consumption is evaluated by inhibition of all activity of oxidative phosphorylation – in this work by addition of rotenone and antimycin A. Residual oxygen consumption is subtracted from all other respirational activity.

2.7.3 Preparation

Table 8: Substrates, uncouplers, inhibitors and their solvents for the SUI protocol of the oxygraph.

Substance	c [mM]	Preparation	Note/storage
Pyruvate	2000	22 mg/ 0.1 mL H ₂ O	Susceptible to decarboxylation. Prepare new every day.
Malate	400	536 mg/ 10 mL H ₂ O	Neutralize with 10 M KOH solution. Aliquot to 0.5 mL portions. Store at -20°C.
ADP	500	501 mg/ 2 mL H ₂ O	Neutralize with 0.45 mL of 5 M KOH. Aliquot to 0.2 mL portions. Store at -80°C.
Succinate	1000	2.701 g/ 10 mL H ₂ O	Aliquot to 0.2 mL portions. Store at -20°C.
Cytochrome C	4	50 mg/ mL H ₂ O	Aliquot to 0.2 mL portions. Store at -20°C.
FCCP	1	2.54 mg/ 10 mL EtOH	Aliquot to 0.2 mL portions in brown glass vials. Store at -20°C.
Rotenone	1	3.94 mg/ 10 mL EtOH	Photosensitive. Store at -20°C.
Oligomycin	5	4 mg/ 1 mL Ethanol	Highly toxic. Aliquot to 0.2 mL portions. Store at -20°C.
Antimycin	5	11 mg/ 4 mL Ethanol	Highly toxic. Aliquot to 0.2 mL portions. Store at -20°C.
Ascorbate	800	1.584 g/ 10 mL	Set pH to ~6 with ascorbic acid to prevent auto-oxidation (137.6 mg/mL). Photosensitive. Store at -20°C.

TMPD	200	47.4 mg/ mL H ₂ O	Add 0.8 M ascorbate (final concentration 10 M) to prevent auto-oxidation. Aliquot to 0.2 mL portions. Store at -20°C.
Azide	4000	260 mg/ mL H ₂ O	Highly toxic. Aliquot to 0.5 mL portions. Store at -20°C.

All steps of the experiment, from storage of the brain to injection of isolated mitochondria into the chambers, are done in respiratory medium MIR05 or MIR05+ PI (see section [2.8.3](#))

Table 9: Composition of MIR05 respiratory medium.

Substance	Amount per liter
EGTA	0.19 g
MgCl ₂ x 6 H ₂ O	0.61 g
Potassium lactobionate	120 mL of 0.5 M potassium lactobionate stock
Taurine	2.5 g
KH ₂ PO ₄	1.36 g
HEPES	4.77 g
Sucrose	37.65 g
BSA	1.0 g
Ultrapure water (Milli Q®)	ad 1000 mL

Preparation of potassium lactobionate stock: Dissolve 35.83 g of lactobionic acid in 10 mL ultrapure water and adjust pH to 7.0 using potassium hydroxide platelets (approximately 20). Afterwards, the volume is filled up to 200 mL and again, the pH is adjusted to 7.0. The other weighed-in substances are dissolved in ultrapure water in a 1 L flask. 120 mL of lactobionate solution are added, the volume is filled up to 1 L and pH is adjusted to 7.1 using 1N HCl or 1N NaOH. The resulting solution is aliquoted into 50 mL falcons® and stored at -20°C.

To prepare MIR05 + PI, one tablet of cOmpete protease inhibitor cocktail (PI) is added to 50 mL MIR05. Aliquoted to 8 mL in 15 mL falcons®, MIR05 +PI can be stored for up to 3 weeks at -20°C.

Isolation of mitochondria

Mice are deeply anesthetized with isoflurane 5% and then decapitated. The skull is cut open and the brain removed. The cerebellum and olfactory bulb are removed from the rest of the brain and discarded. The hemispheres are separated and weighed into two labelled test tubes containing 0.5 mL

ice-cold MIR05+PI. The weight of the hemispheres should be between 80 - 120 mg for optimum respiration (note weight). The hemispheres are then transferred into 2 mL Potter tubes containing 1 mL ice-cold MIR05 + PI. The hemispheres are homogenized with 13 strokes of the Potter homogenizer at 700 rpm. The homogenate is transferred into labelled 2 mL Eppendorf tubes. Next follows the isolation protocol (at 4°C).

1. Centrifuge for 7 minutes at 1.400 g.
2. Transfer supernatant into new 2 mL Eppendorf tube. Centrifuge for 3 minutes at 1.400 g.
3. Transfer supernatant into new 2 mL Eppendorf tube. Centrifuge for 5 minutes at 10.000 g.
4. Mitochondria are now in pellet. Discard supernatant and resuspend pellet in 1 mL MIR05 + PI. Centrifuge for 3 minutes at 1.400 g.
5. Transfer supernatant into 1.5 mL Eppendorf tube. Centrifuge for 5 minutes at 10.000 g.
6. Discard supernatant. Resuspend mitochondria pellet in 250 µL MIR05 + PI.

For analysis of mitochondria, 80 µL are injected into the oxygraph chambers (image 6). The residue is shock-frozen in liquid nitrogen and stored at -80 °C for citrate synthase and protein determinations.

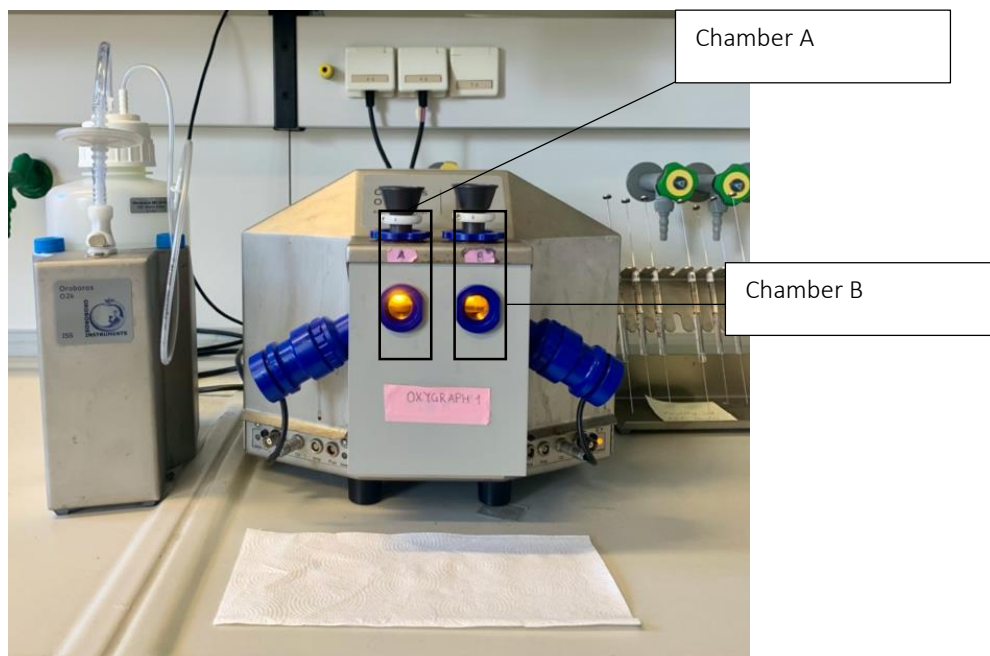


Image 6: Oroboros Oxygraph

2.7.4 Experimental procedure

Before each experiment, the chambers are washed three times with water and then filled with 2.4 mL MIR05. It is left open to equilibrate at 37 °C. In that time the oxygen partial pressure in MIR05 equilibrates to the partial pressure of air. After step 1 of the centrifugation protocol the chambers are closed. 80 µL of mitochondrial suspension are injected into the chambers – 90 µL are mounted into the syringe and the remaining 10 µL are injected back into the Eppendorf tube before freezing. The chambers are left to equilibrate again for a few minutes. Then the Substrate-Uncoupler-Inhibitor-Titration (SUIT-) protocol is started. Each injection of compounds is done after a short time of equilibration (except steps 1 and 9), when O₂ flux shows a plateau and thus stable respiration.

1. Addition of 5 µL pyruvate and 5 µL malate. These substances are complex I substrates. Because complex I needs ADP, which is not available in the mitochondrial suspension, the resulting respiration is not complex I, but leak respiration that occurs in the absence of ADP (non-phosphorylating respiration due to inactive ATP-synthase).
2. Addition of 8 µL ADP. After adding ADP, all complex I related pathways can be measured (CI).
3. Addition of 20 µL succinate, the substrate of complex II (CII). Maximum physiological respiration can be determined by addition of Complex I + Complex II respiration.
4. Addition of 5 µL Cytochrome C. This step is performed to control the integrity of mitochondria. Usually, an experiment is stopped when respiration gain exceeds +10%. In this work, values up to 20% were accepted, as mitochondrial damage is among the results caused by stroke.
5. Addition of 3 µL FCCP in three steps (1 µL at each step). 3 µL were the empirical observation at which respiration does not further increase. This respirational activity is the ETS capacity, the maximum capacity of the electron transfer system. The maximum ETS activity depends on how fast NADH and FADH₂, both reduction equivalents of the TCA cycle, can be fed into the electron transfer system. It also depends on the efficiency of electron transfer in each complex.
6. Addition of 5 µL rotenone: Inhibition of complex I. Isolated complex II respiration is visible after inhibiting complex I respiration.

7. Addition of 1 μL oligomycin (omy). Omy is an inhibitor of ATP-synthase – respiration measured afterwards is thus again leak respiration. After equilibration the chamber is opened for reoxygenation until the oxygen concentration in the chamber is as high as at the beginning of the experiment.
8. Addition of 1 μL antimycin A: inhibition of complex III. Due to inhibition of complex III, proton flux from matrix into intermembrane space is interrupted. Consequently, the entire respiratory chain arrests. In this step the residual oxygen consumption is measured (ROX), i.e. the oxygen consumption independent of mitochondrial activity.
9. Addition of 5 μL TMPD and 5 μL ascorbate. TMPD is an electron donator for Cytochrome C and ascorbate is added for regeneration of TMPD. By adding an infinite source of electrons, a fictive maximum complex IV capacity is obtained.
10. Addition of 60 μL azide: respiration arrests. The chambers are then opened to regain original oxygen concentrations. Later, the oxygen consumption after addition of azide is subtracted from complex IV respiration.

As baseline, ROX respiration is subtracted from all other respiration parameters. An exemplary respiratory measurement according to the SUIT protocol is shown below.

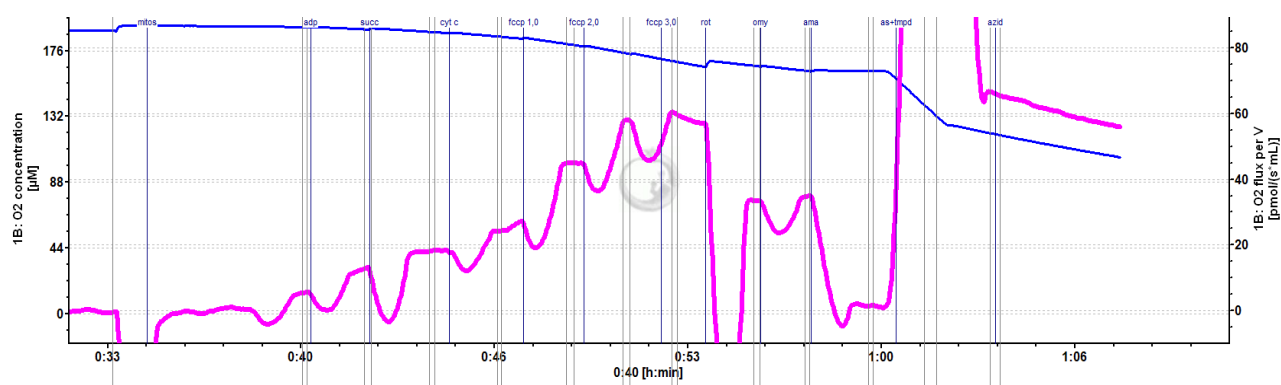


Figure 17: Example of a respiratory analysis of isolated mouse mitochondria. The blue line shows the oxygen concentration and the pink line shows oxygen consumption. Abbreviations: **mitos** injection of mitochondria, **p+m** addition of pyruvate and malate, **adp** addition of ADP, **succ** addition of succinate, **cyt c** addition cytochrome C, **fcp** addition of carbonylcyanid-p-trifluoromethoxyphenyl-hydrizon, **rot** addition of rotenone, **omy** addition of oligomycin, **ama** addition of antimycin, **as+tmpd** addition of ascorbate and tetra-methyl-p-phenylendiamine, **azid** addition of azide.

2.8 Determination of citrate synthase activity

2.8.1 Instruments and materials

Instruments and materials	Manufacturer
Ethanol 70% (for rinsing cuvettes)	Merck (Sigma Aldrich), Darmstadt, D
Pipette tips (filtered)	Nerbe plus GmbH, Winsen, D
Quartz cuvette (1mL)	Hellma Analytics, Müllheim, D
Reaction tube (1.5 mL)	Greiner Bio-One GmbH, Kremsmünster, AT
Spectronic® Genesys 5	Thermo Fisher Scientific, Waltham, MA, USA
Ultrapure water (Milli Q®) (for rinsing cuvettes)	Merck Millipore, Darmstadt, D
Vortex mixer, lab dancer	VWR, Darmstadt, D
Water bath	Thermolab, Prèverenges, CH

Buffers and solutions

The following solutions and buffers were prepared monthly and stored either at 4 °C or -20 °C (see notes).

Compound	Concentration [mM]	Note/Storage
Acetyl-CoA	12.2	10 mg/mL ultrapure water. 250 µL aliquots. Store at -20 °C. Store on ice during experiment.

Compound	Concentration [M]	Note/Storage
Triethanolamine	0.5	4,03 g/ 50 mL ultrapure water

HCl 37% Set pH to 8,0

EDTA 0.05 93,05 mg

Store at 4 °C.

Compound	Concentration [M]	Note/Storage
Tris(hydroxymethyl) ethanolamine	0.5	2 mL of 1M Tris-HCl buffer/ 20 mL ultrapure water.
HCl 37%		Set pH to 7,0 Store at 4 °C.

Compound	Concentration [mM]	Note/Storage
Triton X-100 (100%) nonionic tenside	12.2	10 mg/mL ultrapure water. 250 µL aliquots. Store at -20 °C. Store on ice during experiment.

The following solutions were prepared freshly on the day of experiment.

Compound	Concentration [mM]	Note/Storage
Triethanolamine-HCl buffer	0.1	1.2 mL of 0.5 M triethanolamine-HCl buffer + 4.8 mL ultrapure water.

Compound	Concentration [mM]	Note/Storage
CS standard		2 µL CS standard and 998 µL of 0.1 M triethanolamine- HCl buffer.

Compound	Concentration [mM]	Note/Storage
DTNB	1.01 mM	4 mg/ 10 mL 0.1 triethanolamine- HCl buffer.

Compound	Concentration [mM]	Note/Storage
Oxaloacetate	10 mM	7.8 mg/ 6 mL 0.1 triethanolamine- HCl buffer.

2.8.2 Principle

As the citrate synthase (CS) catalyzes the first and rate-limiting step of the citric acid cycle, it is a suitable quantitative marker for intact mitochondria. It is located within the mitochondrial matrix and catalyzes the condensation of acetyl-CoA and oxaloacetate to citrate.

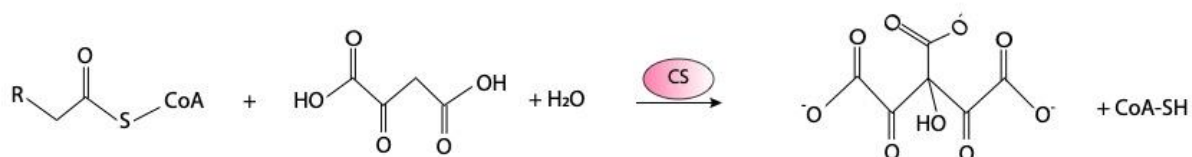


Figure 18: First reaction of citric acid cycle. Citrate synthase catalyzes condensation of acetyl-CoA and oxaloacetate to citric acid.

In the experiment this reaction is coupled to an irreversible chemical reaction in which the thiol group of CoA-SH reacts with 5,5'-dithio-bis-2-nitrobenzoic acid (DTNB, Ellman's reagent). The reaction yields quantitative amounts of 2-nitro-5-thiobenzoate (TNB⁻), which deprotonates to the yellow compound TNB²⁻ in neutral or alkaline solutions. The absorption maximum of TNB²⁻ is at 412 nm wavelength, which makes it quantifiable in an UV-spectrophotometer.

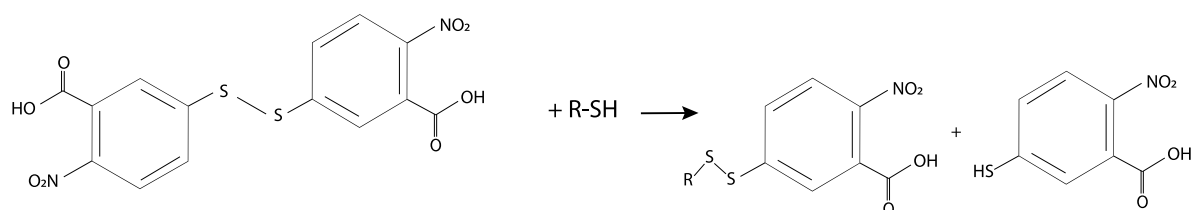


Figure 19: UV spectrophotometrically quantifiable reaction of DTNB and CoA-SH

Citrate synthase activity was determined in isolated mouse mitochondria according to protocol of Oroboros Instruments (Innsbruck, Austria). Mitochondria suspension used in this experiment was earlier used for respiration measurement and stored at -80 °C until needed for measuring citrate synthase activity. All solutions and buffers were stored on ice during the experiment.

2.8.3 Experimental procedure

Before measuring citrate synthase activity in mitochondria,

- 1 mL blank MIR05 (not containing incubation medium),
- 5 µL citrate synthase standard in incubation medium
- And 5 µL citrate synthase standard replica in incubation medium

must be measured.

Incubation medium is prepared in 1.5 mL Eppendorf tubes in a certain order.

1. 795 µL ultrapure water
2. 100 µL DTNB (1.01 mM)
3. 25 µL Triton-X-100 (10%)
4. 50 µL oxaloacetate (10 mM)
5. 25 µL acetyl-CoA (12.2 mM)

The mixture is homogenized with a vortex mixer and incubated at 37 °C for 5 minutes. Then, 10 µL of the mitochondria suspension are added. The mixture is vortexed once again, filled into a quartz cuvette and immediately measured for 200 seconds at a wavelength of 412 nm in the spectrophotometer. The mean value of 2 measurements is calculated. If the values are apart more than 0.005 min⁻¹, citrate synthase activity is measured once more and the mean value is used for calculation of enzyme activity.

Equation 2: Calculation of enzyme activity.

$$v = \frac{rA}{l * \epsilon B * v} * \frac{V_{cuvette}}{V_{sample} * p}$$

v = Enzyme activity [IU= µmol*min⁻¹]

rA = Change of absorption rate [min⁻¹]

l = Optical path length (1 cm)

εB = Extinction coefficient of TNB in the reaction (13.6 mM⁻¹ * cm⁻¹)

v_B = Stoichiometric number of TNB in the reaction (1)

V_{cuvette} = Total volume of solution in cuvette (1000 μL)

V_{sample} = Volume of sample (10 μL)

ρ = Mass concentration (1 $\text{mg} \cdot \text{mL}^{-1}$)

Enzyme activity (v) was calculated through change rate of absorption (r_A) and including the dilution factor of the sample in the measurement solution. The results are shown in international units (IU) [$\mu\text{mol} \cdot \text{min}^{-1}$] and are used for normalization of respiration.

2.9 Photometrical Analysis of Metabolic Intermediates

The energy metabolites glucose, pyruvate and lactate were quantitatively analyzed from plasma samples and microdialysates using the Iscus^{flex} *Microdialysis Analyzer*. Plasma samples were obtained from trunk blood that was collected within seconds after decapitation and diluted 1:10 immediately before analysis.

2.9.1 Instruments and materials

Instrument	Manufacturer
Iscus ^{flex}	M Dialysis AB, Stockholm, SE

Materials	Manufacturer
Caps, 7mm for microvials	Gilson, Middleton, WI, USA
Glucose reagent	M Dialysis AB, Stockholm, SE
Lactate reagent	M Dialysis AB, Stockholm, SE
Pyruvate reagent	M Dialysis AB, Stockholm, SE
Rotilab [®] reaction tubes 250 μL	Carl Roth GmbH & Co. KG, Karlsruhe, D

2.9.2 Principle

The analysis is based on a series of enzymatic reactions and colorimetric detection. Quinonimine (absorption wavelength 530 nm) which is formed in the reaction proportionally to analyte concentrations, allows an indirect determination of glucose, glutamate, glycerol, lactate, pyruvate, and urea.

Glucose

Glucose is oxidized enzymatically by glucose oxidase (GOD). In a following reaction, peroxidase catalyzes a reaction in which hydrogen peroxide, formed in the previous step, phenol and 4-amino antipyrine form quinonimine (red-violet color). The speed of quinonimine formation is proportional to glucose concentration and is detected photometrically at 530 nm.

Analytical parameters

- **Wavelength** 530 nm
- **Temperature** 37 °C
- **Volume of sample** 0.5 μL
- **Detection limit** 0.1 mM

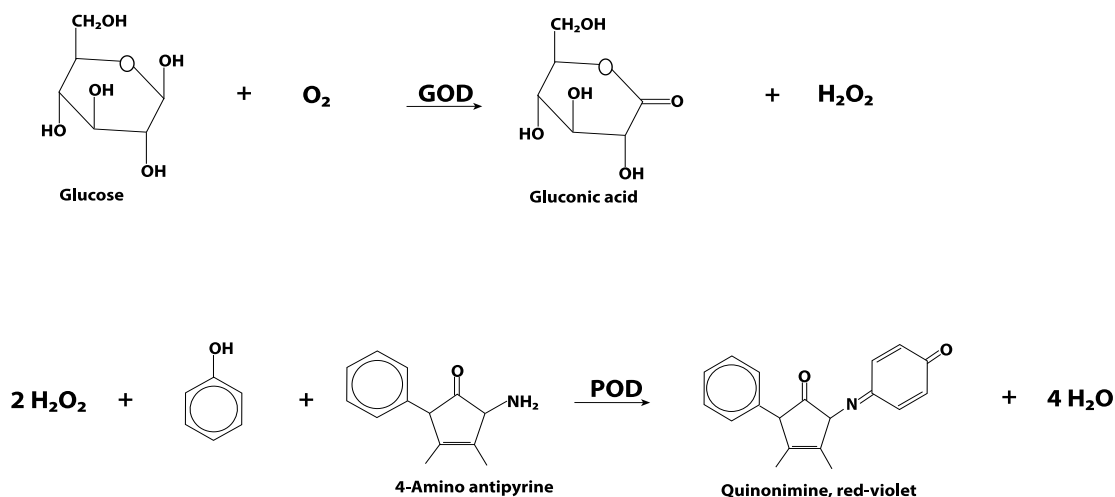


Figure 20: Enzymatic reaction of glucose to gluconic acid under release of H_2O_2 . In a second step, enzymatically catalyzed formation of quinonimine, which is detected colorimetrically at 530 nm wavelength. Abbreviations: **GOD** glucose oxidase, **POD** peroxidase. Figure modified from Christian Viel.

Lactate

Lactate is oxidized enzymatically to pyruvate and hydrogen peroxide by lactate oxidase. As described above, the peroxide oxidase catalyzes the formation of quinonimine from hydrogen peroxide, 4-chlorophenol and 4-aminoantipyrine. The speed of quinonimine formation is proportional to lactate concentration and is detected photometrically at 530 nm.

Analytical parameters

- **Wavelength** 530 nm
- **Temperature** 37 °C
- **Volume of sample** 0.2 µL
- **Detection limit** 0.1 mM

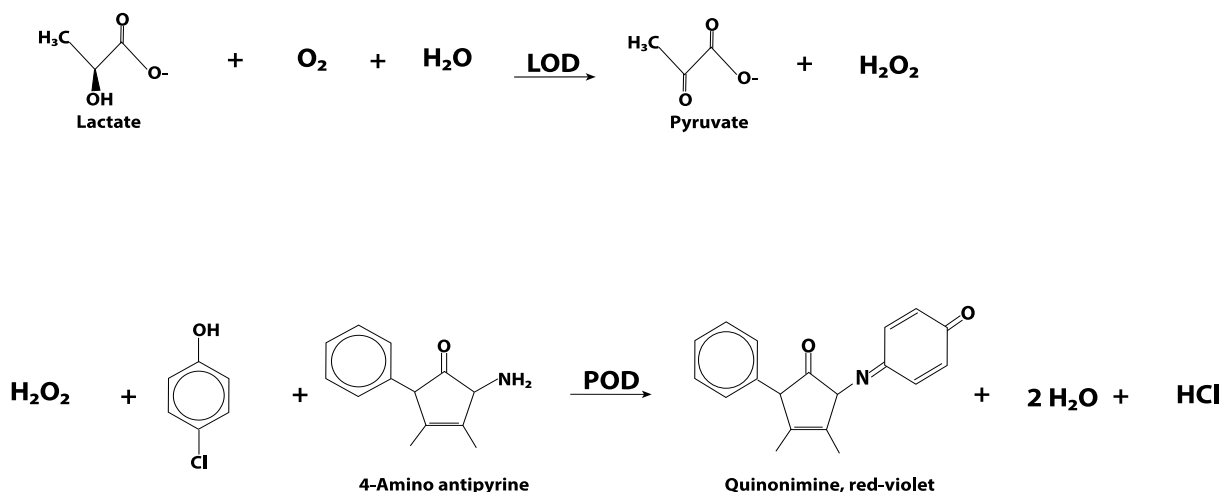


Figure 21: Enzymatic reaction of lactate to pyruvate under release of H₂O₂. Second step, enzymatically catalyzed formation of quinonimine, which is detected colorimetrically at 530 nm wavelength. Abbreviations: LOD lactate oxidase, POD peroxidase. Figure modified from Christian Viel (2022).

Pyruvate

In presence of anorganic phosphate, pyruvate is enzymatically oxidized to hydrogen peroxide by pyruvate oxidase (PyrOx). Peroxide oxidase catalyzes the formation of a quinone diimine from hydrogen peroxide, N-ethyl-N-(2-hydroxy-3-sulfopropyl)-m-toluidin (TOOS) and 4-amino antipyrine. The amount of quinone diimine is proportional to pyruvate concentration.

Analytical parameters

- **Wavelength** 530 nm
- **Temperature** 37 °C
- **Volume of sample** 0.5 µL
- **Detection limit** 0.01 mM

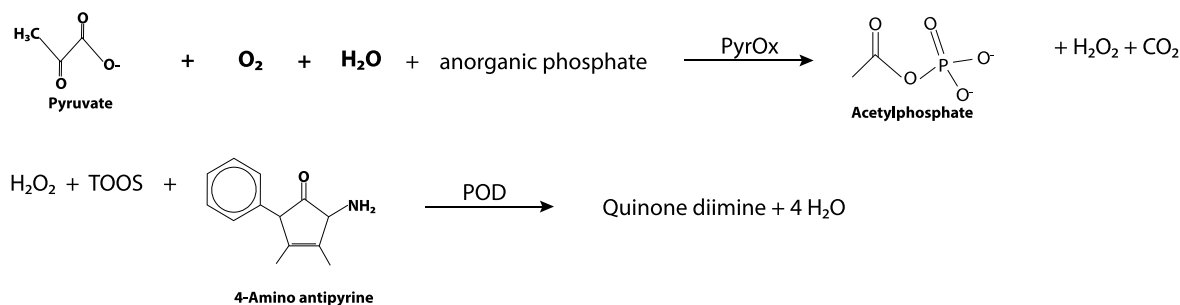


Figure 22: Enzymatic reaction of pyruvate to H₂O₂. Second step, enzymatically catalyzed formation of quinone diimine, which is detected colorimetrically at 530 nm wavelength. Abbreviations: **PyroX** pyruvate oxidase, **TOOS** N-ethyl-N-(2-hydroxy-3-sulfopropyl)-m-toluidin, **POD** peroxidase.

2.10 TTC Staining

2.10.1 Instruments and materials

Table 10: Materials and instruments for TTC staining.

Instrument/Material	Manufacturer
Dino capture camera	Big catch digital products, Torrance, CA, USA
Filter paper	Cytiva life sciences, Marlborough, MA, USA
Tissue chopper	McIlwain, Redding, CA, USA
Water bath	B.Braun, Melsungen, D
2,3,5-Triphenyltetrazoliumchloride (TTC)	Merck (Sigma-Aldrich), Darmstadt, D

Phosphate Buffered Saline (PBS-buffer)

Table 11: Composition of PBS buffer.

Compound	Concentration [mM]
Calcium chloride	0.9
Magnesium chloride	0.9
Potassium chloride	2.7
Potassium dihydrogen phosphate	1.5
Sodium chloride	137
Sodium dihydrogen phosphate	6.5

2.10.2 Principle

2,3,5-Triphenyltetrazoliumchloride (TTC) is a redox indicator. In accepting two electrons and one proton, TTC is transformed to the red-violet compound formazan. In mitochondria this reaction is mainly catalyzed by complex II (succinate dehydrogenase) of the respiratory chain with electrons provided by NADH. Consequently, active mitochondria become red-violet, whereas inactive mitochondria remain colorless.

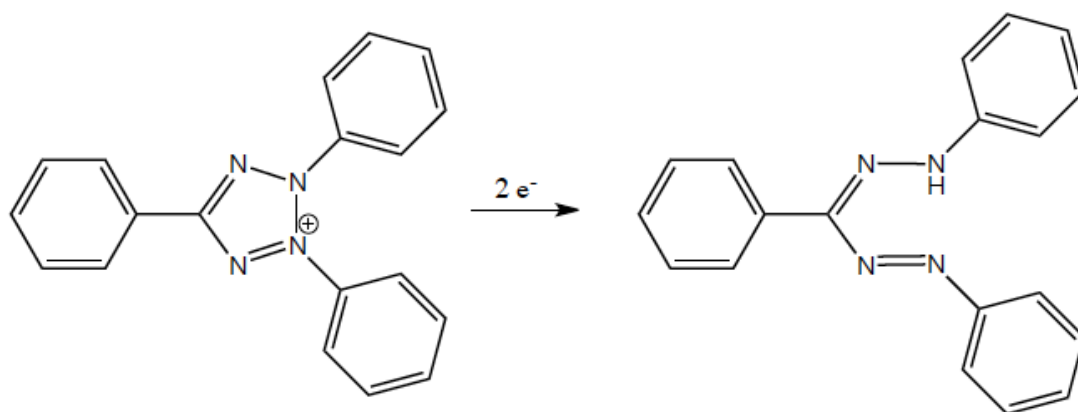


Figure 23: Transformation of 2,3,5-triphenyltetrazoliumchloride (TTC) to formazan. Electrons are donated by NADH. Reaction is catalysed by succinate dehydrogenase (complex II respiration chain).

2.10.3 Experimental procedure

A 1% TTC solution in PBS is prepared and stored light-proof at 4 °C until needed for the experiment. The water bath is heated to 37 °C. Mice were decapitated either 24 hours, 72 hours, or 7 days after reperfusion. The brain is carefully removed from the skull and the entire brain, including cerebellum and olfactory bulb are put into a mouse brain-specific mold, where 1 mm thick slices are cut with a razor blade. Slices are then incubated in the 1% TTC solution for 10 minutes at 37 °C. Afterwards, they are transferred into ice cold PBS to stop the redox reaction. For analysis, brain slices are dried and captured with a magnification camera (Big catch digital products, USA). The extent of stroke was determined by area calculation of colorless tissue (ImageJ 1.42q, National Institutes of Health, USA).

3. Statistical analysis

The statistics of all data shown was calculated by means of the program GraphPad prism 5.0b (GraphPad Software, CA, USA).

Comparison of data sets was performed according to the following scheme.

Non-parametrical	
One-way ANOVA by Kruskal-Wallis with Dunn's post-test	Comparison of > 2 data sets.

Parametrical	
t-test	Comparison of 2 data sets.
t-test with Welch correction	Comparison of 2 data sets with different standard deviations.
One-way ANOVA with Newman-Keuls post-test	Comparison of > 2 data sets.
One-way ANOVA with Tukey post-test	Comparison of > 2 data sets.
Repeated measures ANOVA with Dunnetts post-test	Comparison of data curves.

At first, it had to be determined whether the data follow Gaussian distribution (parametrical), or whether they are distributed non-parametrically. Subsequently, there is a variety of tests and post-tests that can be applied, depending on how many data sets were compared, and the manner in which they should be compared. The significance of data curves was determined by means of repeated measures ANOVA.

All parametrical data sets were shown as mean \pm standard error of the mean (S.E.M.). Non-parametrical data were shown as median \pm interquartile range.

The calculated significance levels are divided into:

Significance levels	
*p < 0.05	significant
**p < 0.01	very significant
***p < 0.001	highly significant

4. Results

This section first shows the results of experiments related to microdialysis, which includes *in vitro*-recovery and change of metabolite concentrations after BHB injection in mice that had not undergone MCAO. The subsequent part shows the results of a small study that was done to determine whether BHB affects mitochondrial respiration *in vitro*. The next part shows detailed results of the MCAO study in which BHB (30 mg/kg bodyweight) was administered upon reperfusion after 90 minutes of cerebral ischemia. Experiments were performed 60 minutes, 24 hours, 72 hours and 7 days after reperfusion. Accordingly, the results are organized by the time after which the experiment was performed. Results beyond 7 days after reperfusion would have been of further interest but were not granted by the local animal committee (Regierungspräsidium Darmstadt). When measuring mitochondrial activity of ischemic and non-ischemic hemispheres, the right (ischemic) hemisphere is referred to as “RH” and the left (non-ischemic) hemisphere is referred to as “LH”.

4.1 Microdialysis

4.1.1 In vitro-recovery

In order to ensure consistent quality of the microdialysis probes, the *in vitro*-recovery rate was determined on a random basis. The values are shown in table 4.1.

Table 12: Recovery rates. Recovery rates are shown as mean values (\pm S.E.M.) of all tested probes with an exchange area of 2 mm and a flow rate of 2 μ L/min. All compounds were measured using the ISCUS[®] microdialysis analyzer (N=4).

	Glucose	Lactate	Pyruvate
Recovery rate [%]	13,30 \pm 0,4	17.42 \pm 1.54	36.02 \pm 5.70

4.1.2 Change of metabolite concentrations after administration of 30 mg/kg β -hydroxybutyrate

Initially, it was investigated whether BHB reaches the brain and if there were any changes in concentrations of the metabolites glucose and lactate. Unfortunately, the GC-MS that was originally used to analyze β -hydroxybutyrate (GC-MS) was irretrievably damaged before the present experiments could be evaluated, which is why β -hydroxybutyrate concentrations could not be measured and older data, obtained by Konrad Koch, is shown instead. Glucose and lactate levels were taken from the present work. Microdialysate was collected every 15 minutes, starting at 30 minutes before injection until 120 minutes after injection. Probes were continually perfused with aCSF at a

flow rate of 2 $\mu\text{L}/\text{min}$. The data shows that injection of BHB leads to a moderate but significant increase of BHB in the brain (Fig. 24) whereas glucose and lactate were unaffected (Fig. 25).

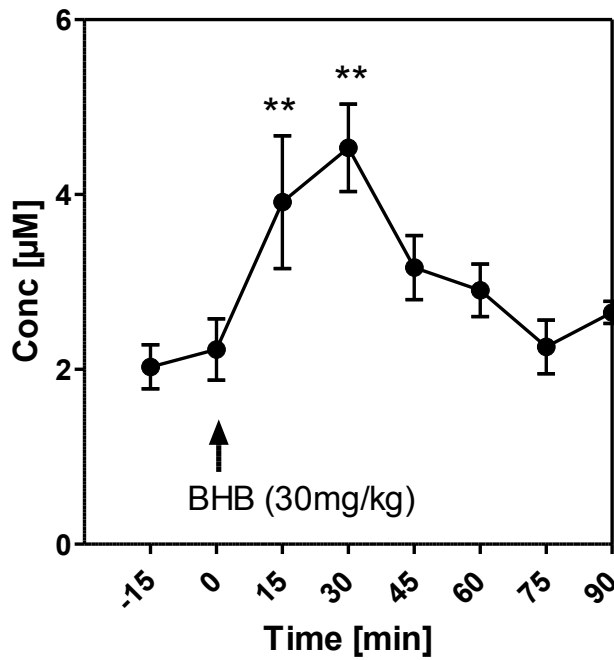


Figure 24: β -Hydroxybutyrate concentrations in microdialysate (mean value \pm S.E.M.) after intraperitoneal injection of β -hydroxybutyrate (30 mg/kg bodyweight). Animals were female CD-1 mice, aged 6-8 weeks. Probes were implanted 24 hours prior to experiment into the left striatum (N=4). Data are shown as absolute concentrations without recovery of each probe. Values adopted from Koch (2017) and Lehto et al. (2022). Data are means \pm S.E.M. of four experiments. Statistics were calculated by repeated measures ANOVA and Dunnett's multiple comparison test. **, $p < 0.01$ vs. basal value at minus 15 min.

The data obtained for glucose and lactate after administration of BHB 30 mg/kg are shown in figure 25. No significant changes were noted.

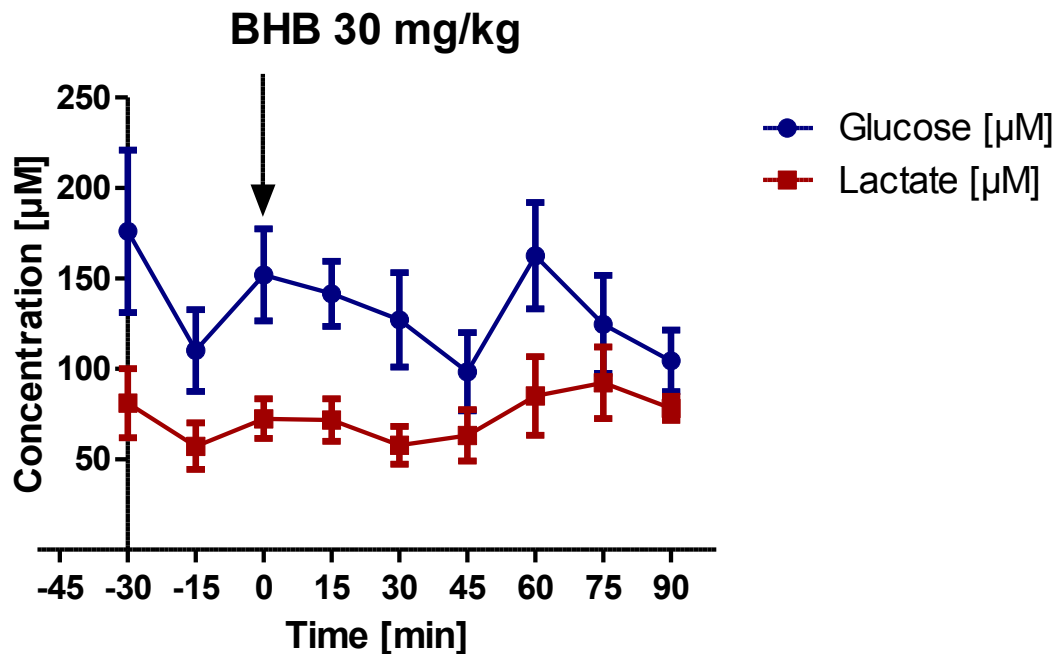


Figure 25: Glucose concentrations in microdialysate (mean values \pm S.E.M.) in blue; lactate concentrations (mean values \pm S.E.M.) in red. Samples were collected starting from 30 minutes before until 90 minutes after injection of β -hydroxybutyrate (30 mg/kg bodyweight; N=9).

4.2. *In vitro* stimulation of mitochondrial respiration with β -hydroxybutyrate

To find out whether BHB administration affects mitochondrial respiration, BHB, pyruvate and succinate were added directly to isolated mitochondria in concentrations of 1 mM, 3 mM and 10 mM. The highest respiration could be observed after addition of succinate (6 times higher than pyruvate alone). It was the only compound in the series of experiments that led to increased respiration in a concentration-dependent manner. Addition of malate to succinate does not further increase respiration (data not shown).

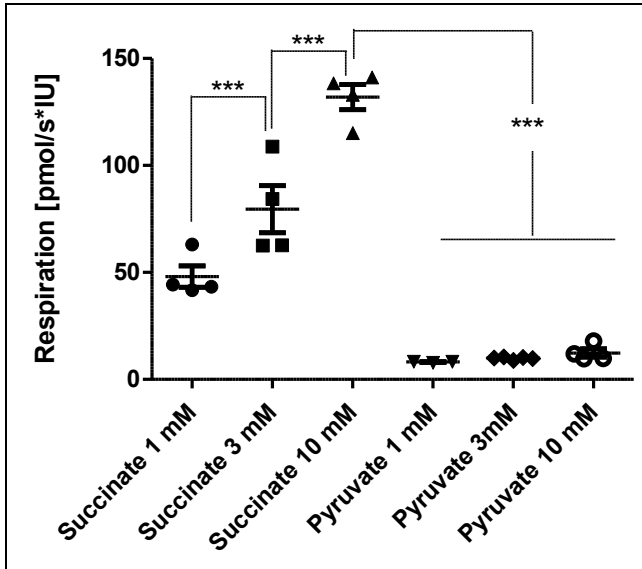


Figure 26: Oxygen consumption measured by respirometry after addition of succinate in concentrations of 1 mM, 3 mM and 10 mM, and pyruvate in concentrations of 1 mM, 3 mM and 10 mM. Statistical analysis: Data are scatter box plots (means \pm S.E.M. are indicated) of 4 independent experiments. Data were analyzed by one-way ANOVA followed by Newman-Keuls post-test: $F_{5,23} = 80.16$. *** $p < 0.0001$.

When adding only BHB and pyruvate, respiration caused by BHB alone was twice as effective as pyruvate alone.

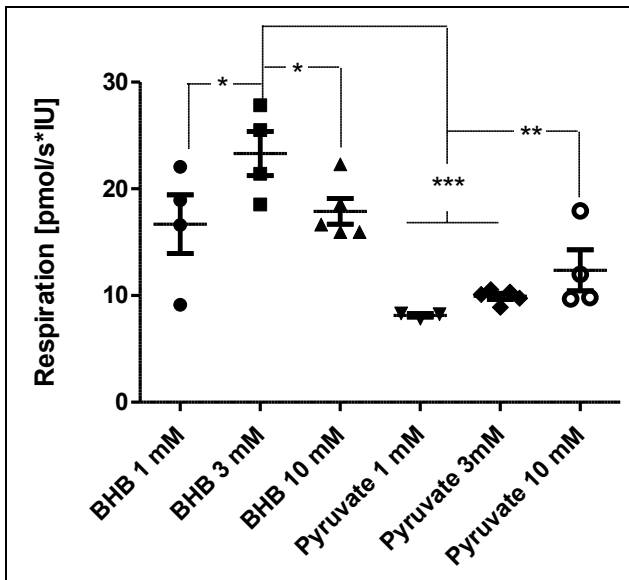


Figure 27: Oxygen consumption measured by respirometry after addition of BHB in concentrations of 1 mM, 3 mM and 10 mM, and pyruvate in concentrations of 1 mM, 3 mM and 10 mM. Statistical analysis: Data are scatter box plots (means \pm S.E.M. are indicated) of 4 independent experiments. Data were analyzed by one-way ANOVA followed by Newman-Keuls post-test: $F_{5,24} = 10.90$. *** $p < 0.0001$, ** $p < 0.01$, * $p < 0.05$.

Respiration induced by BHB was increased by 79% after addition of malate. Interestingly, respiration was highest at concentrations of 3 mM. With BHB alone, the higher concentration of 10 mM reduced respiration, but without statistical significance, whereas, in combination with malate, respiration was not further increased by BHB concentrations of 10 mM (fig. 28).

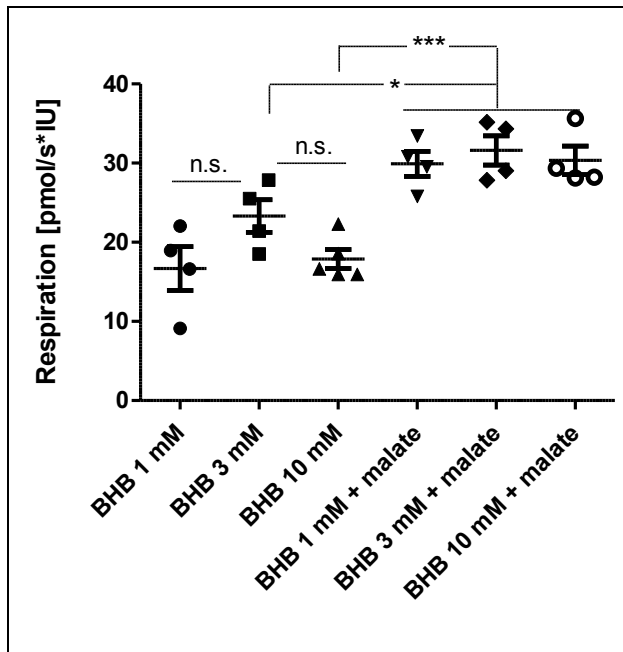


Figure 28: Oxygen consumption measured by respirometry after addition of BHB in concentrations of 1 mM, 3 mM and 10 mM, and BHB and malate in concentrations of 1 mM, 3 mM and 10 mM. Statistical analysis: Data are scatter box plots (means \pm S.E.M. are indicated) of 4 independent experiments. Data were analyzed by one-way ANOVA followed by Newman-Keuls post-test: $F_{5,24} = 12.46$. *** $p < 0.0001$; * $p < 0.05$.

4.3 Reproducibility of transient middle cerebral artery occlusion

Another important control experiment concerned the successful induction of cerebral ischemia by the MCAO technique applied herein. In order to ensure reproducibility of the MCAO surgery, perfusion of the middle cerebral artery (MCA) was measured before surgery, after induction of ischemia, and after reperfusion using a Laser Doppler instrument (see Methods). Figure 29 shows the decline of perfusion of the MCA after placing the suture in it. Surgery was regarded successful when perfusion dropped to < 15%.

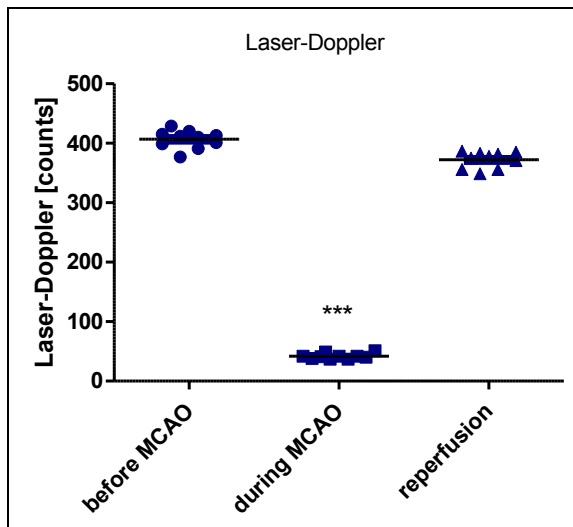


Figure 29: Measurement of Laser-Doppler sonography before ischemia, after induction and after reperfusion (means \pm S.E.M.). Statistical analysis: Data are scatter box plots (means \pm S.E.M. are indicated) of 10 independent experiments. Data were analyzed by one-way ANOVA followed by Newman-Keuls post-test: $F_{2,29} = 2.776$. *** $p < 0.0001$.

4.4 Respiration 60 minutes after reperfusion

4.4.1 Mitochondrial activity

Mitochondria were isolated from mouse brain hemispheres after 90 minutes of MCAO followed by 60 minutes of reperfusion. Mitochondria from the ischemic hemisphere showed significantly lower oxygen consumption than the mitochondria in the contralateral hemisphere, and this was true in both treatment groups, saline and BHB (30 mg/kg bodyweight). Respiration of all complexes, OxPhos and ETS was strongly reduced in the ischemic hemispheres in both groups. Complex I respiration was reduced by 43% in salinetreated animals versus 20% in BHB animals; complex II 51% reduction with saline vs. 45% with BHB. OxPhos and ETS were reduced by approximately 45% in both groups. Absolute values normalized to mitochondrial protein content are shown in figure 30. With the exception of complex I in BHB-treated animals, all complexes as well as ETS and OxPhos are significantly reduced in the right hemispheres regardless of treatment group. In complex I, however, there is a trend that points towards the right hemisphere of BHB-treated animals not being as impaired as the right hemisphere of saline-treated mice.

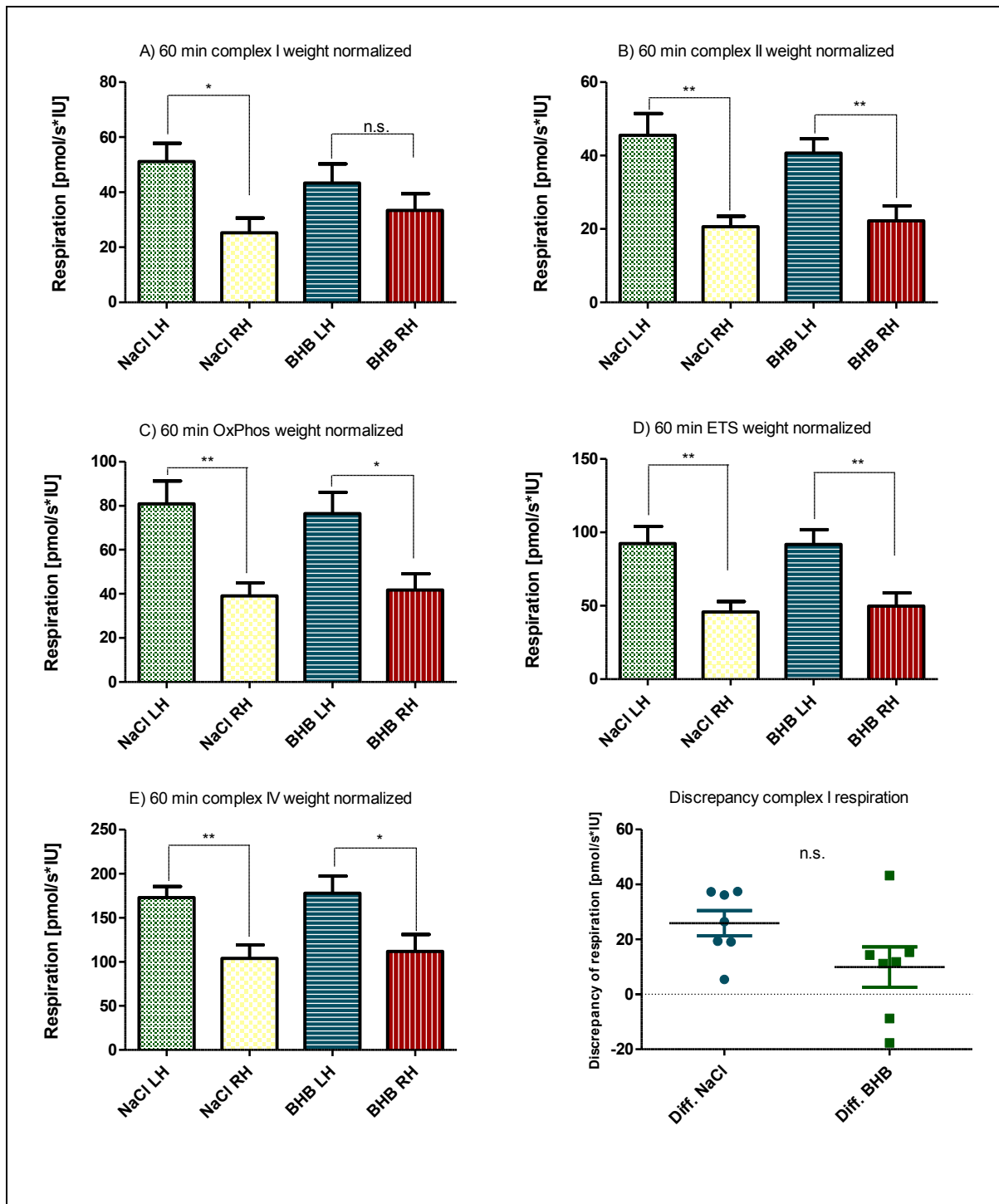


Figure 30: Oxygen consumption measured by respirometry 60 minutes after transient ischemia. Raw data were normalized to mitochondrial protein content. Statistical analysis: Data are vertical column bar graphs (means \pm S.E.M. are indicated) of 14 independent experiments (BHB: N=7, NaCl: N=7). A)-E) Data were analyzed by one-way ANOVA followed by Newman-Keuls post-test. F) Data were analyzed by unpaired t-test.

A) Oxygen consumption of complex I, $F_{3,27} = 3.253$; * $p = 0.05$; B) Oxygen consumption of complex II, $F_{3,27} = 8.633$; *** $p < 0.0005$; C) OxPhos respiration, $F_{3,27} = 7.060$, ** $p = 0.0014$; D) ETS respiration, $F_{3,27} = 7.297$, ** $p = 0.0011$; E) Oxygen consumption of complex IV, $F_{3,27} = 5.401$, ** $p = 0.0053$. F) Discrepancy of respiration of complex I in left and right hemisphere, $p = 0.090$.

The difference of complex I respiration between saline and BHB treated animals becomes more pronounced when analyzing right and left hemispheres separately by paired t-test. Whereas the difference between RH and LH is not significant in complex I in BHB treated animals ($p= 0.227$), it is so in saline treated animals (** $p= 0.0013$).

When comparing ratios of left and right hemisphere, there was no significant difference between the intervention and control group (fig. 31) for either complex. However, for complex I, a trend without statistical significance is visible that points to lower impairment of the ischemic hemisphere in animals treated with BHB. Administration of a single dose of BHB seems to have mildly beneficial effects immediately after stroke.

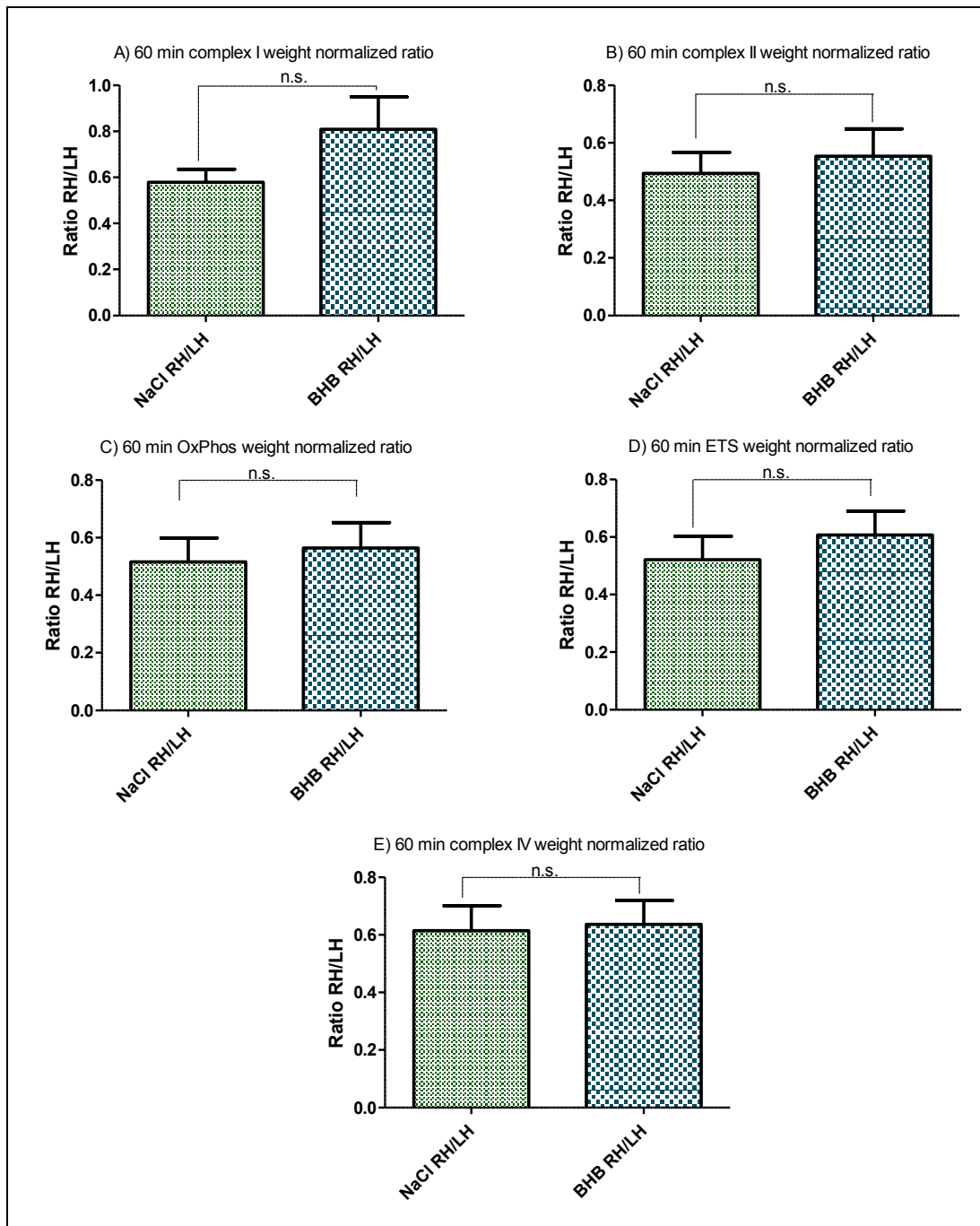


Figure 31: Ratio of mitochondrial respiration of right hemispheres in proportion to unaffected left hemispheres 60 minutes after transient ischemia. Statistical analysis: Data are vertical column bar graphs (means \pm S.E.M. are indicated) of 14 independent experiments (BHB: N=7, NaCl: N=7). Data were analyzed by unpaired t-test: A) Complex I: $p=0.15$ B) Complex II: $p=0.62$; C) OxPhos: $p=0.69$; D) ETS: $p=0.47$; E) Complex IV: $p=0.86$. Citrate synthase activity in the right hemisphere was significantly reduced in both groups 60 minutes after reperfusion (fig. 32).

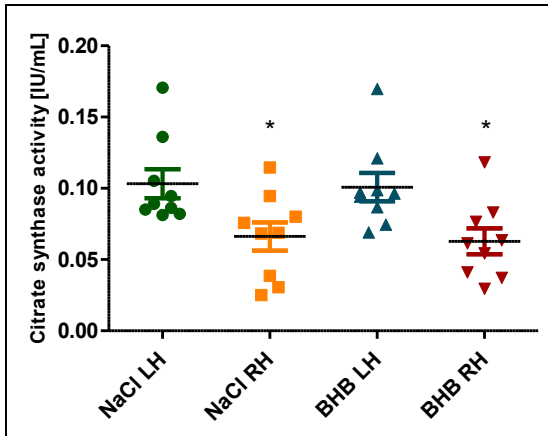


Figure 32: Citrate synthase activity 60 minutes after transient ischemia. Statistical analysis: Data are scatter box plots (means \pm S.E.M. are indicated) of 18 independent experiments (BHB: N=9, NaCl: N=9). Data were analyzed by one-way ANOVA followed by Newman-Keuls post-test: $F_{3,35}=4.924$, $**p=0.0063$, * $p<0.05$ vs. left hemisphere.

Consequently, when normalized to citrate synthase activity, the effect of stroke almost entirely disappeared (complexes I, II and IV shown exemplary in fig. 33), leading to the conclusion that mitochondria that have not died during MCAO are unimpaired. Presumably, there is a higher amount of non-oxygen consuming tissue in the right hemisphere. As there is no difference visible in citrate-normalized respiration values, ratios are not shown.

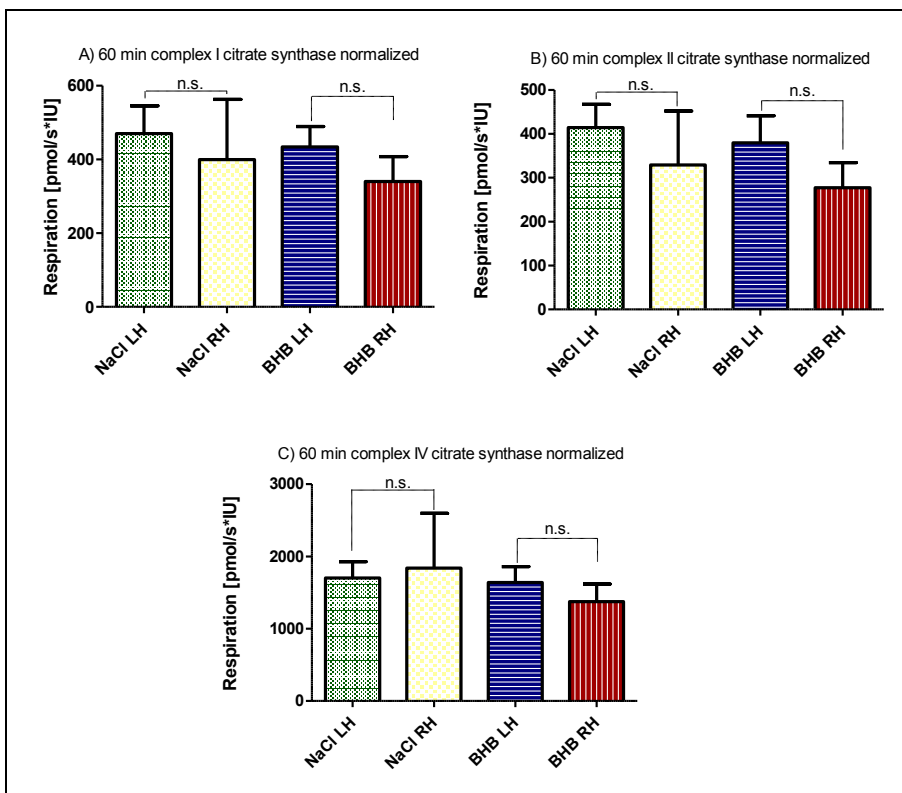


Figure 33: Oxygen consumption measured by respirometry 60 minutes after transient ischemia with raw data normalized to citrate synthase activity. Statistical analysis: Data are vertical column bar graphs (means \pm S.E.M.

are indicated) of 14 independent experiments (BHB: N=7, NaCl: N=7). Data were analyzed by one-way ANOVA followed by Newman-Keuls post-test. A) Complex I: $F_{3,28} = 0.306$, $p = 0.821$; B) Complex II: $F_{3,28} = 0.605$, $p = 0.618$; C) Complex IV: $F_{3,28} = 0.212$ $p = 0.887$

4.5 Respiration 24 hours after reperfusion

4.5.1 Mitochondrial activity

24 hours after reperfusion, the activity of complexes I and II was reduced more strongly in the untreated group. Whereas complex I respiration of the right hemisphere is significantly reduced in saline treated animals, the difference between right and left hemisphere is not significant in BHB treated mice. Complex II respiration is decreased regardless of treatment group. However, the difference is significantly higher in saline treated mice. OxPhos, being the sum of complex I and complex II respiration, was also significantly increased in the treated group. Complex IV activity was unaffected by BHB treatment and complex IV respiration was no longer impaired 24 hours after reperfusion. ETS, the sum of complexes I-IV, was unchanged compared to saline (fig. 34).

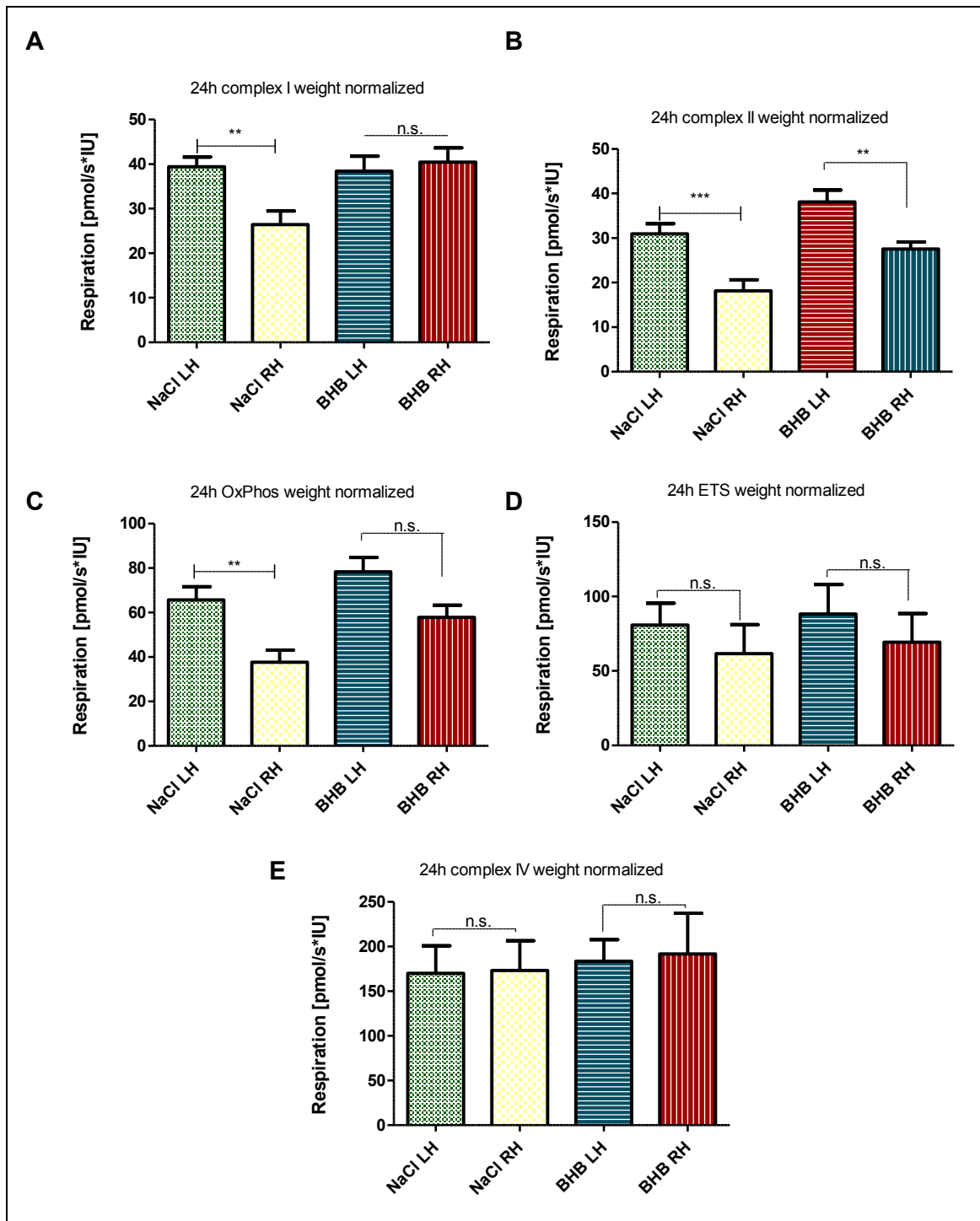


Figure 34: Oxygen consumption measured by respirometry 24 hours after transient ischemia. Raw data were normalized to mitochondrial protein content. Statistical analysis: Data are vertical column bar graphs (means \pm S.E.M. are indicated) of 12 independent experiments. Data were analyzed by one-way ANOVA followed by Newman-Keuls post-test. A) Complex I: $F_{3,47} = 4.86$, $p = 0.005$; B) Complex II: $F_{3,47} = 30.93$, $p < 0.001$; C) OxPhos: $F_{3,47} = 18.77$, $p < 0.001$; D) ETS: $F_{3,17} = 0.40$, $p = 0.76$. E) Complex IV: $F_{3,47} = 1.33$, $p = 0.28$. * $p < 0.05$, ** $p < 0.01$.

The ratio of left and right hemisphere was increased in complex I in the BHB group, pointing to a beneficial effect of BHB 24 hours after reperfusion (fig. 35). All other ratios showed no statistically significant difference and the data is not shown.

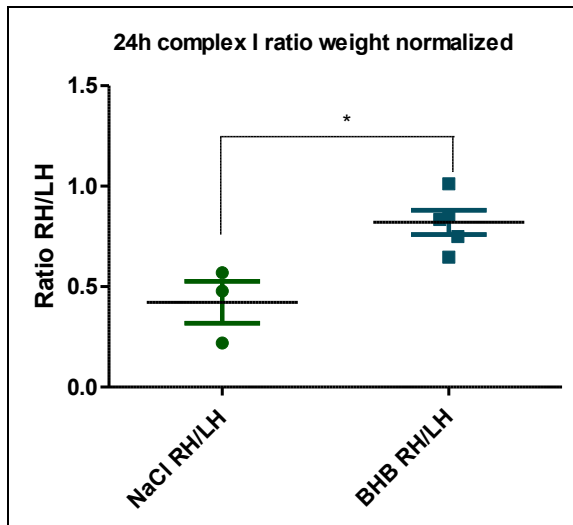


Figure 35: Ratio of mitochondrial complex I respiration of right hemispheres in proportion to unaffected left hemispheres 24 hours after transient ischemia. Statistical analysis: Data are scatter box plots (means \pm S.E.M. are indicated) of 8 independent experiments (BHB: N=5, NaCl: N=3). Data were analyzed by unpaired t-test: *p= 0.0117.

As observed 60 minutes after reperfusion, the effect of stroke itself almost entirely disappeared when normalizing respiration to citrate synthase activity. Inevitably, possible effects of BHB disappeared as well. Complex I is shown exemplary, other data is not shown.

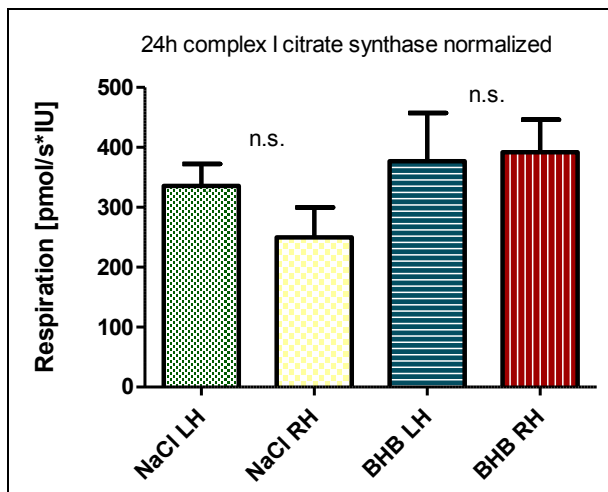


Figure 36: Oxygen consumption measured by respirometry 24 hours after transient ischemia with raw data normalised to citrate synthase activity. Statistical analysis: Data are vertical column bar graphs (means \pm S.E.M. are indicated) of 10 independent experiments. Data were analyzed by one-way ANOVA followed by Newman-Keuls post-test: $F_{3,17} = 1.05$, $p = 0.402$.

It is, however, noteworthy that citrate synthase activity itself was higher in the right hemispheres of BHB treated mice. Citrate synthase activity in left hemispheres was unchanged in both groups.

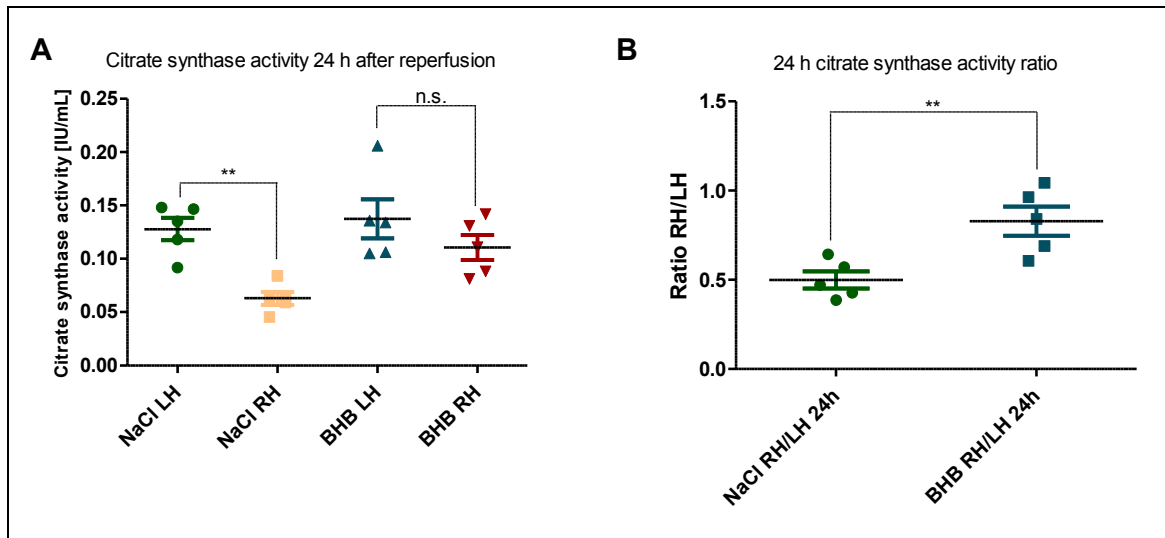


Figure 37: A) Citrate synthase activity 24 hours after transient ischemia, absolute values. Statistical analysis: Data are scatter box plots (means \pm S.E.M. are indicated) of 10 independent experiments (BHB: N=5, NaCl: N=5). Data were analyzed by one-way ANOVA followed by Newman-Keuls post-test: $F_{3,19}=7.028$, $**p=0.0031$. B) Citrate synthase activity 24 hours after transient ischemia, absolute values. Statistical analysis: Data are scatter box plots (means \pm S.E.M. are indicated) of 10 independent experiments. Data were analyzed by unpaired t-test: $**p=0.0082$.

4.5.2 Plasma metabolites

Earlier experiments from our group (Koch et al., 2017) showed pronounced ketosis in untreated animals 24 hours after 90 minutes of MCAO. The effect was particularly strong when animals had been fed a fat-rich diet. Plasma BHB concentrations in untreated animals were approximately 3 times as high as in animals treated with 30 mg/kg BHB and more than 5,000 times as high as in sham-operated animals (image 7).

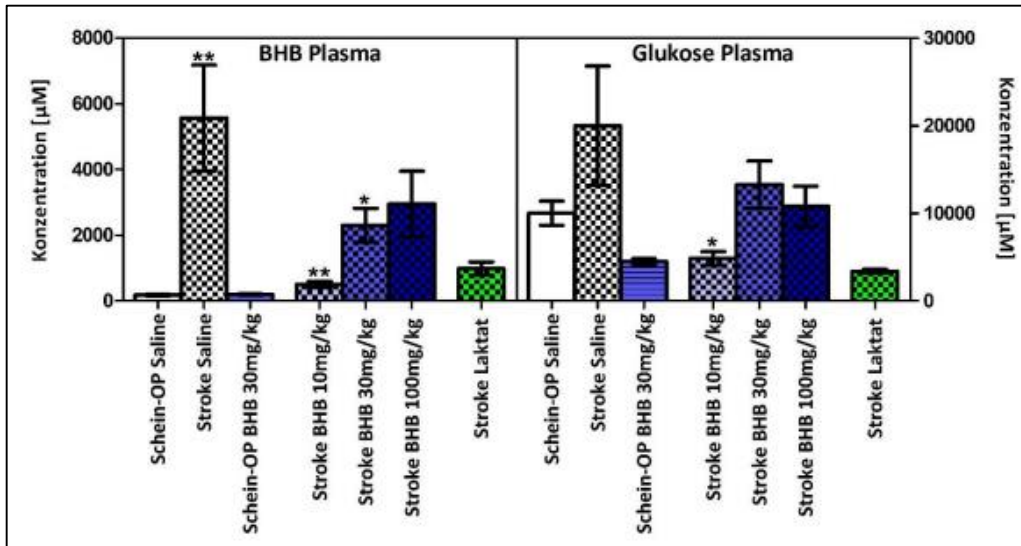


Image 7: BHB and glucose levels after various treatment regiments following MCAO or sham operation. Left: BHB levels (means \pm S.E.M), right: glucose levels (means \pm S.E.M) in plasma 24 hours after reperfusion. Data are vertical column bar graphs of N=9 independent experiments. Data were analyzed by one-way ANOVA followed by Tukey-post left: $F_{4,34} = 6$; * $p < 0,05$; right: $F_{1,66} = 3.6$. Values adopted from Konrad Koch (2017).

In the present study, the data on BHB plasma and tissue concentrations could not be reconfirmed since there was no more possibility to measure BHB and other ketone bodies. Plasma glucose concentrations were similar to the previous set of experiments in sham-operated animals and in animals treated with saline or BHB. Plasma lactate levels were increased in both groups that underwent stroke compared to sham-operated animals, although the difference was not statistically significant. Plasma pyruvate levels, however, were significantly higher in animals that have had MCAO than in sham-operated animals. The BHB-treated group showed the highest concentrations of pyruvate, but again, the increase in comparison to the saline group did not reach statistical significance. Calculation of the lactate-pyruvate-ratio shows no statistically significant difference between all groups.

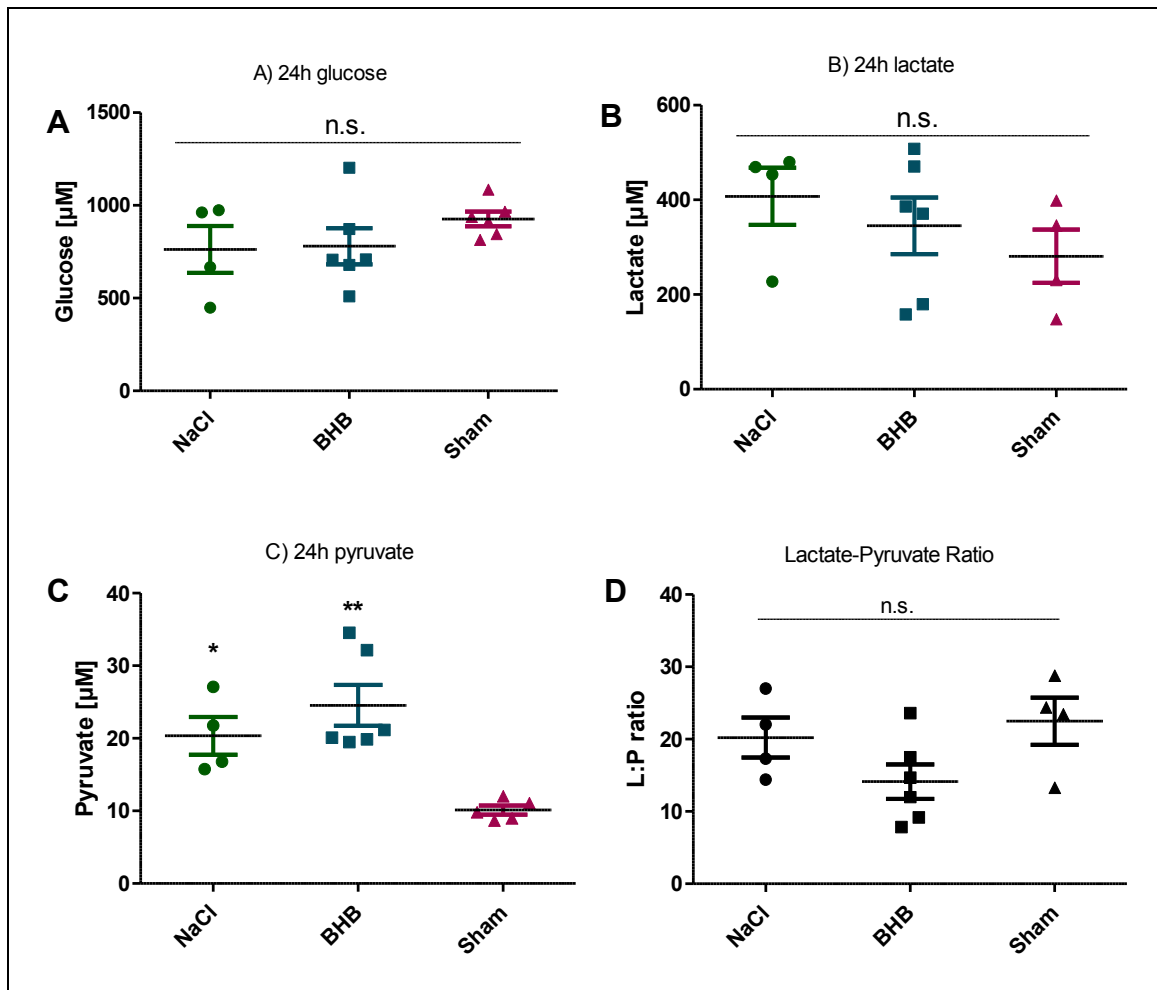


Figure 38: Concentrations of A) glucose, B) lactate and C) pyruvate in plasma. Mice underwent transient cerebral ischemia for 90 min and were given saline or β -hydroxybutyrate (BHB; 30 mg/kg) by i.p. injection immediately after reperfusion ("NaCl"; "BHB"). For sham-operated mice, the carotid artery was prepared but not occluded. Blood samples were taken 24 hours after BHB administration. Statistical analysis: Data are scatter box plots (means \pm S.E.M) of 16 independent experiments (BHB: N=6, NaCl: N=4, sham: N=6). Data were analyzed by one-way ANOVA followed by Tukey's post-test. A) $F_{2,15} = 1.121$, $p = 0.356$; B) $F_{2,13} = 0.937$, $p = 0.421$; C) $F_{2,14} = 10.79$, $**p=0.0021$, $*p < 0.05$; D) $F_{2,13} = 3.08$, $p = 0.09$.

4.5.3 Behavioral tests

Corner test

The corner test was performed to determine the extent of unilateral motor impairment. Mice are given the chance to turn left or right in a corner, and the movements are counted after 10 attempts. When the animals were trained for three days before MCAO, turns were always nearly 1:1 in both directions.

A laterality index of 0 means that turns were equal in both directions, an index of +10 means right turns only, an index of -10 only left turns. In this experiment BHB-treated mice showed substantial

improvement compared to saline (fig. 39). Whereas saline-treated mice turned right almost exclusively, the animals treated with BHB had far more heterogenous patterns of turning. Only two animals from the BHB group turned solely in one direction.

Chimney test

In this experiment, the time was recorded in which an animal climbs backwards out of a 20 cm long vertical tube. Here, the motor impairment after a 90-minute stroke is clearly visible 24 hours after reperfusion (fig. 39). Animals treated with BHB, however, performed better in this experiment. It took the animals approximately 16 seconds to exit the tube backwards, whereas it took saline-treated mice 21.5 seconds on average. Before MCAO it took the animals 2.7 seconds on average to leave the tube.

Rotarod

Rotarod tests motoric coordination, and again, a very clear effect of stroke can be seen. Whereas the animals can walk on the rotating rod effortlessly for 60 seconds after sham surgery, they fall off after approximately 30 seconds after MCAO, regardless of the treatment. BHB had no significant effect.

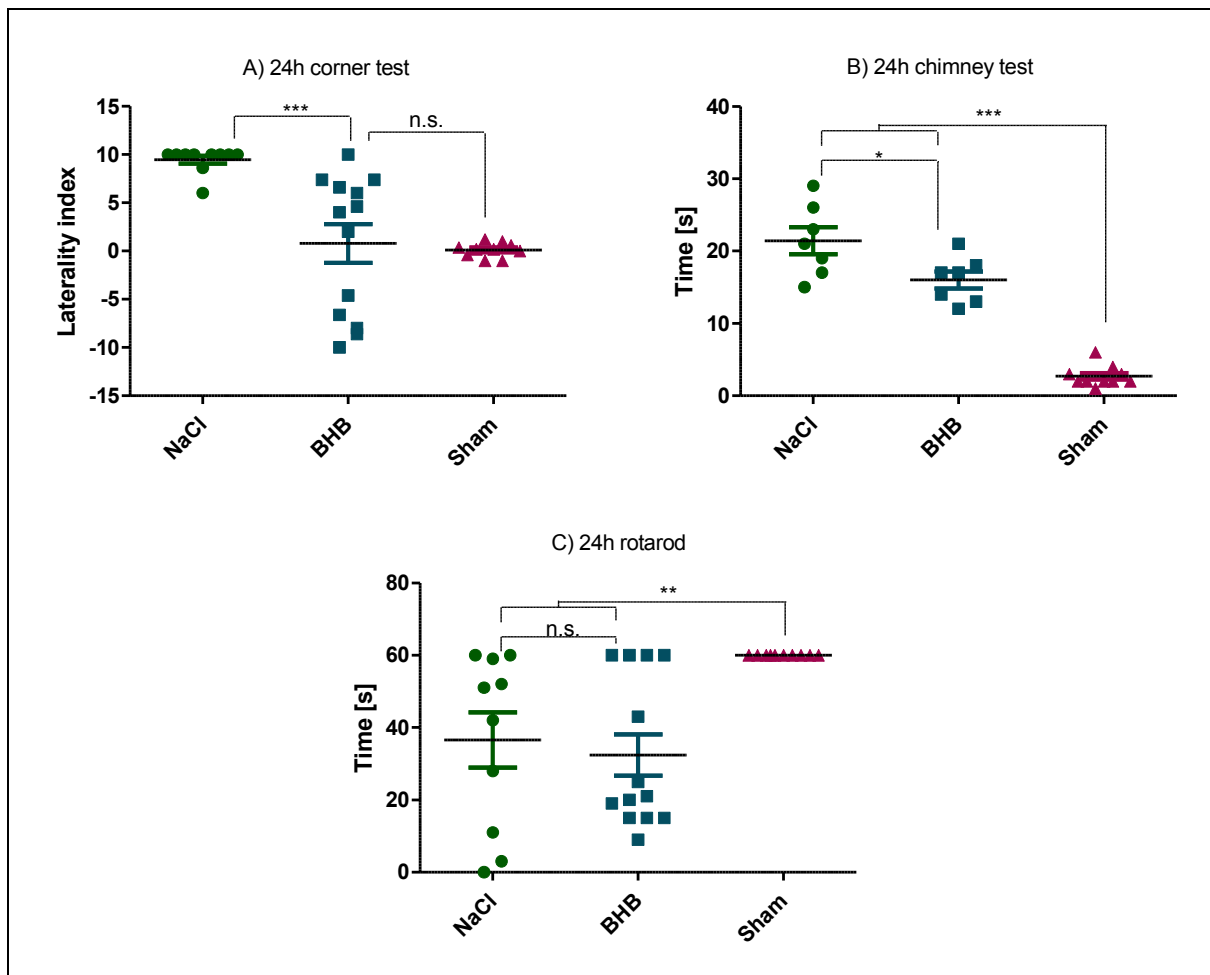


Figure 39: Effect of β -hydroxybutyrate (BHB) on mouse motoric function. Mice underwent transient cerebral ischemia for 90 min and were given saline or BHB (30 mg/kg) by i.p. injection immediately after reperfusion ("NaCl"; "BHB"). Data are scatter box plots (means \pm S.E.M. are indicated) of 10-12 independent experiments.

A) and B): Data were analyzed by one-way ANOVA followed by Newman-Keuls post-test. C) Data were analyzed by Kruskal-Wallis test followed by Dunn's post-test. A) Corner Test after 24 hours. This test determines the preferred side to leave a corner. A score of zero represents equal number of turns to both sides, a score of 10 indicates that the animal always turned contra-laterally to the brain lesion. $F_{2,32} = 13.08$, $***p < 0.0001$. B) Chimney Test after 24 hours. This test measures the performance expressed in time (sec) needed to exit a tube backwards (maximum value 120 sec). $F_{2,23} = 74.36$, $***p < 0.001$, $*p < 0.05$. C) Rotarod after 24 hours. This test determines an animals' ability to walk on a rotating beam for at least 60 seconds. $**p = 0.0029$.

4.5.4 TTC stainings

Beneficial effects of BHB regarding infarction volume have been found by Suzuki et al. (2002). In the present study, TTC stainings were done with two animals at maximum because the brains were used for measuring mitochondrial respiration. Accordingly, the images shown are only exemplary and not statistically representative. The infarction area was determined using imageJ. The core region of the saline treated mouse was 3.66% of the total area, the penumbra was 11.13%. In the brain of the BHB treated animal, the core region was 0.68% and penumbra 6.83%.

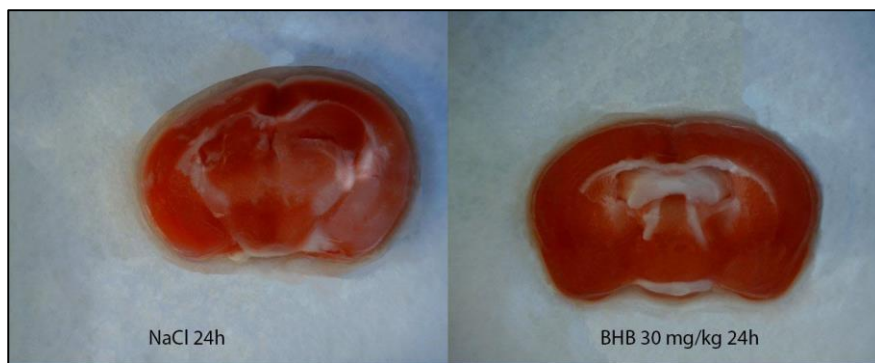


Image 8: TTC stainings 24 hours after reperfusion.

4.6. Respiration 72 hours after reperfusion

4.6.1 Weight loss

Between 24 and 72 hours after stroke the animals visibly deteriorated. Due to motor impairment, they had difficulties eating, which may have been exacerbated by continuous administration of buprenorphine. Within the first 72 hours, the animals lose around 20% of their original bodyweight on average regardless of treatment group (fig. 40)

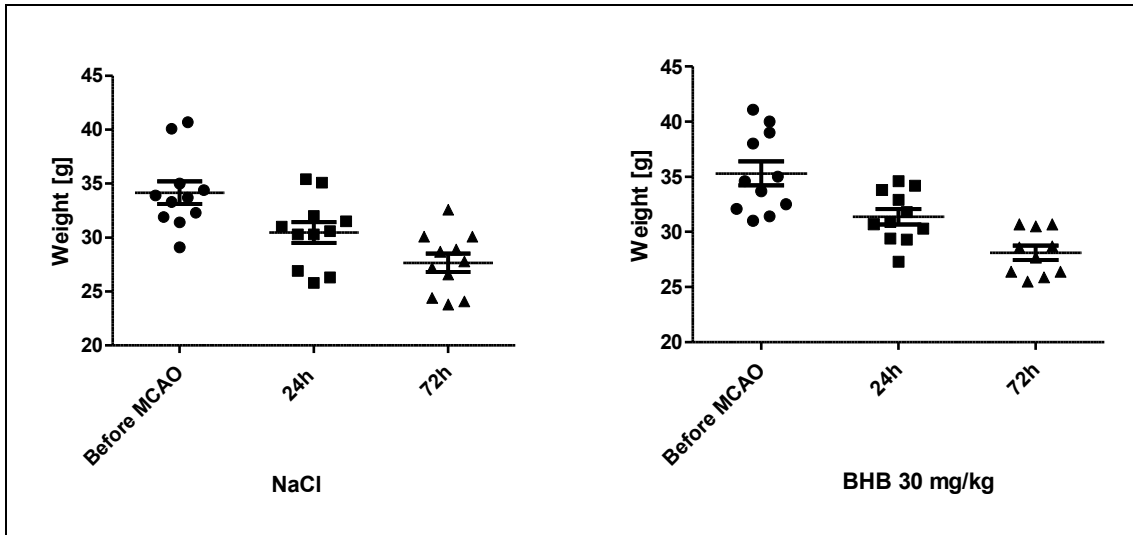


Figure 40: Development of mouse weight after undergoing 90-minute transient cerebral ischemia and receiving either saline (left) or BHB (30 mg/kg) (right) by i.p. injection immediately after reperfusion. Data are scatter box plots (means \pm S.E.M. are indicated) of 11-independent experiments.

4.6.2 Mitochondrial respiration

72 hours after reperfusion, respiration of complexes I and II of saline-treated right hemispheres is still significantly reduced. As 24 hours after reperfusion, respiration was reduced by averagely 58% compared to the healthy left hemisphere. In the group treated with BHB, complex I and II respiration deteriorated. Whereas complex I respiration in the right hemispheres of BHB-treated mice 24 hours after stroke was at 85% compared to the left hemisphere, it was at 66% on average after 72 hours (fig. 41). This trend, however, narrowly fails to reach statistical significance.

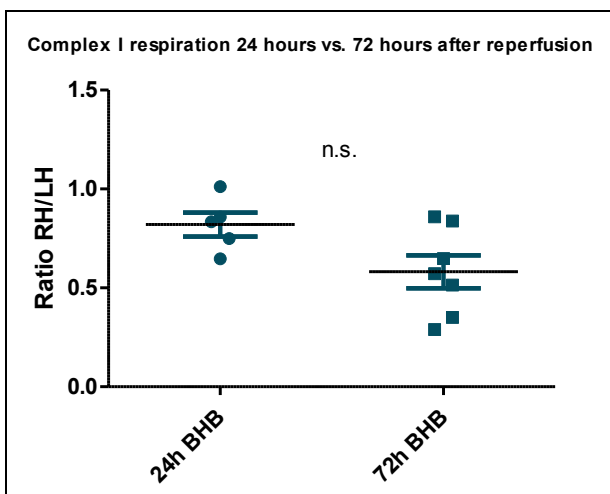


Figure 41: Ratio of mitochondrial complex I respiration of right hemispheres in proportion to unaffected left hemispheres 24 and 72 hours after transient ischemia. Data are scatter box plots (means \pm S.E.M. are indicated) of 5-7 independent experiments. Data were analyzed by unpaired t-test, $p = 0.059$.

At this point, complexes I and II in the right hemisphere were significantly impaired in the BHB-treated group as well. Still, when comparing ratios, there is a trend that complex I is functioning better in the BHB-treated group.

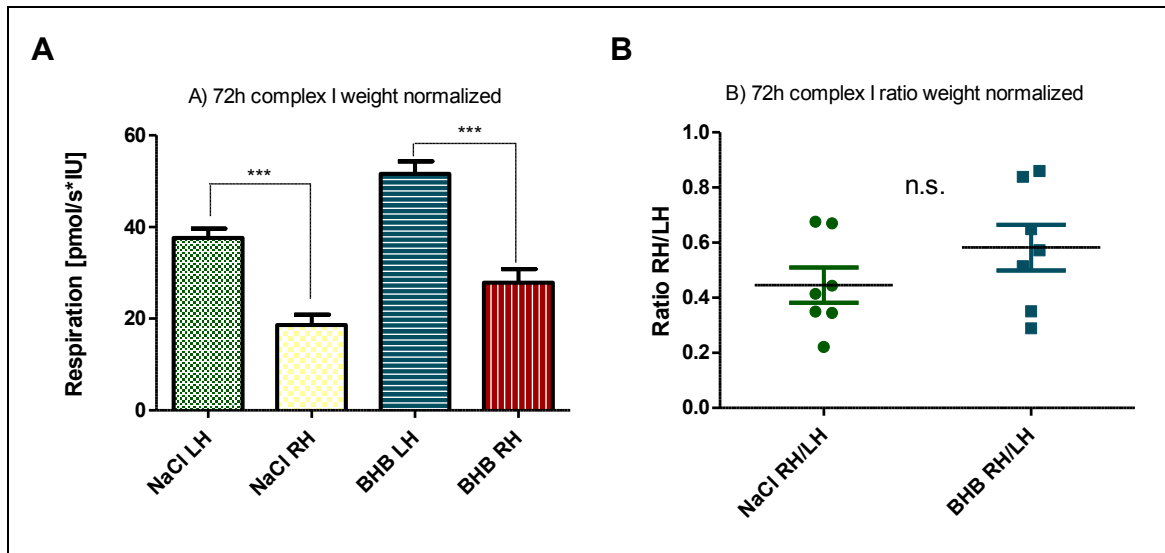


Figure 42: A) Oxygen consumption of complex I, measured by respirometry 72 hours after transient ischemia. Mice underwent transient cerebral ischemia for 90 min and were given saline or BHB (30 mg/kg) by i.p. injection immediately after reperfusion (“NaCl”; “BHB”). Raw data were normalized to mitochondrial protein content. Statistical analysis: Data are vertical column bar graphs (means \pm S.E.M. are indicated) of 14 independent experiments (BHB: N=7, NaCl: N=7). Data were analyzed by one-way ANOVA followed by Newman-Keuls post-test: $F_{3,28}=32.89$, $***p < 0.0001$. B) Ratio of mitochondrial respiration of right hemispheres in proportion to unaffected left hemispheres 72 hours after transient ischemia. Data of 14 independent experiments (BHB: N=7, NaCl: N=7) are shown as scatter box plots (means \pm S.E.M.). Data were analyzed by unpaired t-test, $p = 0.020$.

The ratio of right and left hemisphere for complex II is significantly better in the BHB group than in the saline group.

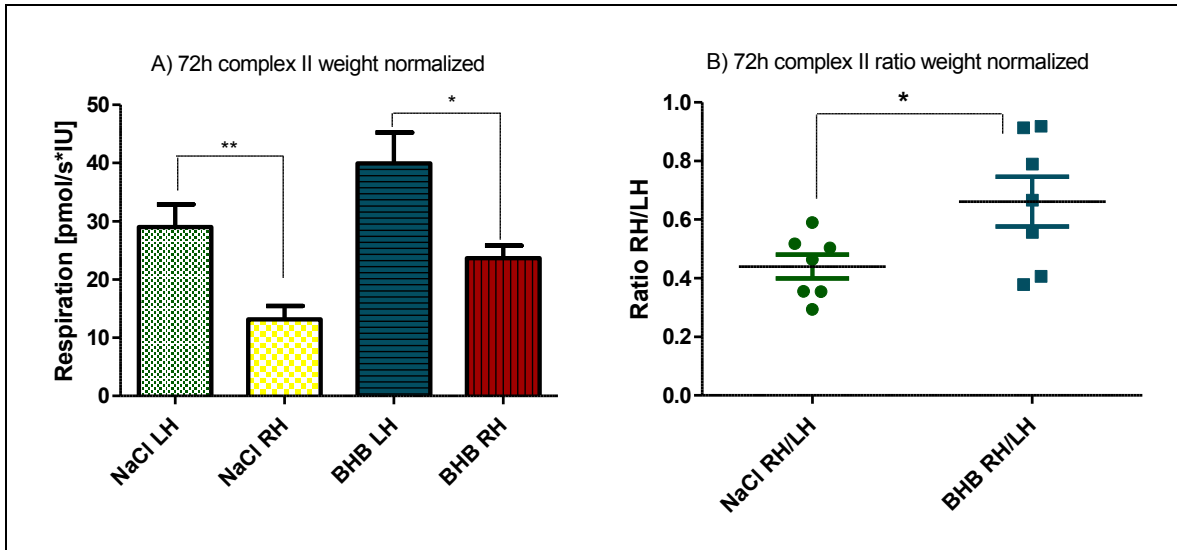


Figure 43: A) Oxygen consumption of complex II, measured by respirometry 72 hours after transient ischemia. Mice underwent transient cerebral ischemia for 90 min and were given saline or BHB (30 mg/kg) by i.p. injection immediately after reperfusion ("NaCl"; "BHB"). Raw data were normalised to mitochondrial protein content. Statistical analysis: Data are vertical column bar graphs (means \pm S.E.M. are indicated) of 14 independent experiments (BHB: N=7, NaCl: N=7). Data were analyzed by one-way ANOVA followed by Newman-Keuls post-test: $F_{3,28}=10.11$, *** $p=0.0002$; ** $p<0.01$; * $p<0.05$. B) Ratio of mitochondrial respiration of right hemispheres in proportion to unaffected left hemispheres 72 hours after transient ischemia. Data of 14 independent experiments (BHB: N=7, NaCl: N=7) are shown as scatter box plots (means \pm S.E.M.). Data were analyzed by unpaired t-test: $F=4.376$, * $p=0.0365$.

As expected, OxPhos respiration is similarly impaired as complex I and II, as is ETS. At this point, even complex IV is damaged in the right hemisphere. None of the ratios are significantly different from another in the two groups (fig. 44), therefore, absolute values are not shown.

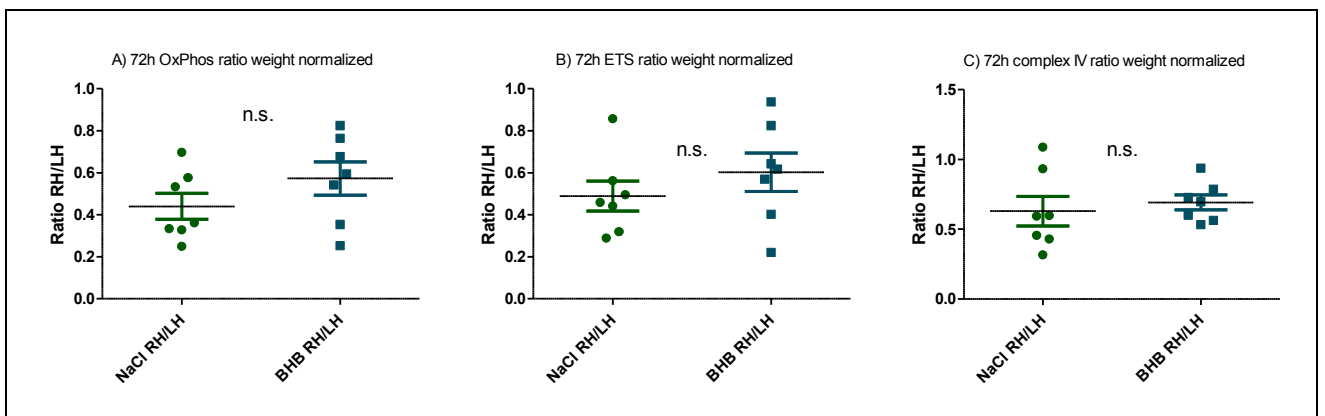


Figure 44: Ratio of mitochondrial respiration of right hemispheres in proportion to unaffected left hemispheres 72 hours after transient ischemia. Statistical analysis: Data are shown as scatter box plots (means \pm S.E.M. are

indicated) of 14 independent experiments (BHB: N=7, NaCl: N=7). Data were analyzed by unpaired t-test: A) Ratio of OxPhos respiration, $p=0.211$. B) Ratio of ETS, $p=0.350$. C) Ratio of complex IV respiration, $p=0.612$.

As observed 60 minutes and 24 hours after reperfusion, citrate synthase normalization neutralizes the effect of stroke and thereby any possible effect of BHB treatment (fig. 45). The following figure shows the ratios of complex I and complex II respiration of right and left hemisphere in both groups in an exemplary fashion, because an effect of BHB was visible here when normalized to weight. Data for complex IV, OxPhos and ETS are not shown.

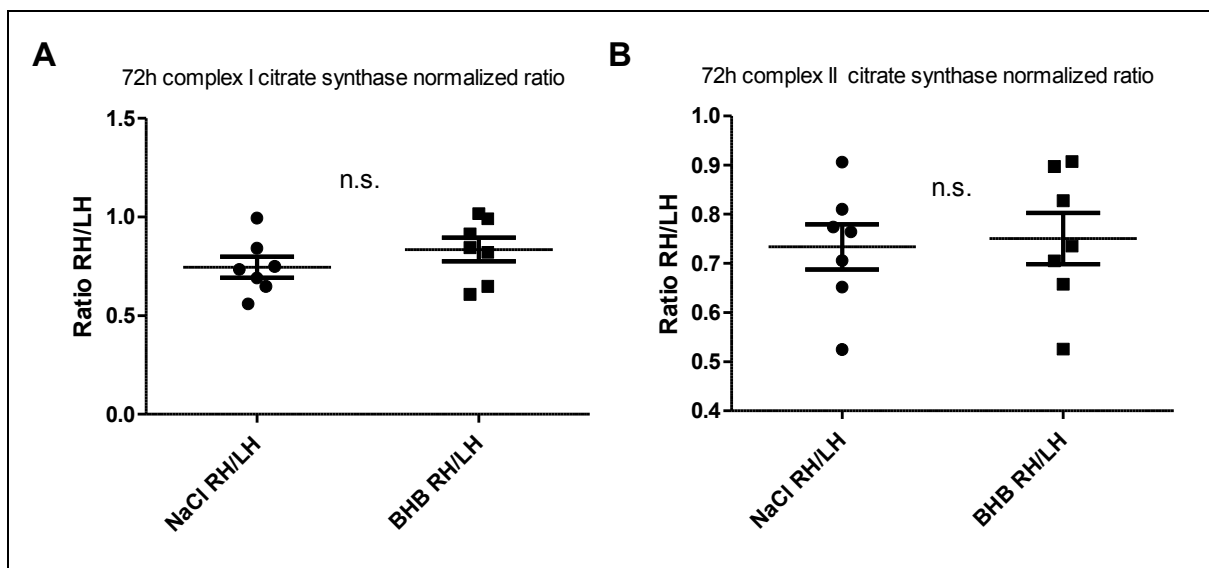


Figure 45: Ratio of mitochondrial respiration of right hemispheres in proportion to unaffected left hemispheres 72 hours after transient ischemia, normalized to citrate synthase activity. Statistical analysis: Data are shown as scatter box plots (means \pm S.E.M.) of 14 independent experiments (BHB: N=7, NaCl: N=7). Data were analyzed by unpaired t-test. A) Ratio of complex I respiration, $p=0.285$. B) Ratio of complex II respiration, $p=0.810$.

4.6.3 Plasma metabolites

In order to monitor metabolic changes after stroke, metabolite levels were determined once again by collecting blood samples after decapitation. Plasma glucose levels in BHB-treated and sham operated mice are almost equal 72 hours after surgery. Glucose levels in saline treated mice, however, are strongly reduced. Lactate levels were significantly increased in the plasma of the BHB treated group when compared to that of saline treated animals. Compared to sham operated animals, the lactate levels seem to be higher in the BHB group, though not statistically significant. Plasma pyruvate levels were increased in both groups that underwent stroke in comparison to sham-operated animals. Pyruvate levels between the two MCAO groups did not differ from each other (fig. 46).

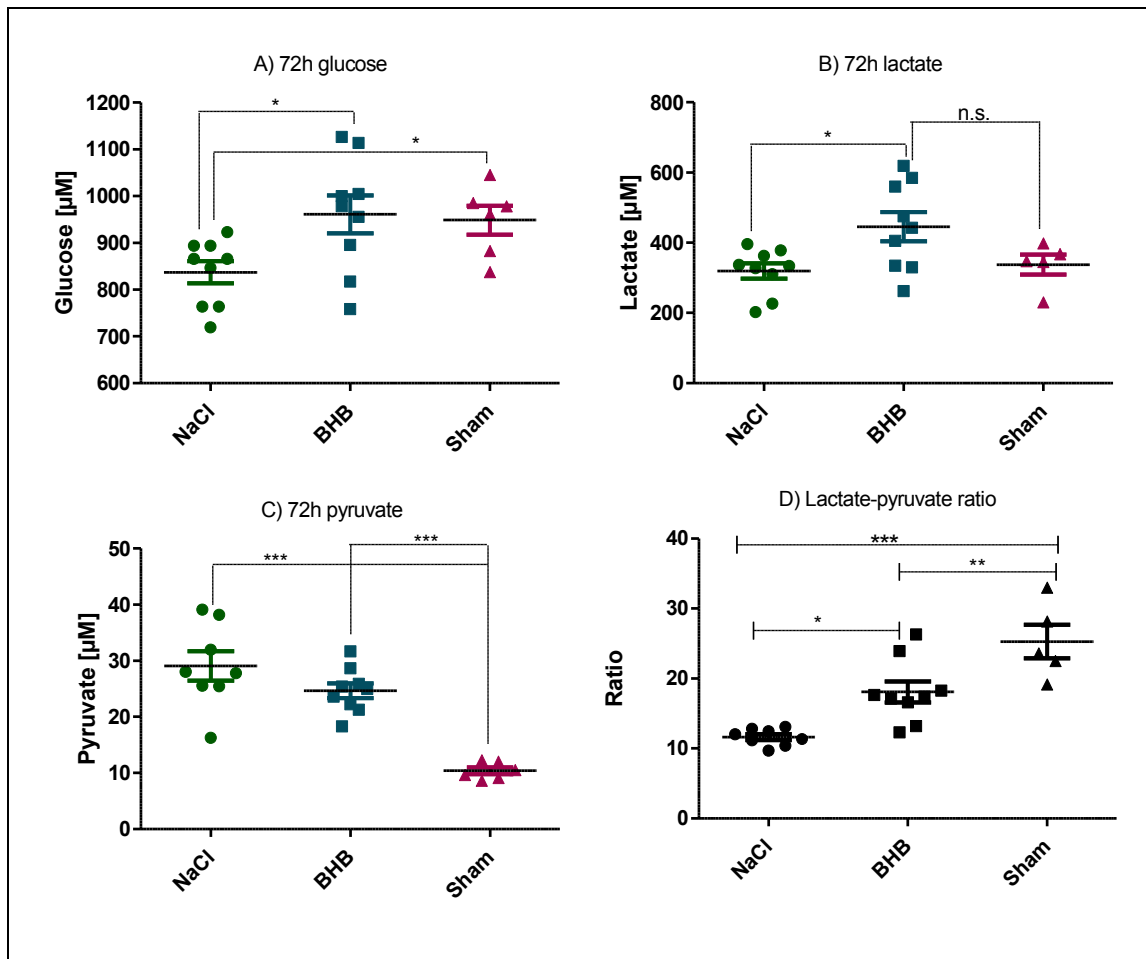


Figure 46: Concentrations of A) glucose, B) lactate and C) pyruvate in plasma. Mice underwent transient cerebral ischemia for 90 min and were given saline or β -hydroxybutyrate (BHB; 30 mg/kg) by i.p. injection immediately after reperfusion (“Stroke Saline”; “Stroke BHB”). For sham-operated mice, the carotid artery was prepared but not occluded. Blood samples were withdrawn 72 hours after BHB administration. Statistical analysis: Data are scatter box plots (means \pm S.E.M) of 23 independent experiments (BHB: N=9, NaCl: N=9, sham: N=5). Data were analyzed by one-way ANOVA followed by Tukey post-test: A) $F_{2,22}= 4.441$, $*p= 0.0246$; B) $F_{2,22}= 4.557$, $*p=0.0234$ C) $F_{2,22}=24.30$, $***p<0.0001$, D) $F_{2,21}= 19.62$, $***p< 0.0001$, $**p< 0.01$, $*p< 0.05$.

4.6.4 Behavioral tests

Corner test

Whereas BHB-treated mice performed significantly better in the Corner test 24 hours after reperfusion, this effect is no longer visible after 72 hours. 24 hours after stroke, the animals turning patterns were still strongly heterogenous – after 72 hours there is a significant preference towards right turns. In saline treated animals, the unilateral turns tend to improve over time (not statistically significant) and the difference to BHB treated animals is no longer significant after 72 hours. Unilateral motor impairment seems to come into effect in a delayed manner in BHB treated animals.

Chimney test

The Chimney test showed no improvement after 72 hours within the groups. However, the BHB treated group performed significantly better after 72 hours than did the saline group. Whereas it took the saline treated animals approximately 22 seconds to walk backwards out of the tube, it took the BHB animals 16 seconds on average. Both groups are clearly impaired in comparison to sham-operated animals that took averagely 2.4 seconds to leave the tube.

Rotarod

In both groups the animals were able to walk longer on the rotating rod than 24 hours after reperfusion (fig. 47). Improvement within the BHB group was on average + 17 seconds (from 32 seconds after 24 hours to 49 seconds after 72 hours), with none of these results reaching statistical significance. The saline group, too, did not improve in a statistically significant manner (improvement by 11 seconds from 36 seconds after 24 hours to 47 seconds after 72 hours). At 72 hours after stroke, the animals in the BHB group no longer performed poorer in the Rotarod test than sham-operated animals.

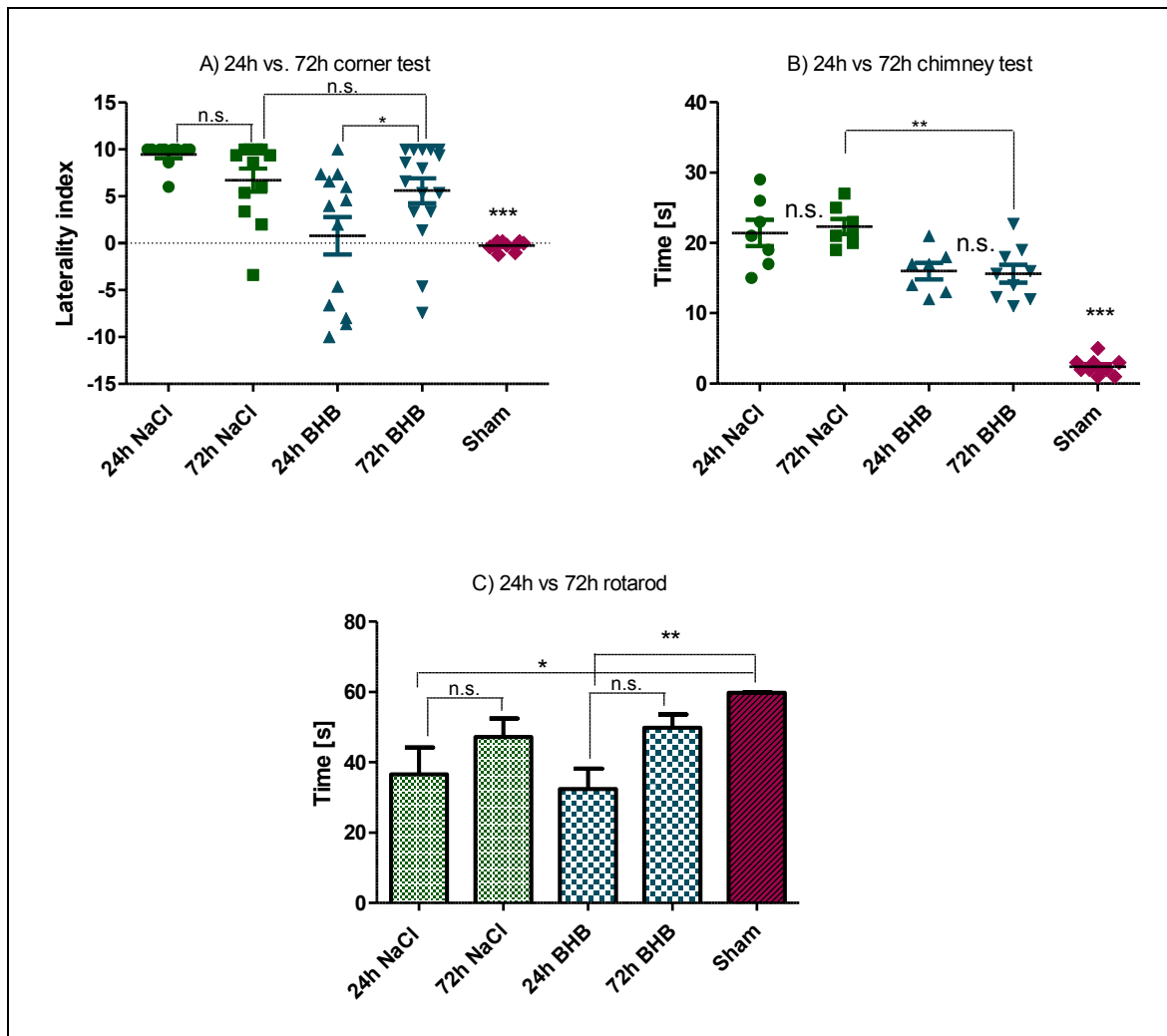


Figure 47: Effect of β -hydroxybutyrate (BHB) on mouse motoric function after 24 and 72 hours. Mice underwent transient cerebral ischemia for 90 min and were given saline or BHB (30 mg/kg) by i.p. injection immediately after reperfusion (“NaCl”; “BHB”). A) and B) Data are scatter box plots (means \pm S.E.M. are indicated) of 10-16 independent experiments. C) Data are vertical column bar graphs (means \pm S.E.M. are indicated) of 10- 16 independent experiments. Data were analyzed by one-way ANOVA followed by Tukey’s post-test. A) Corner Test after 24 and 72 hours. This test determines the preferred side to leave a corner. A score of zero represents equal number of turns to both sides, a score of 10 indicates that the animal always turned contra-laterally to the brain lesion, $F_{4,60} = 8.050$; $***p < 0.0001$, $**p < 0.01$, $*p < 0.05$ B) Chimney Test after 24 and 72 hours. This test measures the performance expressed in time (sec) needed to exit a tube backwards (maximum value 120 sec), $F_{4,39} = 51.37$; $***p < 0.0001$, $**p < 0.01$, $*p < 0.05$ C) Rotarod after 24 and 72 hours. This test determines an animals’ ability to balance on a rotating beam for at least 60 seconds, $F_{4,60} = 4.31$; $**p = 0.0041$, $*p < 0.05$.

4.6.5 TTC staining

This experiment, again, was performed with only two animals in each group and the results are not of any statistical value. Therefore, only two exemplary images are shown (image 9). The core region was 3.05% and 9.14% of the total surface in the saline group, the penumbra 14.37% and 26.00%, respectively. In BHB treated animals, the core area was 5.01% in one animal and 4.92% in the other, and penumbra 14.21% and 16.78%, respectively.

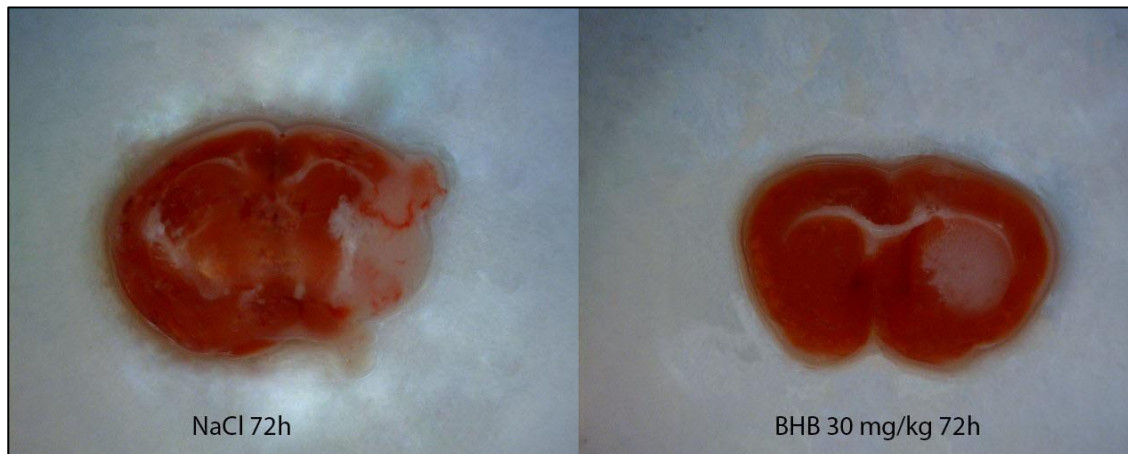


Image 9: Exemplary pictures of TTC stained brain slices from brains obtained 72 hours after reperfusion. Left: TTC stained brain slice of an animal treated with saline solution directly after reperfusion. Right: TTC stained brain slice of an animal treated with BHB 30 mg/kg upon reperfusion.

4.7. Respiration 7 days after reperfusion

4.7.1 Weight development

As shown in the previous section, the animals in both groups suffer from massive weight loss after MCAO (fig. 48)

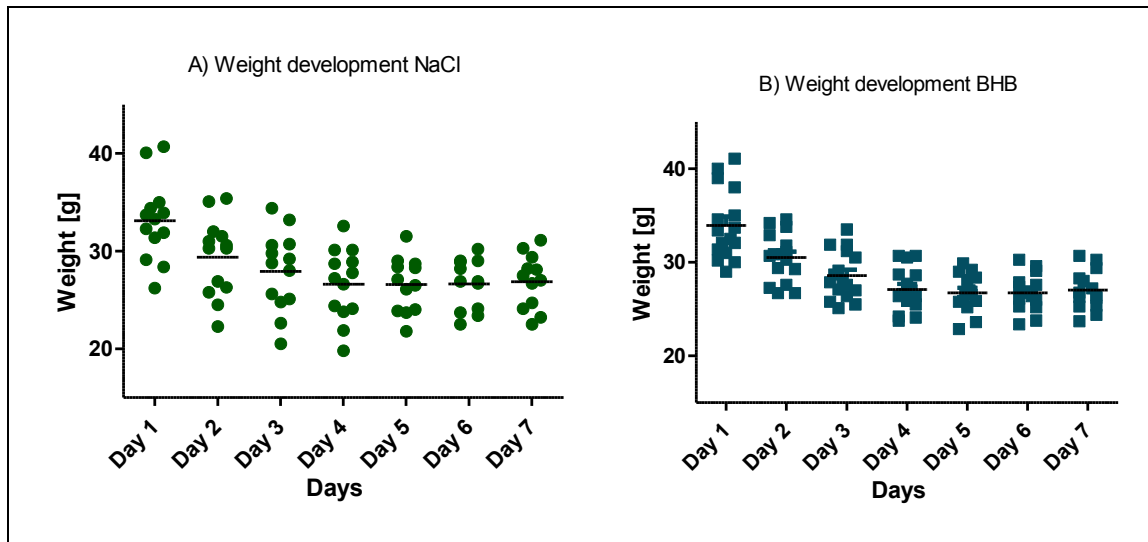


Figure 48: Development of mouse weight throughout one week after undergoing 90-minute transient cerebral ischemia and receiving either saline (left) or BHB (30 mg/kg) (right) by i.p. injection immediately after reperfusion. Data are shown as grouped column scatter (mean) of 7-16 animals.

Regardless of treatment, the animals lose approximately 20% of their initial weight within the first 72 hours. Weight loss then stabilizes and tends to recover after 7 days (fig. 49).

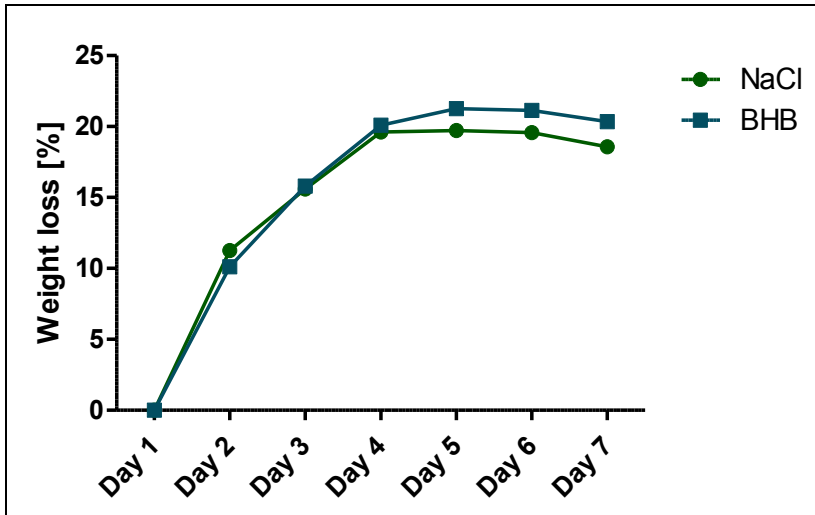


Figure 49: Weight loss in percent throughout one week after undergoing 90-minute transient cerebral ischemia and receiving either saline (left) or BHB (30 mg/kg) (right) by i.p. injection immediately after reperfusion.

4.7.2 Mitochondrial respiration

One week after stroke complex I respiration remains strongly impaired in both groups (fig. 50). In saline treated animals, respiration in the right hemisphere is reduced by averagely 50%. The right hemispheres of BHB treated mice seem to be less affected by stroke than those of saline treated animals. This effect, however, is no longer statistically significant.

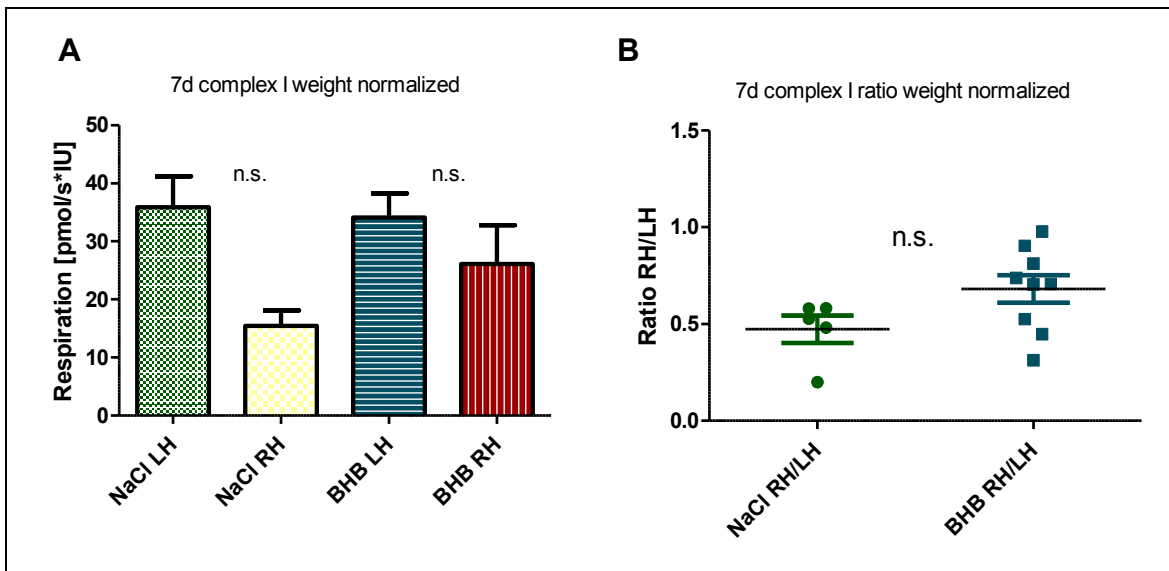


Figure 50: A) Oxygen consumption of complex I measured by respirometry 7 days after transient ischemia. Mice underwent transient cerebral ischemia for 90 min and were given saline or BHB (30 mg/kg) by i.p. injection immediately after reperfusion ("NaCl"; "BHB"). Raw data were normalised to mitochondrial protein content. Statistical analysis: Data are vertical column bar graphs (means \pm S.E.M. are indicated) of 14 independent experiments (BHB: N=9, NaCl: N=5). Data were analyzed by one-way ANOVA followed by Newman-Keuls post-test; $F_{3,25} = 2.472$, $p = 0.089$ Right: Ratio of mitochondrial respiration of complex I of right hemispheres in

proportion to unaffected left hemispheres 7 days after transient ischemia. Data of 14 independent experiments (BHB: N=7, NaCl: N=7) are shown as scatter box plots (means \pm S.E.M.). Data were analyzed by unpaired t-test; $p=0.085$.

Complex II respiration, which was significantly improved in BHB treated animals 72 hours after reperfusion, is no longer significantly different from saline treated animals. Saline treated animals seem to recover from stroke as well (from 46% to 64% of function compared to left hemisphere), whereas recovery in BHB treated animals stagnates (66% to 78% compared to left hemisphere).

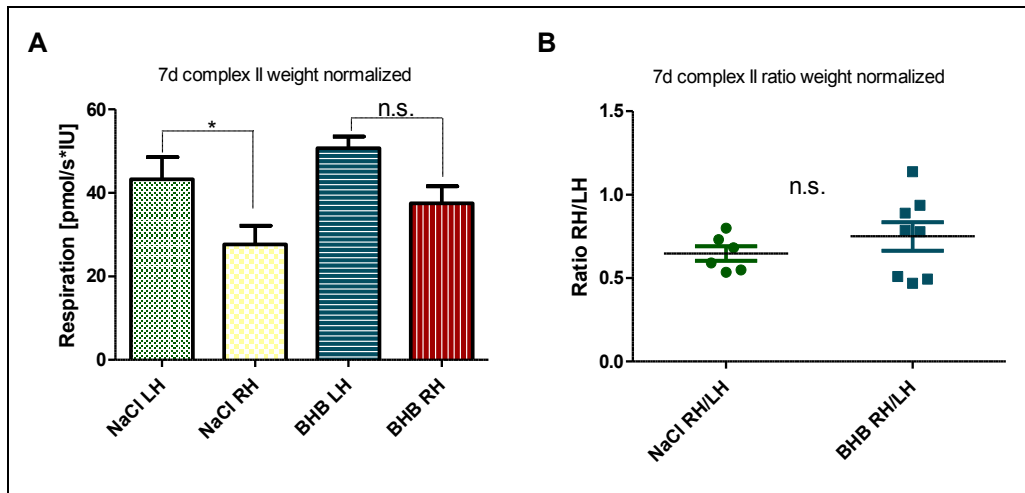


Figure 51: A) Oxygen consumption of complex II measured by respirometry 7 days after transient ischemia. Mice underwent transient cerebral ischemia for 90 min and were given saline or BHB (30 mg/kg) by i.p. injection immediately after reperfusion (“NaCl”; “BHB”). Raw data were normalised to mitochondrial protein content. Statistical analysis: Data are vertical column bar graphs (means \pm S.E.M. are indicated) of 14 independent experiments (BHB: N=9, NaCl: N=5). Data were analyzed by one-way ANOVA followed by Newman-Keuls post-test: $F_{3,28}=5.729$, $**p=0.0040$. B) Ratio of mitochondrial respiration of complex II of right hemispheres in proportion to unaffected left hemispheres 7 days after transient ischemia. Data of 14 independent experiments (BHB: N=7, NaCl: N=7) are shown as scatter box plots (means \pm S.E.M.). Data were analyzed by unpaired t-test; $p=0.354$.

As expected, OxPhos respiration is similarly impaired as complex I and II. Ratios, however, do not significantly differ from one another, as observed in earlier experiments. ETS and complex IV as well do not differ from each other. Therefore, only ratios are shown (fig. 52).

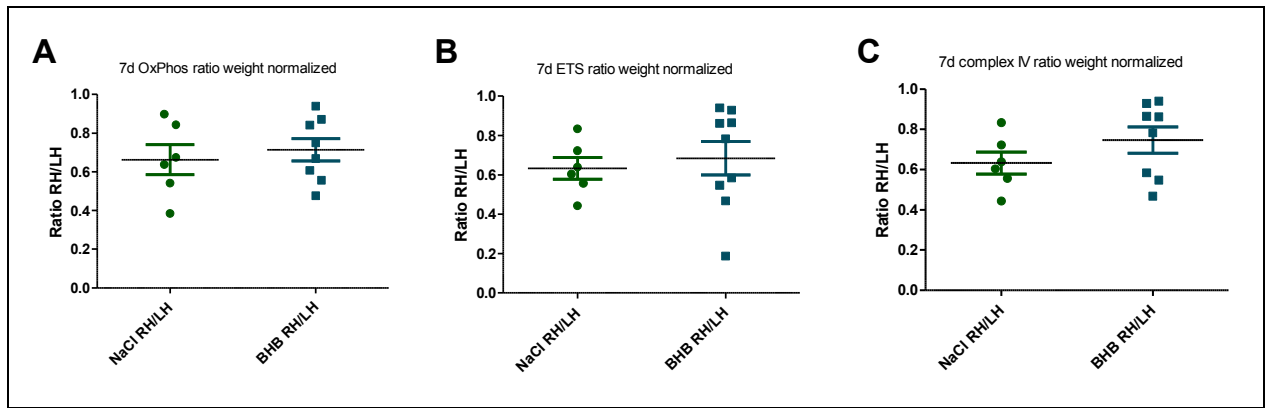


Figure 52: Ratio of mitochondrial respiration of right hemispheres in proportion to unaffected left hemispheres 7 days after transient ischemia. Statistical analysis: Data are shown as scatter box plots (means \pm S.E.M. are indicated) of 14 independent experiments (BHB: N=9, NaCl: N=5). Data were analyzed by unpaired t-test: A) Ratio of OxPhos respiration, $p=0.601$. B) Ratio of ETS, $p=0.659$. C) Ratio of complex IV respiration, $p=0.230$.

4.7.3 Plasma metabolites

7 days after reperfusion glucose levels have normalized, also in the saline treated group, and no longer differ from sham-operated animals. Lactate levels remain elevated compared to sham animals. This effect is significant in the saline treated group, but not in BHB animals. There is no statistical difference between both stroke groups.

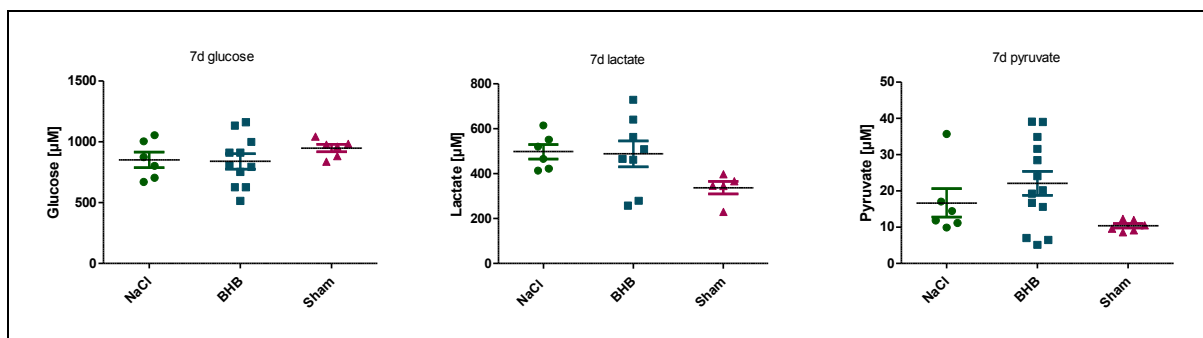


Figure 53: Concentrations of A) glucose, B) lactate and C) pyruvate in plasma. Mice underwent transient cerebral ischemia for 90 min and received saline or β -hydroxybutyrate (BHB; 30 mg/kg) by i.p. injection immediately after reperfusion (“Stroke Saline”; “Stroke BHB”). For sham-operated mice, the carotid artery was prepared but not occluded. Blood samples were withdrawn 72 hours after BHB administration. Statistical analysis: Data are scatter box plots (means \pm S.E.M) of 5-13 independent experiments (BHB: N=13, NaCl: N=6, sham: N=5). Data were analyzed by one-way ANOVA followed by Tukey post-test. A) $F_{2,22}=0.839$; $p=0.447$. B) $F_{2,18}=3.040$; $p=0.076$. C) $F_{2,24}=2.889$; $p=0.077$.

4.7.4 Behavioral tests

Corner test

As in the experiments at the previous time points, BHB treated animals turns are more heterogenous than those of saline treated animals. This effect, however, fails to reach statistical significance. In both groups there is still a nearly exclusive preference for right turns.

Chimney test

The time that it takes mice to exit the vertical tube backwards remains unchanged compared to 72 hours. Saline treated animals still need an average of 22.8 seconds, BHB treated animals 16.3 seconds. At this point, with respect to this experiment, the effect of BHB is significant. Still, both groups remain strongly impaired compared to sham-operated animals.

Rotarod

With exception of two animals in each group, all animals were able to walk on the rotating rod for 60 seconds. This is an improvement of 8 seconds on average in the saline group and 6 seconds in the BHB group compared to experiments 72 hours after reperfusion (saline 47.3 seconds after 72 hours, BHB 49.8 seconds). At this point the animals in both stroke groups perform no different than do those in the sham operated group (fig. 54).

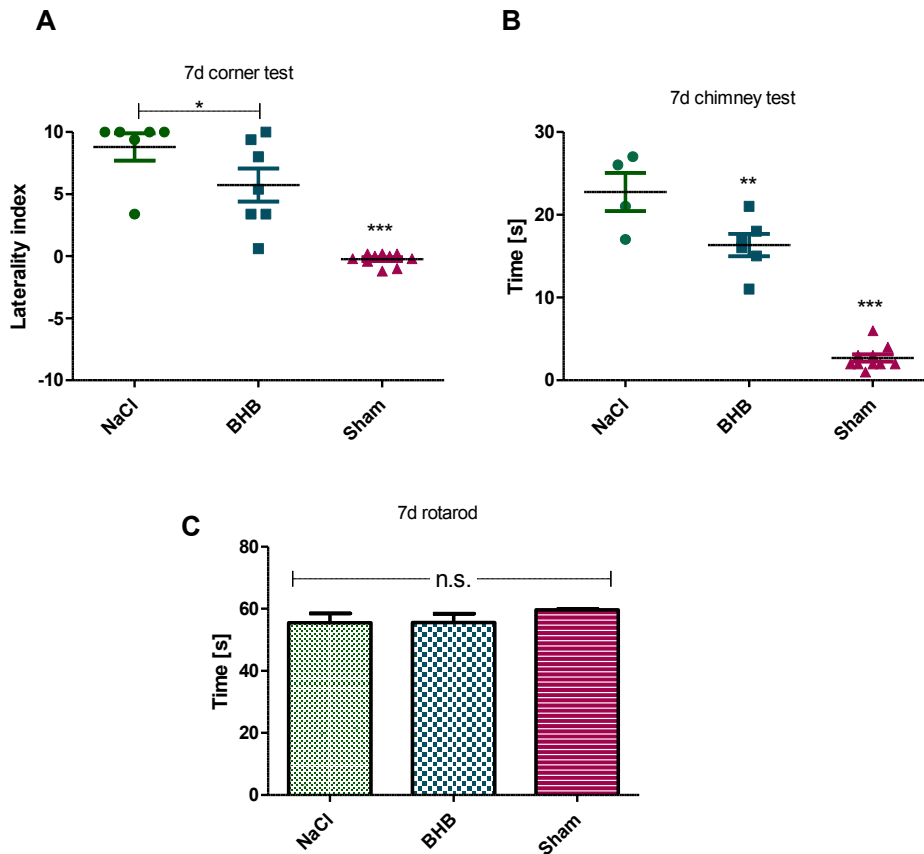


Figure 54: Effect of β -hydroxybutyrate (BHB) on mouse motoric function 7 days after transient cerebral ischemia. Mice underwent transient cerebral ischemia for 90 min and were given saline or BHB (30 mg/kg) by i.p. injection immediately after reperfusion (“NaCl”; “BHB”). A) Corner Test after 7 days. This test determines the preferred side to leave a corner. A score of zero represents equal number of turns to both sides, a score of 10 indicates that the animal always turned contra-laterally to the brain lesion. B) Chimney Test after 7 days. This test measures the performance expressed in time (sec) needed to exit a tube backwards (maximum value 120 sec). C) Rotarod after 24 and 72 hours. This test determines an animals’ ability to walk on a rotating beam for at least 60 seconds. A) and B) Data are scatter box plots (means \pm S.E.M. are indicated); C) Data are vertical column bar graphs (means \pm S.E.M. are indicated) of 6-10 independent experiments. Data were analyzed by one-way ANOVA followed by Newman-Keuls post-test A) $F_{2,22} = 30.38$; $***p < 0.0001$, $*p < 0.05$. B) $F_{2,19} = 86.80$; $***p < 0.0001$, $**p < 0.01$. C) $F_{2,22} = 1.591$; $p = 0.228$.

5. Discussion

First, this chapter will discuss the methods used to obtain the results of this work before discussing the results themselves.

5.1 Discussion of methods

5.1.1 Microdialysis

In vivo-microdialysis is a minimally invasive sampling technique that is used to obtain and analyze small, solved molecules like energy metabolites (e.g. glucose, lactate, pyruvate) or neurotransmitters (acetylcholine, for example) from the extracellular space.

Compared to other *in vivo* techniques, microdialysis has some advantages and disadvantages that must be taken into consideration.

The use of a stereotaxic device allows microdialysis in nearly all regions of the brain. Samples of various compounds can be taken simultaneously from conscious and freely moving animals. The semi-permeable membrane is a physical barrier between perfusate and tissue, and it functions as a filter for larger compounds. The probes used in the experiments in this work had a molecular cut-off of 30 kDa, meaning that the obtained samples are virtually free from cells or proteins. Thus, no further cleaning steps are required prior to analysis. Furthermore, the semi permeable membrane has a protective effect, because it shields tissue from turbulent currents of the perfusion solution. Finally, there is the advantage that substances can be infused directly into the brain through retrodialysis. One of the disadvantages of microdialysis is local damage of brain tissue. Early after implantation, the integrity of the blood brain barrier (BBB) is impaired. Sumbria et al. (2011) found the blood brain barrier to be higher permeable only immediately (15 minutes) after probe implantation. The consequence of decreased integrity of the BBB is reduced blood flow and disrupted release of neurotransmitters (Benveniste and Diemer 1987). 1.5 hours after implantation the blood brain barrier had already been restored. Measurement of metabolites, on the contrary, were decreased compared to basal levels (Sumbria et al. 2011). This problem is avoided by starting microdialysis experiments 18-24 hours after probe implantation, as the integrity of the blood brain barrier is restored after 18 hours (Benveniste and Diemer 1987). Due to low time resolution of 1-10 minutes, changes, especially of neurotransmitter levels, do not reflect synaptic dynamics but rather long-term changes of neuronal activity. Furthermore, the direction of flow cannot be specified through this method. The time resolution depends on the inner volume of the probes, diffusion rate of the compound of interest through the membrane, and perfusion rate, which is usually 1-2 $\mu\text{L}/\text{min}$. Microdialysis allows the determination of substances in the extracellular space.

Absolute concentrations can be approximated by correcting measured values with the *in vitro*-recovery rate. For determining recovery *in vitro*, the probe is perfused with a solution that contains substances in known concentrations. The dialysate is then measured and the quotient from measured concentration and true concentration equals the recovery rate.

Alternatively, recovery can be determined *in vivo*. Korth et al. (2001) describe various methods that can be used for *in vivo*-recovery. They will be briefly discussed in the following paragraph.

Zero flow method

The perfusion rate is gradually lowered, and the concentration of the analyte is measured in the dialysate. By means of non-linear regression, the concentration at the flow rate of zero is determined. This concentration is equivalent to a recovery rate of 100% and to the analyte concentration in the extracellular space. As equilibrium has to be established at all flow rates, this method takes a lot of time. The method's biggest advantage is that it can be applied to any analyte.

Near-equilibrium method

A microdialysis probe with a large membrane for exchange is perfused with the lowest flow rate possible. This way, an equilibrium between the analyzed compartment and microdialysate is established. A problem of this method are the small volumes of the resulting dialysate. On the other hand, it is very precise and yields recoveries of 100% at flow rates as low as 0.3 $\mu\text{L}/\text{min}$.

No net flux method

The underlying principle of this method is bidirectional flux through the semi permeable membrane of the microdialysis probe. The analytes are added to the perfusion solution in various concentrations that are higher or lower than expected in the dialyzed tissue. The concentrations in the dialysate are graphically plotted against the applied concentrations. Then, by means linear regression, the concentration is determined at which net transport no longer takes place. The determined concentration is equivalent to the analyte concentration in the extracellular space. This method is particularly suitable for determining extracellular concentrations of endogenous compounds. It is not as applicable for exogenous substances like drugs, as extracellular concentrations of the compound must be constant throughout measurement.

Retrodialysis

Retrodialysis is predominantly used in pharmacological investigations. In retrodialysis, the agent is added to the perfusion solution and the decrease of concentration is determined from the dialysate. This method is most suitable for determining the recovery rate of exogenous substances (Korth & Klein, 2001).

Finally, there is the possibility to determine analytes by using an internal standard.

Diffusion in tissue (brain tissue, in this work) is generally slower than in an aqueous solution, due to lower liquid volume and higher diffusion path (Benveniste and Hüttemeier 1990). Variations in results while using microdialysis in this work were most likely due to the fact that the probes are self-built and implanted manually. It must be assumed that the probes and surgeries weren't always identical. Therefore, due to methodical variations in addition to biological variations, increased S.E.M.s can be seen when using this method. In this work, the focus was on determining changes of metabolite concentrations. Absolute concentrations were of secondary interest. Therefore, the recovery rate was determined through the relatively simple *in vitro*- method.

In conclusion, microdialysis is a sampling method that, though minimally invasive, does very little harm to the laboratory animal. It allows the determination of metabolites, neurotransmitters and other small molecules, all at once. Through *in vivo*- recovery determination, compound concentrations can be measured precisely. The dialysate that is yielded from microdialysis can be analyzed in a wide range, for example by GC-MS, making detection of several small molecules possible. This is not the case for any other sampling method that can be performed *in vivo*. A limiting factor may be low concentrations of the analyzed compound in combination with the small volumes that result from microdialysis, as flow rates are as low as 1-10 $\mu\text{L}/\text{min}$. As a consequence, highly sensitive analytical methods are required.

5.1.2 Intraluminal suture middle cerebral artery occlusion (MCAO) model

As briefly discussed in section 2.4.2, the occlusion of the middle cerebral artery caused by the intraluminal suture model is a reproducible method for models of cerebral ischemia. Because this model does not require craniectomy, it can be considered as minimally invasive, and it allows transient as well as permanent ischemia. Other possibilities for inducing MCAO in rodents will be discussed in the next section 5.1.3.

Depending on how far the suture is advanced into the artery, the MCA may be blocked selectively or together with the posterior communicating artery. Either way yields reproducible infarction areas in frontoparietal cortex and lateral caudoputamen (Durukan and Tatlisumak 2007). Besides, silicone coated sutures are available in different sizes, making this stroke model possible in various animals (e.g. mice, rats, dogs) (Howells et al. 2010). However, there are disadvantages of the intraluminal suture model. The most severe disadvantage is the possibility of rupture of vessels and consequently subarachnoid hemorrhage, leading to sudden death of the animal shortly after or during surgery. Especially in less experienced experimenters, where the suture may have to be repositioned into the correct location, or if the suture is advanced too high into the MCA with too much force, this occurs more frequently.

The opposite, insufficient blockade of the middle cerebral artery, can also become a disadvantage, as perfusion, in that case, is too high to imitate an ischemic stroke. This can happen if the suture is placed too hesitant, or if the suture is advanced into the maxillary artery (PPA) (image 10). Insufficient stroke can be detected through Laser-Doppler measurement and corrected by repositioning the suture or advancing it further up the internal carotid artery.

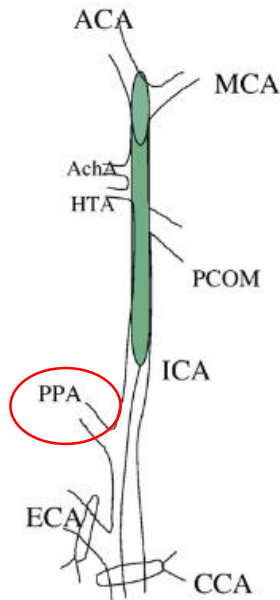


Image 10: Intraluminal middle cerebral artery occlusion model. Image shows Koizumi's method where the silicone coated suture is inserted in the CCA and blocks the MCA, AchA and HTA. ACA, anterior carotid artery; AchA, anterior choroidal artery; CCA, common carotid artery; ECA, external carotid artery; ICA, internal carotid artery; HTA, hypothalamic artery; PPA, pterygopalatine artery (maxillary artery); PCOM, posterior communicating artery. Image modified from Durukan and Tatlisumak (2007).

Further, there is the translational issue – as mentioned in section [1.1.5.](#), the relevance of any kind of animal stroke is questionable, as most neuroprotective agents fail when tested in humans after successful preclinical studies. Timing of the treatment is critical in this respect. Mice and rats per se are suitable for imitating stroke in humans, because they as well have a circle of Willis and are thereby similar to humans regarding the anatomy of cerebral blood vessels. However, in experimental stroke models, mostly young animals with no preexisting cardiovascular or metabolic diseases are used. Studies in the past have had contradictory results with regard to whether older animals are more susceptible to larger infarct volumes. Whereas Wang et al. (2003) found no correlation of rat age and extent of stroke, Sieber et al. (2011) found beneficial effects of older age in regard to infarct volumes, and Liu and McCullough (2011) found older animals to be more susceptible to stroke. Sieber et al. (2011) conclude that older animals may not have as strong inflammatory reactions to stroke, whereas

Zhang et al. (2005) argue that reduced angiogenesis and poor neurological recovery cause older animals to be more susceptible to ischemic stroke.

In addition, there are studies that suggest that even different animal strains react more or less sensitive to stroke. This effect is so significant that infarct size and even dynamics of the penumbra vary strongly in different strains of animals. A possible explanation is the heterogeneous cerebrovascular anatomy between strains (Bardutzky et al. 2005). Differences within the same strain were also seen when animals of the same strain were obtained from different vendors. Furthermore, there is a well-known difference between sexes. Female animals suffer from smaller infarct sizes than do males. However, this observation can no longer be seen when female animals are gonadectomized at young age (Manwani et al. 2015). To minimize variabilities due to strain, gender and age, only female mice of a single strain, CD-1, aged six to eight weeks, by the vendor Charles River, were used in the experiments of this work.

5.1.3 Other MCAO models

There are four other procedures by which MCAO can be induced in rodents. In this chapter, these methods will be described briefly and discussed as to why they were less suited for the experiments in the present work.

Craniectomy model

As indicated by the name, this MCAO model requires craniectomy, i.e. drilling of the skull bone, as well as the dissection of the dura mater to access the MCA. Once exposed, the MCA is cauterized and dissected, leading to permanent occlusion of the artery (Tamura et al. 1981). This model was later modified by using microaneurysm clips or ligatures to enable transient occlusion (Fluri et al. 2015). Another possibility to induce ischemic stroke using craniectomy is through three-vessel occlusion. In this case, both common CCAs and the MCA are occluded. The occlusion can be permanent through cauterization or transient through microclips. Infarct sizes resulting from the craniectomy-based models depend on whether the occlusion is permanent or transient (Yanamoto et al. 2003). Advantages of models based on craniectomy are the reproducibility of infarct sizes, the possibility of transient or permanent occlusion and that success of the procedure can be confirmed visually (Fluri et al. 2015).

The major disadvantage of the model is the craniectomy itself. The procedure may damage the cortex below the skull, or cause ruptures of blood vessels, by drilling or cauterization. Moreover, intracranial pressure and integrity of the blood-brain barrier are affected by craniectomy. Finally, this method, as the intraluminal MCAO model, requires considerable surgical skills.

As it was not sure if later experiments would require microdialysis paired with MCAO, a craniectomy-based model was not considered for the experiments in the present work.

Photothrombosis model

In the photothrombosis model, ischemia is caused by intravascular photo-oxidation. The resulting stroke affects the cortex and, in part, the striatum (Watson et al. 1985; Kuroiwa et al. 2009). Ischemia is induced by i.p. or i.v. injection of photoactive dyes (e.g., erythrosin B), and activated by radiation of the skull at the wavelength needed for photoactivation. The core region can be further specified by using a stereotaxic device (Watson et al. 1985; Kleinschnitz et al. 2008). One of the main advantages of this model is that it is noninvasive. Furthermore, mortality is low and it is highly reproducible. The main limitation to this model is that it does not lead to the formation of an ischemic penumbra (Fluri et al. 2015). Thus, the photothrombosis model, despite being minimally to noninvasive, was unsuited for the purpose in this work.

Endothelin-1 model

Endothelin-1 (ET1), a potent vasoconstrictive peptide, is either injected into the exposed MCA, administered as an intracerebral injection using a stereotaxic device, or injected onto the cortical surface. The result of ET1 injection into the MCA and intracerebral injection is a dose-dependent ischemic stroke, similar to permanent MCAO (Fluri et al. 2015). Cortical ET1 injection leads to infarctions in all cortical layers. This model provides ischemic strokes with perfusion reduced by 70-90% for several hours (Biernaskie et al. 2001). Further advantages of the ET1 model are low mortality and versatility in stroke regions, as ischemia can be induced in superficial or deep regions of the brain. The main limitation of this model is the fact that ET1 receptors and ET1 converting enzymes are expressed by neurons and astrocytes. Uesugi et al. (1998) found ET1 to cause astrocytosis and axonal sprouting, which may distort the interpretability of experiments that investigate neural repair.

As it was not sure if later experiments would require microdialysis paired with MCAO, model that requires drilling of the skull was not chosen for the experiments in the present work.

Embolic stroke model

There are two categories into which the embolic stroke model can be divided – stroke models induced in microspheric or macrospheric manner, and thromboembolic clot models.

For microsphere-induced stroke, spheres with a diameter of 20-50 μM (e.g., dextran, ceramic or TiO_2) are injected into the MCA or into the ICA (through the ECA) by means of a microcatheter. Via blood flow, the microspheric compounds are then carried into the circle of Willis. The result of this model

are multifocal and heterogeneous ischemic infarctions with lesion sizes increasing slowly up to 24 hours after injection. Furthermore, the extent stroke depends on size and dosage of the injected particles (Mayzel-Oreg et al. 2004; Fukuchi et al. 1999). Macrosphere- induced stroke is established through injection of particles of 100-400 μM diameter into the ICA. This model leads to focal ischemia comparable to the suture model. Furthermore, it does not block blood supply to the hypothalamus, preventing ischemia in hypothalamic regions, which can lead to hyperthermia in the suture MCAO model (Gerriets et al. 2003).

In the thromboembolic clot model, either spontaneously formed or thrombin-induced clots from autologous blood are injected into the ICA (via ECA), or thrombin is injected into the intracranial part of the ICA or into the MCA (Overgaard et al. 1992; Niessen et al. 2003; Zhang et al. 1997b; Ansar et al. 2014). The thromboembolic clot model, compared to other MCAO models, is most similar to ischemic stroke in humans. As ischemia in this model is caused by thrombi, it allows investigations of thrombolytics alone or in combination with other compounds of interest. However, there are some limitations to this model. The infarct volume is highly variable and depends on several factors: size and elasticity of the clot determine the infarct size, as well as endogenous thrombolysis. Endogenous thrombolysis, which can be found between 1 hour to 24 hours after clot injection, leads to uncontrolled recanalization. The speed at which a clot disintegrates depends on the composition of the clot and its concentrations of thrombin and erythrocytes (Overgaard et al. 1992).

Altogether, this model, although most similar to human stroke, has many disadvantages, making the method unsuited for the experiments of this work. Multifocal ischemia with variable infarction sizes and localizations and uncontrolled endogenous thrombolysis yield a non-reproducible MCAO.

In conclusion, the intraluminal suture model was the most suitable model for the experiments in this work, as it results in reproducible occlusion of the MCA, success of the surgery can be monitored by means of the Laser-Doppler and occlusion can be upheld stably for the desired time. Intraluminal MCAO results in a considerable penumbra, which was required for investigating the effects of BHB (Li and Murphy 2008). Additionally, microdialysis would have been possible if needed.

5.1.4 Measurement of mitochondrial respiration with the Oroboros oxygraph

The oroboros oxygraph allows exact determination of mitochondrial oxygen consumption (Hütter et al. 2006). The biggest benefit of using this analysis method is that, by addition of various substrates and inhibitors of the respiratory chain, isolated activity of the complexes I, II and IV, leak respiration, total respiration (OxPhos) and the electron transport system (ETS) can be measured. All other methods that can be used to assess mitochondrial activity are enzyme assays that allow determination of each

complex, but separately and not in one single experiment. Another method by which mitochondrial activity can be investigated, is by use of the Seahorse analyzer. Through this method, ATP-dependent respiration, proton leak respiration and maximum respiration can be determined. Investigation of precise complex respiration is not possible using the Seahorse analyzer. As this work was aimed at investigating possible beneficial effects of BHB on individual mitochondrial complexes, the Oroboros oxygraph was the most precise analyzer for this purpose.

5.1.5 Measurement of mitochondrial respiration in regard to hypoxia

When investigating mitochondria that have been exposed to hypoxic conditions as in this present work, the conditions in which they are analyzed must be taken into consideration as well. As mitochondria are removed from their physiological environment and transferred into a respiratory medium, possible damage of the mitochondria through change of oxygen concentrations must be ruled out. Impairment of respiratory capacities following ischemia or other forms of hypoxia were considered by the manufacturer (Gnaiger 2001). According to their studies, mild hypoxia protects from oxidative stress and leads to economization of electron transport through the respiratory chain. High oxygen levels would inhibit oxidative phosphorylation and lead to less efficient mitochondrial respiration (Gnaiger et al. 2000). The studies mentioned above were performed to determine the ideal oxygen concentrations in the chambers of the oxygraph. Mitochondrial damage caused by stroke, of course, is far more severe. Ischemic stroke has no protective properties of oxidative stress, but oxidative stress occurs in a very pronounced manner upon reperfusion (Manzanero et al. 2013; Dirnagl et al. 1999). Nonetheless, the analysis of ideal oxygen concentrations in the respiratory chambers of the oxygraph makes a more detailed comparison of hypoxic conditions *in vivo* due to ischemia, and oxygen conditions throughout the process from isolation of mitochondria to respiration measurement plausible. Immediately after decapitation, the brain is transferred into the respiration medium MirO5, a medium with the composition to stabilize mitochondrial structures and provide glucose and oxygen. Furthermore, for the isolation steps a protease inhibitor is added to MirO5 to prevent degradation of mitochondrial structures. Optimum conditions for mitochondrial respiration are maintained in the oxygraph and throughout analysis. Additionally, all substrates are added in sufficient amounts during the experiment. *In vivo*, in contrast, conditions are no longer optimal for mitochondrial respiration after ischemia, as oxygen and glucose become scarce. Shortage of oxygen and glucose lead to secondary scarcity of further substrates, strongly impairing mitochondrial respiration (Sims and Muyderman 2010). Mitochondria used in the experiments of the present work underwent ischemia of 90 minutes *in vivo* before isolation. This is the most physiological way to expose the mitochondrial respiratory chain to ischemia. Transfer into a medium with optimal conditions, however, mimics

unphysiological reperfusion (for detailed literature regarding reperfusion injury, see (Blomgren et al. 2003; Sanderson et al. 2013)). Reperfusion damage is unlikely after isolation of mitochondria. The centrifugation protocol, described in section 2.8.3 in Materials and Methods clears mitochondria of cellular compartments that cause inflammation and secondary damages, such as caspases and death receptors. However, mitochondria of the ischemic brain may be able to recover from prior shortage of glucose and oxygen *in vivo*. As all experiments were performed in the same way, this combination of *in vivo* and *ex vivo* is a carefully designed experimental setup for analysis of mitochondrial respiration after ischemic stroke. In conclusion, the oxygen concentrations are controlled throughout the isolation process, and consequently, hypoxia-related damage of the isolated mitochondria in this work is unlikely.

5.1.6 Neurological outcome

The neurological outcome after stroke may be assessed through a variety of behavioral tests following stroke. They were performed to assess the animals' motoric abilities before and after stroke, as well as the influence of the treatment with β -hydroxybutyrate. The tests employed in this work were designed for stroke research as they enable the evaluation of impaired motor functions under the influence of hemiparesis (Bouët et al. 2007).

Advantages of behavioral tests are that they are easy to perform, even for an untrained experimenter, and they require only little time. However, due to a number of reasons, neurological deficits are problematic to evaluate. First, all the tests are highly subjective and may vary when carried out by different investigators. In addition, blinding is crucial, as assessment by an unblinded experimenter is likely to lead to distorted results. The animals become used to the experiment over the course of time, which may further distort results if using untrained animals. Finally, small animals recover more easily from brain injury, further complicating assessment because effects of neuroprotective compounds may blur (Durukan and Tatlisumak 2007). As precaution, all behavioral experiments in this work were performed by one experimenter that the animals were used to. The animals were trained 3 days prior to stroke and the experimenter was blinded while assessing the behavioral tests.

Because of all the disadvantages mentioned above, behavioral tests are suitable for supporting the findings obtained through less subjective and higher reproducible analysis methods.

5.2. Discussion of results

5.2.1 Weight development

On average, the animals lost 20% of their initial bodyweight within 72 hours after cerebral ischemia, regardless of treatment group. After that, weight loss stagnated and by 7 days after ischemia some animals started regaining weight. Weight loss may lead to motor impairment following stroke, which was visible and measured by behavioral tests. On the other hand, it is possible that weight loss is a consequence of motor impairment. The animals visibly had difficulties standing upright to grab food and chew it. Surprisingly, they also did not eat the liquid food standing on the ground of the cage. A further explanation could be that the mice received buprenorphine until 72 hours after stroke. Opioids are well known to reduce food intake in rodents (Jirkof 2017). Possibly, weight loss in the first 72 hours after stroke was exacerbated by continuous and prolonged administration of buprenorphine. When the animals were no longer treated with the analgesic, they started eating the liquid food and took interest in pellet food, although most animals were unable to chew solid food until the end of the experiments.

5.2.2 In vitro stimulation of mitochondria with various compounds

There are three enzymes that convert the ketone bodies BHB and acetoacetate into two acetyl-CoA: namely BHB dehydrogenase, 3-oxoacid CoA-transferase and acetyl-CoA acetyltransferase (m-thiolase). Thus, the metabolism of BHB to acetyl-CoA in the liver is well known. Similarly well known is the transport of BHB across the blood brain barrier. Monocarboxylate transporters (MCTs) in endothelial cells and astroglia allow ketone bodies and lactate to cross the blood brain barrier. However, the question as to how BHB is transferred into mitochondria remains unanswered to this day (Berg et al. 2013). In isolated mitochondria of the non-ischemic brain, BHB was able to stimulate oxygen consumption. This finding proves that BHB is somehow transported into and utilized by isolated brain mitochondria. BHB has been shown to stimulate mitochondrial respiration before and various mechanisms have been discussed. BHB affects the energy metabolism through interconversion by NAD⁺-linked β -hydroxybutyrate dehydrogenase in the mitochondrial matrix. Hereby, the NADH/NAD⁺ equilibrium is shifted towards NADH, which in turn favors complex I (NADH dehydrogenase) activity. In course of its metabolic pathway, BHB also generates succinate, the substrate for complex II. However, BHB does not stimulate mitochondrial oxygen consumption as strongly as succinate. This is not surprising as BHB undergoes numerous metabolic steps to generate succinate (Tieu et al. 2003). Furthermore, BHB was found to affect the mitochondrial redox state by

increasing the oxidation state of coenzyme Q (Brown et al. 1990; Newman and Verdin 2017). Compared to pyruvate, BHB generates more combustion heat, increasing the efficiency of mitochondrial ATP production (Veech 2004). This finding is consistent with the findings of this work, where pyruvate alone did not lead to oxygen consumption, whereas BHB did. Succinate, the positive control substance, stimulates mitochondrial oxygen consumption through direct complex II activation.

5.2.3 Citrate synthase normalization

The citrate synthase (CS) catalyzes the first and rate-limiting step of the citric acid cycle. This makes it a suitable quantitative marker for intact mitochondria. It is located within the mitochondrial matrix and catalyzes the condensation of acetyl-CoA and oxaloacetate to citrate.

Mitochondrial activity is often either normalized to protein content of the homogenates or to mitochondrial citrate synthase activity. In the present study, normalization to citrate synthase activity neutralized the effect of stroke. Generally, citrate synthase is a good correcting factor for measurement of mitochondrial functions. As the amount of weighed brain differs from one experiment to another, mitochondrial respiration is normalized to the number of functioning mitochondria in the sample via citrate synthase activity (McLaughlin et al. 2020). In other words, citrate synthase is used as a quantitative marker (Gnaiger 2020). In the experiments in this work, however, ischemia causes mitochondria to die. Consequently, normalization to remaining functioning mitochondria causes the effect of stroke to entirely disappear. This could be observed for normalization to citrate synthase activity throughout all time points of mitochondrial respiration. However, citrate synthase activity itself was significantly increased in mitochondria of BHB treated animals in comparison to mitochondria of saline-treated animals 24 hours after ischemia. Presumably, this is an indicator for the neuroprotective effect of BHB that prevents mitochondria from dying after ischemia.

As citrate synthase normalization was unsuited for evaluation of mitochondrial respiration, absolute values were normalized to mitochondrial protein content. This way, non-functioning protein and tissue was also taken into calculation. The further discussion exclusively refers to weight normalized mitochondrial respiration.

5.2.4 Mitochondrial respiration: early events

The Oroboros oxygraph allows exact determination of mitochondrial oxygen consumption (Hütter et al. 2006). Addition of various substrates and inhibitors according to the SUIT protocol, (explained in

detail in section 2.8.3 in Materials and Methods) of the respiratory chain makes isolated measurement of the complexes I, II and IV, leak respiration, total respiration (OxPhos) and the electron transport system (ETS) possible, enabling detailed analysis of mitochondria. In this work, 90-minute ischemia was induced in the right hemisphere, mitochondria were isolated, and respiration was compared to the mitochondria of the unaffected contralateral hemisphere. As expected, ischemia caused oxygen consumption of all mitochondrial complexes to drastically decline. Of all complexes, complex I was the most affected (50% compared to control). These results are in line with those of prior research. Janssens et al. (2000) found strongly reduced activity of complexes I and II after transient ischemia. Complex III respiration, which has never been reported to be affected after ischemia, was not investigated in this work. Further, preceding research showed strongly reduced OxPhos respiration and moderately reduced complex IV respiration (Nelson and Silverstein 1994; Ginsberg et al. 1977). The extent of damage of each complex of the respiratory chain seems to depend on the severity of ischemia. Complex I for example has been shown to suffer from damage only after massive ischemia (Allen et al. 1995). The results in this work are consistent with this finding – complex I was particularly impaired regardless of treatment group after 90-minute ischemia.

60 minutes after reperfusion all mitochondrial complexes showed strongly reduced respiration. The treatment with BHB showed no effect this early after ischemia. Since the mechanism by which BHB takes action is not fully understood, reasons for the delayed effect can only be guessed at this point. One of the reasons for the delayed effect may be the complex metabolic pathway through which BHB generates substrates that can be fed into the citric acid cycle. Another possibility is that BHB has secondary effects on mitochondria. BHB, being an inhibitor of histone deacetylase enzymes, may affect gene expression to regulate the response to oxidative stress (Newman and Verdin 2014).

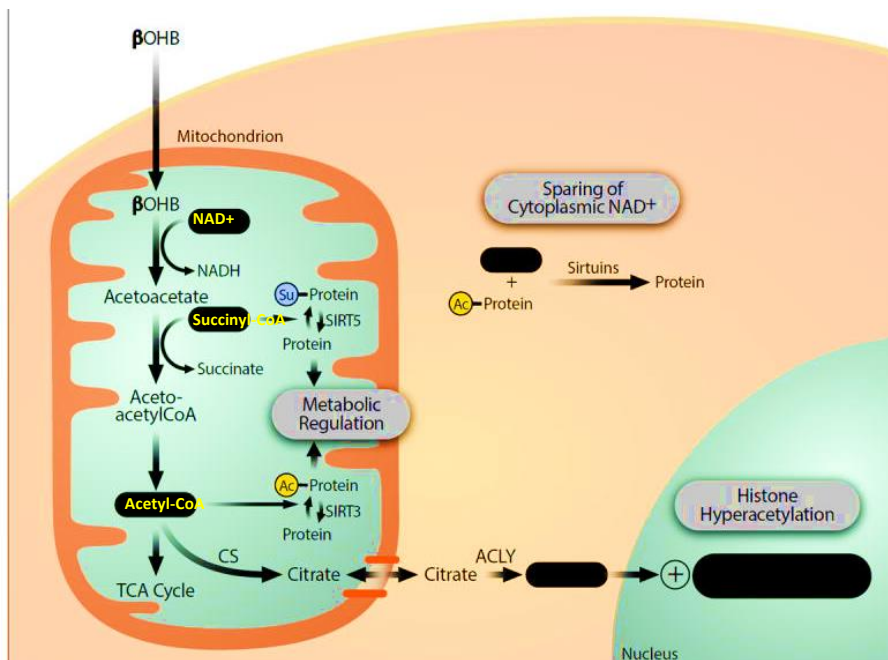


Figure 55: Metabolic pathway of BHB and cellular signaling functions of its metabolites. Degradation of BHB leads to increased cellular acetyl-CoA concentrations, whereas levels of succinyl-CoA and NAD⁺ decrease. Secondary effects include increase acetylation of mitochondrial protein and decrease of succinylation of mitochondrial protein. This may have regulatory effects on numerous metabolic enzymes. Another secondary effect of BHB may be established through acetyl-CoA, the degradation product of BHB generated in mitochondria, which is transported into the nucleus, where it serves as substrate for histone acetyltransferases (Newman and Verdin 2014). Figure adapted from Newman and Verdin (2014).

5.2.5 Mitochondrial respiration: later events

24 hours after reperfusion, complex IV activity seems to have recovered. However, the assay in the present work measures complex IV activity under optimum conditions of substrate supply. Consequently, complex IV activity is very high, and it must be assumed that activity measured *ex vivo* does not reflect the activity *in situ*. Complex I and II activity, and the combination of both, OxPhos, were significantly reduced in the ischemic hemispheres of saline and BHB treated groups. BHB administration, however, significantly improved mitochondrial respiration in complex I. Complex II and OxPhos seem to be improved, although the effect failed to reach statistical significance. Li et al. (2021) found BHB to have a protective effect with respect to oxidative stress and apoptosis induced by mitochondria in the ischemic brain 24 hours after reperfusion. These authors, too, found improved complex I activity and suggest a protective effect of BHB against ROS.

After 72 hours the improving effect of BHB on complex I is still visible. Until this point after reperfusion, a single administration of BHB seems to have neuroprotective properties. In the BHB-treated group, complex II significantly improved. For OxPhos, there is a trend towards improvement in the BHB group,

but not statistically significant. 7 days after reperfusion, differences between BHB and saline treated groups were no longer significant. This observation confirms prior work by Suzuki et al. (2002), who found that BHB, given to rats that had undergone 120 minutes of ischemia in the same dosage of 30 mg/kg bodyweight, reduced cerebral infarct areas, cerebral edema and neurological deficits 24 hours after reperfusion.

Consequently, the effect of a single administration of BHB may be transient, similar to the results found in the behavioral assays. In other words, a similar time course was observed for BHB's actions on mitochondrial respiration and on functional outcomes.

However, the mechanism over which BHB exerts its effect remains unknown. As mentioned in section 1.3.3 in the introduction, numerous mechanisms of action have been suggested for BHB effects: Some work suggested an inhibition of neuroinflammation through HCA2 receptors (Rahman et al. 2014; Offermanns and Schwaninger 2015), other studies favored reductions of reactive oxygen species (antioxidative mechanism) or epigenetic mechanisms through histone deacetylase inhibition (Julio-Amilpas et al. 2015; Yin et al. 2015). While the study in the present work does not exclude these mechanisms, its results suggest that BHB's beneficial action is associated with the improvement of mitochondrial respiration. Earlier studies have also reported mitochondrial effects in animal models (Julio-Amilpas et al. 2015). In one study, an increase of succinate was suggested to mediate BHB's actions (Tieu et al. 2003). Experiments from our lab could show that total brain succinate levels were stable after BHB administration, but dynamic local changes of citric acid cycle metabolites cannot be excluded (Lehto et al. 2022). Nevertheless, based on the model used in this work, BHB presumably acts through improvement of complex I and II activities and therefore, mitochondrial function.

5.2.6 Metabolites

During ischemia, brain extracellular concentrations of glucose, lactate and pyruvate change drastically. The reason for changing concentrations of the mentioned metabolites is an increase of anaerobic glycolysis. Oxidative degradation of glucose is only possible through glycolysis with pyruvate as final product. If there are insufficient amounts of oxygen, NADH builds up and pyruvate is reduced to lactate. Lactate accumulation leads to decreasing pH values as low as 6.0. However, no consistent metabolic changes could be observed in plasma after stroke. Plasma glucose levels are decreased in saline-treated mice compared to BHB-treated and sham-operated mice 72 hours after surgery. 24 hours after reperfusion, all mice that had undergone ischemia received Ringer's lactate once per day, leading to stable plasma glucose levels in both groups. The differences in plasma glucose levels after 72 hours may be a first indicator for BHB-treated animals starting to eat again. Pyruvate and lactate levels appeared to differ from sham-operated animals in both groups 24 hours and 72 hours after reperfusion. The lactate-pyruvate ratio, however, was not significantly different from sham. It seems

likely that metabolic changes of the compounds are mostly limited to the ischemic tissue (Tóth et al. 2020). Notably, in prior studies of this lab, metabolite levels drastically changed after cerebral ischemia when fed a fat-rich diet (Koch et al. 2017). This, however, does not apply to animals fed a standard, carbohydrate-based diet and fluctuations of pyruvate and lactate concentrations are mitigated when calculating the lactate-pyruvate ratio. Thus, metabolic changes are most likely limited to the ischemic tissue (Tóth et al. 2020). This hypothesis is further supported by one study that suggested an increase of succinate to mediate BHB's actions (Tieu et al. 2003). In our hands, total brain succinate and citrate levels were stable after ischemia and administration of BHB, but we cannot exclude dynamic local changes of citric acid cycle metabolites (Lehto et al. 2022)

5.2.7 Behavioral tests

The results of the behavioral tests further support the beneficial effects of administration of BHB after ischemic stroke that was previously seen in mitochondrial respiration.

The extent of hemiparesis can be measured by means of the Corner test. Due to ischemia in the right hemisphere, motor functions of the contralateral side are impaired, resulting in one-sided movement. Before ischemia, when the animals were trained, the LI was consistently nearly 0, as was the LI of sham operated animals. The animals were tested 24 hours, 72 hours and 7 days after ischemic stroke or sham surgery. 24 hours after reperfusion, a significant beneficial effect is visible for BHB. However, this effect was no longer visible after 72 hours. Both treatment groups had a similar laterality index (both groups turned almost exclusively left) and BHB and saline were no longer statistically different from one another. Sham operated mice still had an arbitrary turning pattern with a LI of nearly 0.

The Chimney test, in which mice must climb backwards out of a vertical tube, requires muscular effort and motor coordination. Here, the animals that had undergone MCAO were clearly impaired compared to sham. The effect of BHB on motor functions was visible until 7 days after reperfusion. On average, BHB-treated animals required 6 seconds less to exit the tube than saline-treated animals (~16 seconds versus ~22 seconds at all time points).

The Rotarod is also performed to assess coordinative abilities of the animals. The mouse walks on an accelerating rotating cylinder for 60 seconds. Prior to ischemia, all animals were able to walk on the cylinder for the entire 60 seconds. 24 hours after reperfusion, a clear effect of ischemia was visible in both groups, but there was no difference between BHB and saline treated animals. It must be pointed out that the animals performed very heterogeneously in the Rotarod experiment, ranging from 0 seconds to 60 seconds. This suggests that the induced stroke leads to varying motor deficits. Possibly, MCAO causes inconsistent damage to the motor cortex, as it may be in the penumbra of ischemic stroke in the striatum, leading to heterogenous performance in the Rotarod behavioral experiment.

Both groups recovered in the following days, although after 72 hours, they still performed significantly poorer than sham operated animals. 7 days after reperfusion, there were no more differences between animals that had undergone ischemia and sham operated animals.

The validity of the Rotarod is questionable for this experimental setting, as it leads to inconsistent results. Furthermore, there is a training effect in animals that were in the experiment until 7 days after reperfusion, which may further contort the results. In total it can be said that the effect of a single dose of BHB is most likely transient, possibly delaying the effect of stroke. This is in line with the findings of Suzuki et al. (2002) who also found no effect of a single dose of BHB beyond 24 hours using infarct volume as outcome parameter.

6. Conclusion

This work was aimed at investigating the neuroprotective properties of the ketone body BHB. Microdialysis in the striatum of mice showed an increase of extracellular BHB concentrations upon BHB application, proving that BHB crosses the blood brain barrier (Lehto et al. 2022). However, the increase of BHB is limited. This can most likely be attributed to an extensive uptake of BHB by other organs, which has been investigated in the past (Kesi et al. 2016; Pan et al. 2002). The effect of BHB was then tested when given as a single acute dose after 90 minutes of transient cerebral ischemia. 24 hours after reperfusion, the behavioral tests and neurological scores suggested that BHB administration at 30 mg/kg has beneficial effects on the outcome of ischemic stroke. Interestingly, neither a low dosage of 10 mg/kg, nor a high dosage of 100 mg/kg BHB was able to affect neurological outcomes (Lehto et al., 2022). Consequently, dosage seems to be relevant for beneficial effects. The reason as to why BHB was ineffective at higher doses remains unknown because the toxicity of BHB is low.

In this work, BHB was shown to improve mitochondrial function and behavioral outcomes until 72 hours after stroke when given immediately after transient cerebral ischemia in mice. The effect has been shown to be dose-dependent and transient since improvements decline after 72 hours and are no longer detectable after 7 days (Lehto et al. 2022). Furthermore, BHB has an effect primarily on complex I and in part on complex II. The exact mechanism, however, remains unknown. Potentially beneficial effects of continuous and prolonged administration of BHB after ischemic stroke should be investigated. Also, plasma metabolites such as pyruvate, lactate and glucose seem to be unsuitable markers for assessing recovery after ischemia when fed a normal diet.

Since therapeutic options of ischemic stroke are strongly limited to this day, the effect of BHB should be considered as a substance for clinical studies in humans. At least, future studies should consider testing the effect of BHB in the setting of ischemic stroke in larger animals such as dogs or pigs to

investigate whether the effect is limited to rodents. An initial treatment with an acute dose of BHB may stabilize mitochondrial function until thrombolysis is initiated and may prolong the therapeutic window.

List of references

- Adibhatla, Rao Muralikrishna; Hatcher, J. F. (2008): Phospholipase A(2), reactive oxygen species, and lipid peroxidation in CNS pathologies. In: *BMB reports* 41 (8), S. 560–567. DOI: 10.5483/bmbrep.2008.41.8.560.
- Akiyama, H. (2000): Inflammation and Alzheimer's disease. In: *Neurobiology of Aging* 21 (3), S. 383–421. DOI: 10.1016/S0197-4580(00)00124-X.
- Albers, G. W.; Goldstein, L. B.; Hall, D.; Lesko, L. M. (2001): Aptiganel hydrochloride in acute ischemic stroke: a randomized controlled trial. In: *JAMA* 286 (21), S. 2673–2682. DOI: 10.1001/jama.286.21.2673.
- Alexander, Mihaela; Forster, Colleen; Sugimoto, Koreaki; Clark, H. Brent; Vogel, Stefanie; Ross, M. Elizabeth; Iadecola, Costantino (2003): Interferon regulatory factor-1 immunoreactivity in neurons and inflammatory cells following ischemic stroke in rodents and humans. In: *Acta neuropathologica* 105 (5), S. 420–424. DOI: 10.1007/s00401-002-0658-x.
- Allen, K. L.; Almeida, A.; Bates, T. E.; Clark, J. B. (1995): Changes of respiratory chain activity in mitochondrial and synaptosomal fractions isolated from the gerbil brain after graded ischaemia. In: *Journal of neurochemistry* 64 (5), S. 2222–2229. DOI: 10.1046/j.1471-4159.1995.64052222.x.
- Al-Mudallal, A. S.; LaManna, J. C.; Lust, W. D.; Harik, S. I. (1996): Diet-induced ketosis does not cause cerebral acidosis. In: *Epilepsia* 37 (3), S. 258–261. DOI: 10.1111/j.1528-1157.1996.tb00022.x.
- Ansar, Saema; Chatzikonstantinou, Eva; Wistuba-Schier, Anja; Mirau-Weber, Silvia; Fatar, Marc; Hennerici, Michael G.; Meairs, Stephen (2014): Characterization of a new model of thromboembolic stroke in C57 black/6J mice. In: *Translational stroke research* 5 (4), S. 526–533. DOI: 10.1007/s12975-013-0315-9.
- Bardutzky, Juergen; Shen, Qiang; Henninger, Nils; Bouley, James; Duong, Timothy Q.; Fisher, Marc (2005): Differences in ischemic lesion evolution in different rat strains using diffusion and perfusion imaging. In: *Stroke* 36 (9), S. 2000–2005. DOI: 10.1161/01.STR.0000177486.85508.4d.
- Beckman, J. S.; Koppenol, W. H. (1996): Nitric oxide, superoxide, and peroxynitrite: the good, the bad, and ugly. In: *The American journal of physiology* 271 (5 Pt 1), C1424-37. DOI: 10.1152/ajpcell.1996.271.5.c1424.
- Bellido, T.; Huening, M.; Raval-Pandya, M.; Manolagas, S. C.; Christakos, S. (2000): Calbindin-D28k is expressed in osteoblastic cells and suppresses their apoptosis by inhibiting caspase-3 activity. In: *The Journal of biological chemistry* 275 (34), S. 26328–26332. DOI: 10.1074/jbc.M003600200.
- Belrose, Jillian C.; Caetano, Fabiana A.; Yang, Kai; Lockhart, Brian M. W.; Jackson, Michael F.; MacDonald, John F. (2012): Mechanisms of Calcium Influx Following Stroke. In: Yang V. Li und John H. Zhang (Hg.): *Metal Ion in Stroke*. New York, NY: Springer New York, S. 15–39.
- Benveniste, H.; Diemer, N. H. (1987): Cellular reactions to implantation of a microdialysis tube in the rat hippocampus. In: *Acta neuropathologica* 74 (3), S. 234–238. DOI: 10.1007/BF00688186.
- Benveniste, Helene; Hüttemeier, Peter Christian (1990): Microdialysis—Theory and application. In: *Progress in Neurobiology* 35 (3), S. 195–215. DOI: 10.1016/0301-0082(90)90027-e.
- Berg, Jeremy M.; Tymoczko, John L.; Stryer, Lubert (2013): *Stryer Biochemie*. Berlin, Heidelberg: Springer Berlin Heidelberg.
- Bhatia, Rohit; Hill, Michael D.; Shobha, Nandavar; Menon, Bijoy; Bal, Simerpreet; Kochar, Puneet et al. (2010): Low rates of acute recanalization with intravenous recombinant tissue plasminogen activator in ischemic stroke: real-world experience and a call for action. In: *Stroke* 41 (10), S. 2254–2258. DOI: 10.1161/STROKEAHA.110.592535.
- Biernaskie, J.; Corbett, D.; Peeling, J.; Wells, J.; Lei, H. (2001): A serial MR study of cerebral blood flow changes and lesion development following endothelin-1-induced ischemia in rats. In: *Magnetic resonance in medicine* 46 (4), S. 827–830. DOI: 10.1002/mrm.1263.
- Blomgren, Klas; Zhu, Changlian; Hallin, Ulrika; Hagberg, Henrik (2003): Mitochondria and ischemic reperfusion damage in the adult and in the developing brain. In: *Biochemical and Biophysical Research Communications* 304 (3), S. 551–559. DOI: 10.1016/S0006-291X(03)00628-4.

- Bokhari, Faraz Ahmed; Shakoory, Tania A.; Butt, Ambreen; Ghafoor, Farkhanda (2014): TNF-alpha: a risk factor for ischemic stroke. In: *Journal of Ayub Medical College, Abbottabad : JAMC* 26 (2), S. 111–114.
- Bouët, Valentine; Freret, Thomas; Toutain, Jérôme; Divoux, Didier; Boulouard, Michel; Schumann-Bard, Pascale (2007): Sensorimotor and cognitive deficits after transient middle cerebral artery occlusion in the mouse. In: *Experimental neurology* 203 (2), S. 555–567. DOI: 10.1016/j.expneurol.2006.09.006.
- Bough, Kristopher J.; Wetherington, Jonathon; Hassel, Bjørnar; Pare, Jean Francois; Gawryluk, Jeremy W.; Greene, James G. et al. (2006): Mitochondrial biogenesis in the anticonvulsant mechanism of the ketogenic diet. In: *Annals of neurology* 60 (2), S. 223–235. DOI: 10.1002/ana.20899.
- Broughton, Brad R. S.; Reutens, David C.; Sobey, Christopher G. (2009): Apoptotic mechanisms after cerebral ischemia. In: *Stroke* 40 (5), e331-9. DOI: 10.1161/STROKEAHA.108.531632.
- Brown, G. C.; Lakin-Thomas, P. L.; Brand, M. D. (1990): Control of respiration and oxidative phosphorylation in isolated rat liver cells. In: *European journal of biochemistry* 192 (2), S. 355–362. DOI: 10.1111/j.1432-1033.1990.tb19234.x.
- Bruce, A. J.; Boling, W.; Kindy, M. S.; Peschon, J.; Kraemer, P. J.; Carpenter, M. K. et al. (1996): Altered neuronal and microglial responses to excitotoxic and ischemic brain injury in mice lacking TNF receptors. In: *Nature medicine* 2 (7), S. 788–794. DOI: 10.1038/nm0796-788.
- Caplan, Louis R.; Reis, Donald J.; Siesjo, Bo K. (1997a): *Primer on Cerebrovascular Diseases*. 1. Aufl. s.l.: Elsevier professional.
- Caplan, Louis R.; Reis, Donald J.; Siesjo, Bo K. (1997b): *Primer on Cerebrovascular Diseases*. 1. Aufl. s.l.: Elsevier professional.
- Chamorro, Angel; Hallenbeck, John (2006): The harms and benefits of inflammatory and immune responses in vascular disease. In: *Stroke* 37 (2), S. 291–293. DOI: 10.1161/01.STR.0000200561.69611.f8.
- Chandel, Navdeep Singh (2015): *Navigating metabolism*. Unter Mitarbeit von Pete Jeffs. Cold Spring Harbor, New York: Cold Spring Harbor Laboratory Press.
- Cheng, Baohua; Yang, Xinxin; An, Liangxiang; Gao, Bo; Liu, Xia; Liu, Shuwei (2009): Ketogenic diet protects dopaminergic neurons against 6-OHDA neurotoxicity via up-regulating glutathione in a rat model of Parkinson's disease. In: *Brain research* 1286, S. 25–31. DOI: 10.1016/j.brainres.2009.06.060.
- Cherian, L.; Peek, K.; Robertson, C. S.; Goodman, J. C.; Grossman, R. G. (1994): Calorie sources and recovery from central nervous system ischemia. In: *Critical care medicine* 22 (11), S. 1841–1850.
- Colak, Gozde; Filiano, Anthony J.; Johnson, Gail V. W. (2011): The application of permanent middle cerebral artery ligation in the mouse. In: *Journal of visualized experiments : JoVE* (53). DOI: 10.3791/3039.
- Conn, P. Michael (2006): *Handbook of models for human aging*. Unter Mitarbeit von P. Michael Conn. Amsterdam: Elsevier Academic Press.
- Connolly, E. S.; Winfree, C. J.; Springer, T. A.; Naka, Y.; Liao, H.; Yan, S. D. et al. (1996): Cerebral protection in homozygous null ICAM-1 mice after middle cerebral artery occlusion. Role of neutrophil adhesion in the pathogenesis of stroke. In: *The Journal of clinical investigation* 97 (1), S. 209–216. DOI: 10.1172/JCI118392.
- Cowman, Seamus; Royston, Maeve; Hickey, Anne; Horgan, Frances; McGee, Hannah; O'Neill, Desmond (2010): Stroke and nursing home care: a national survey of nursing homes. In: *BMC geriatrics* 10, S. 4. DOI: 10.1186/1471-2318-10-4.
- Crowell, R. M.; Marcoux, F. W.; DeGirolami, U. (1981): Variability and reversibility of focal cerebral ischemia in unanesthetized monkeys. In: *Neurology* 31 (10), S. 1295–1302. DOI: 10.1212/WNL.31.10.1295.
- Cullingford, Tim E. (2004): The ketogenic diet; fatty acids, fatty acid-activated receptors and neurological disorders. In: *Prostaglandins, leukotrienes, and essential fatty acids* 70 (3), S. 253–264. DOI: 10.1016/j.plefa.2003.09.008.
- D'Agostino, R. B.; Wolf, P. A.; Belanger, A. J.; Kannel, W. B. (1994): Stroke risk profile: adjustment for antihypertensive medication. The Framingham Study. In: *Stroke* 25 (1), S. 40–43. DOI: 10.1161/01.str.25.1.40.

- D'Amelio, M.; Cavallucci, V.; Cecconi, F. (2010): Neuronal caspase-3 signaling: not only cell death. In: *Cell death and differentiation* 17 (7), S. 1104–1114. DOI: 10.1038/cdd.2009.180.
- Dardzinski, B. J.; Smith, S. L.; Towfighi, J.; Williams, G. D.; Vannucci, R. C.; Smith, M. B. (2000): Increased plasma beta-hydroxybutyrate, preserved cerebral energy metabolism, and amelioration of brain damage during neonatal hypoxia ischemia with dexamethasone pretreatment. In: *Pediatric research* 48 (2), S. 248–255. DOI: 10.1203/00006450-200008000-00021.
- Del Zoppo, G. J.; Schmid-Schönbein, G. W.; Mori, E.; Copeland, B. R.; Chang, C. M. (1991): Polymorphonuclear leukocytes occlude capillaries following middle cerebral artery occlusion and reperfusion in baboons. In: *Stroke* 22 (10), S. 1276–1283. DOI: 10.1161/01.STR.22.10.1276.
- Delgado, J.; DeFeudis, F.; Roth, Robert; Ryugo, David; Mitruka, B. (1972): Dialytrode for long term intracerebral perfusion in awake monkeys. In: *Archives internationales de pharmacodynamie et de thérapie* 198, S. 9–21.
- Dinapoli, Vincent A.; Rosen, Charles L.; Nagamine, Tomoaki; Crocco, Todd (2006): Selective MCA occlusion: a precise embolic stroke model. In: *Journal of neuroscience methods* 154 (1-2), S. 233–238. DOI: 10.1016/j.jneumeth.2005.12.026.
- Dirnagl, Ulrich; Iadecola, Costantino; Moskowitz, Michael A. (1999): Pathobiology of ischaemic stroke: an integrated view. In: *Trends in Neurosciences* 22 (9), S. 391–397. DOI: 10.1016/s0166-2236(99)01401-0.
- Dittmar, Michael; Spruss, Thilo; Schuierer, Gerhard; Horn, Markus (2003): External carotid artery territory ischemia impairs outcome in the endovascular filament model of middle cerebral artery occlusion in rats. In: *Stroke* 34 (9), S. 2252–2257. DOI: 10.1161/01.STR.0000083625.54851.9A.
- Durukan, Aysan; Tatlisumak, Turgut (2007): Acute ischemic stroke: overview of major experimental rodent models, pathophysiology, and therapy of focal cerebral ischemia. In: *Pharmacology, biochemistry, and behavior* 87 (1), S. 179–197. DOI: 10.1016/j.pbb.2007.04.015.
- Endres, M.; Namura, S.; Shimizu-Sasamata, M.; Waeber, C.; Zhang, L.; Gómez-Isla, T. et al. (1998): Attenuation of delayed neuronal death after mild focal ischemia in mice by inhibition of the caspase family. In: *Journal of cerebral blood flow and metabolism : official journal of the International Society of Cerebral Blood Flow and Metabolism* 18 (3), S. 238–247. DOI: 10.1097/00004647-199803000-00002.
- Ercińska, M.; Nelson, D.; Daikhin, Y.; Yudkoff, M. (1996): Regulation of GABA level in rat brain synaptosomes: fluxes through enzymes of the GABA shunt and effects of glutamate, calcium, and ketone bodies. In: *Journal of neurochemistry* 67 (6), S. 2325–2334. DOI: 10.1046/j.1471-4159.1996.67062325.x.
- Feigin, Valery L.; Mensah, George A.; Norrving, Bo; Murray, Christopher J. L.; Roth, Gregory A. (2015): Atlas of the Global Burden of Stroke (1990-2013): The GBD 2013 Study. In: *Neuroepidemiology* 45 (3), S. 230–236. DOI: 10.1159/000441106.
- Feigin, Valery L.; Norrving, Bo; Mensah, George A. (2017): Global Burden of Stroke. In: *Circulation research* 120 (3), S. 439–448. DOI: 10.1161/CIRCRESAHA.116.308413.
- Fluri, Felix; Schuhmann, Michael K.; Kleinschnitz, Christoph (2015): Animal models of ischemic stroke and their application in clinical research. In: *Drug design, development and therapy* 9, S. 3445–3454. DOI: 10.2147/DDDT.S56071.
- Fonarow, Gregg C.; Smith, Eric E.; Saver, Jeffrey L.; Reeves, Mathew J.; Bhatt, Deepak L.; Grau-Sepulveda, Maria V. et al. (2011): Timeliness of tissue-type plasminogen activator therapy in acute ischemic stroke: patient characteristics, hospital factors, and outcomes associated with door-to-needle times within 60 minutes. In: *Circulation* 123 (7), S. 750–758. DOI: 10.1161/CIRCULATIONAHA.110.974675.
- Forster, C.; Clark, H. B.; Ross, M. E.; Iadecola, C. (1999): Inducible nitric oxide synthase expression in human cerebral infarcts. In: *Acta neuropathologica* 97 (3), S. 215–220. DOI: 10.1007/s004010050977.
- Fraser, D. D.; Whiting, S.; Andrew, R. D.; Macdonald, E. A.; Musa-Veloso, K.; Cunnane, S. C. (2003): Elevated polyunsaturated fatty acids in blood serum obtained from children on the ketogenic diet. In: *Neurology* 60 (6), S. 1026–1029. DOI: 10.1212/01.WNL.0000049974.74242.C6.
- Freeman, John; Veggiotti, Pierangelo; Lanzi, Giovanni; Tagliabue, Anna; Perucca, Emilio (2006): The ketogenic diet: from molecular mechanisms to clinical effects. In: *Epilepsy research* 68 (2), S. 145–180. DOI: 10.1016/j.eplepsyres.2005.10.003.

- Fujimura, M.; Morita-Fujimura, Y.; Murakami, K.; Kawase, M.; Chan, P. H. (1998): Cytosolic redistribution of cytochrome c after transient focal cerebral ischemia in rats. In: *Journal of cerebral blood flow and metabolism : official journal of the International Society of Cerebral Blood Flow and Metabolism* 18 (11), S. 1239–1247. DOI: 10.1097/00004647-199811000-00010.
- Fukao, Toshiyuki; Lopaschuk, Gary D.; Mitchell, Grant A. (2004): Pathways and control of ketone body metabolism: on the fringe of lipid biochemistry. In: *Prostaglandins, leukotrienes, and essential fatty acids* 70 (3), S. 243–251. DOI: 10.1016/j.plefa.2003.11.001.
- Fukuchi, K.; Kusuoka, H.; Watanabe, Y.; Nishimura, T. (1999): Correlation of sequential MR images of microsphere-induced cerebral ischemia with histologic changes in rats. In: *Investigative radiology* 34 (11), S. 698–703. DOI: 10.1097/00004424-199911000-00006.
- Furukawa, K.; Sopher, B. L.; Rydel, R. E.; Begley, J. G.; Pham, D. G.; Martin, G. M. et al. (1996): Increased activity-regulating and neuroprotective efficacy of alpha-secretase-derived secreted amyloid precursor protein conferred by a C-terminal heparin-binding domain. In: *Journal of neurochemistry* 67 (5), S. 1882–1896. DOI: 10.1046/j.1471-4159.1996.67051882.x.
- Gandolfo, C.; Sandercock, P.; Conti, M. (2002): Lubeluzole for acute ischaemic stroke. In: *The Cochrane database of systematic reviews* (1), CD001924. DOI: 10.1002/14651858.CD001924.
- García, O.; Massieu, L. (2001): Strategies for neuroprotection against L-trans-2,4-pyrrolidine dicarboxylate-induced neuronal damage during energy impairment in vitro. In: *Journal of neuroscience research* 64 (4), S. 418–428. DOI: 10.1002/jnr.1093.
- Gasior, Maciej; Rogawski, Michael A.; Hartman, Adam L. (2006): Neuroprotective and disease-modifying effects of the ketogenic diet. In: *Behavioural pharmacology* 17 (5-6), S. 431–439.
- Gerriets, Tibo; Li, Fuhai; Silva, Matthew D.; Meng, Xiangjun; Brevard, Mathew; Sotak, Christopher H.; Fisher, Marc (2003): The macrosphere model. In: *Journal of neuroscience methods* 122 (2), S. 201–211. DOI: 10.1016/s0165-0270(02)00322-9.
- Ginsberg, M. D.; Mela, L.; Wrobel-Kuhl, K.; Reivich, M. (1977): Mitochondrial metabolism following bilateral cerebral ischemia in the gerbil. In: *Annals of neurology* 1 (6), S. 519–527. DOI: 10.1002/ana.410010603.
- Ginsberg, Myron D. (1995): REVIEW ■ : Neuroprotection in Brain Ischemia: An Update (Part I. In: *Neuroscientist* 1 (2), S. 95–103. DOI: 10.1177/107385849500100206.
- Ginsberg, Myron D. (2008): Neuroprotection for ischemic stroke: past, present and future. In: *Neuropharmacology* 55 (3), S. 363–389. DOI: 10.1016/j.neuropharm.2007.12.007.
- Gnaiger, E.; Méndez, G.; Hand, S. C. (2000): High phosphorylation efficiency and depression of uncoupled respiration in mitochondria under hypoxia. In: *Proceedings of the National Academy of Sciences of the United States of America* 97 (20), S. 11080–11085. DOI: 10.1073/pnas.97.20.11080.
- Gnaiger, Erich (2001): Bioenergetics at low oxygen: dependence of respiration and phosphorylation on oxygen and adenosine diphosphate supply. In: *Respiration Physiology* 128 (3), S. 277–297. DOI: 10.1016/s0034-5687(01)00307-3.
- Gnaiger, Erich (2020): Mitochondrial Pathways and Respiratory Control. Unter Mitarbeit von Erich Gnaiger.
- Hakim, Antoine M. (2012): The future of stroke thrombolysis. In: *Annals of the New York Academy of Sciences* 1268, S. 8–13. DOI: 10.1111/j.1749-6632.2012.06706.x.
- Hara, H.; Friedlander, R. M.; Gagliardini, V.; Ayata, C.; Fink, K.; Huang, Z. et al. (1997): Inhibition of interleukin 1beta converting enzyme family proteases reduces ischemic and excitotoxic neuronal damage. In: *Proceedings of the National Academy of Sciences of the United States of America* 94 (5), S. 2007–2012. DOI: 10.1073/pnas.94.5.2007.
- Hass, Bruce S.; Hart, Ronald W.; Lu, Ming H.; Lyn-Cook, Beverly D. (1993): Effects of caloric restriction in animals on cellular function, oncogene expression, and DNA methylation in vitro. In: *Mutation Research/DNAging* 295 (4-6), S. 281–289. DOI: 10.1016/0921-8734(93)90026-y.

- HILL, N. C.; MILLIKAN, C. H.; WAKIM, K. G.; SAYRE, G. P. (1955): Studies in cerebrovascular disease. VII. Experimental production of cerebral infarction by intracarotid injection of homologous blood clot; preliminary report. In: *Proceedings of the staff meetings. Mayo Clinic* 30 (26), S. 625–633.
- Hillis, Argye E.; Baron, Jean-Claude (2015): Editorial: the ischemic penumbra: still the target for stroke therapies? In: *Frontiers in neurology* 6, S. 85. DOI: 10.3389/fneur.2015.00085.
- Horn, J.; Haan, R. J. de; Vermeulen, M.; Limburg, M. (2001): Very Early Nimodipine Use in Stroke (VENUS): a randomized, double-blind, placebo-controlled trial. In: *Stroke* 32 (2), S. 461–465. DOI: 10.1161/01.STR.32.2.461.
- Hossmann, K. A. (1996): Periinfarct depolarizations. In: *Cerebrovascular and brain metabolism reviews* 8 (3), S. 195–208.
- Howells, David W.; Porritt, Michelle J.; Rewell, Sarah S. J.; O'Collins, Victoria; Sena, Emily S.; van der Worp, H. Bart et al. (2010): Different strokes for different folks: the rich diversity of animal models of focal cerebral ischemia. In: *Journal of cerebral blood flow and metabolism : official journal of the International Society of Cerebral Blood Flow and Metabolism* 30 (8), S. 1412–1431. DOI: 10.1038/jcbfm.2010.66.
- Hütter, E.; Unterluggauer, H.; Garedew, A.; Jansen-Dürr, P.; Gnaiger, E. (2006): High-resolution respirometry--a modern tool in aging research. In: *Experimental gerontology* 41 (1), S. 103–109. DOI: 10.1016/j.exger.2005.09.011.
- Iadecola, C.; Salkowski, C. A.; Zhang, F.; Aber, T.; Nagayama, M.; Vogel, S. N.; Ross, M. E. (1999): The transcription factor interferon regulatory factor 1 is expressed after cerebral ischemia and contributes to ischemic brain injury. In: *The Journal of experimental medicine* 189 (4), S. 719–727. DOI: 10.1084/jem.189.4.719.
- Iadecola, Costantino (1997): Bright and dark sides of nitric oxide in ischemic brain injury. In: *Trends in Neurosciences* 20 (3), S. 132–139. DOI: 10.1016/S0166-2236(96)10074-6.
- Janssens, D.; Delaive, E.; Remacle, J.; Michiels, C. (2000): Protection by bilobalide of the ischaemia-induced alterations of the mitochondrial respiratory activity. In: *Fundamental & clinical pharmacology* 14 (3), S. 193–201. DOI: 10.1111/j.1472-8206.2000.tb00016.x.
- Jirkof, Paulin (2017): Side effects of pain and analgesia in animal experimentation. In: *Lab animal* 46 (4), S. 123–128. DOI: 10.1038/labani.1216.
- Johnson, Catherine Owens; Nguyen, Minh; Roth, Gregory A.; Nichols, Emma; Alam, Tahiya; Abate, Degu et al. (2019): Global, regional, and national burden of stroke, 1990–2016: a systematic analysis for the Global Burden of Disease Study 2016. In: *The Lancet Neurology* 18 (5), S. 439–458. DOI: 10.1016/S1474-4422(19)30034-1.
- Jones, S. (2002): Clusterin. In: *The International Journal of Biochemistry & Cell Biology* 34 (5), S. 427–431. DOI: 10.1016/S1357-2725(01)00155-8.
- Julio-Amilpas, Alberto; Montiel, Teresa; Soto-Tinoco, Eva; Gerónimo-Olvera, Cristian; Massieu, Lourdes (2015): Protection of hypoglycemia-induced neuronal death by β -hydroxybutyrate involves the preservation of energy levels and decreased production of reactive oxygen species. In: *Journal of cerebral blood flow and metabolism : official journal of the International Society of Cerebral Blood Flow and Metabolism* 35 (5), S. 851–860. DOI: 10.1038/jcbfm.2015.1.
- Kannel, William B. (1979): Diabetes and Cardiovascular Disease. In: *JAMA* 241 (19), S. 2035. DOI: 10.1001/jama.1979.03290450033020.
- Kesl, Shannon L.; Poff, Angela M.; Ward, Nathan P.; Fiorelli, Tina N.; Ari, Csilla; van Putten, Ashley J. et al. (2016): Effects of exogenous ketone supplementation on blood ketone, glucose, triglyceride, and lipoprotein levels in Sprague-Dawley rats. In: *Nutrition & metabolism* 13, S. 9. DOI: 10.1186/s12986-016-0069-y.
- Kiewert, Cornelia; Kumar, Vikas; Hildmann, Oksana; Hartmann, Joachim; Hillert, Markus; Klein, Jochen (2008): Role of glycine receptors and glycine release for the neuroprotective activity of bilobalide. In: *Brain research* 1201, S. 143–150. DOI: 10.1016/j.brainres.2008.01.052.
- Kiewert, Cornelia; Mdzinarishvili, Alexander; Hartmann, Joachim; Bickel, Ulrich; Klein, Jochen (2010): Metabolic and transmitter changes in core and penumbra after middle cerebral artery occlusion in mice. In: *Brain research* 1312, S. 101–107. DOI: 10.1016/j.brainres.2009.11.068.

- Kleinschnitz, Christoph; Braeuninger, Stefan; Pham, Mirko; Austinat, Madeleine; Nölte, Ingo; Renné, Thomas et al. (2008): Blocking of Platelets or Intrinsic Coagulation Pathway–Driven Thrombosis Does Not Prevent Cerebral Infarctions Induced by Photothrombosis. In: *Stroke* 39 (4), S. 1262–1268. DOI: 10.1161/STROKEAHA.107.496448.
- Koch, Konrad; Berressem, Dirk; Konietzka, Jan; Thinnies, Anna; Eckert, Gunter P.; Klein, Jochen (2017): Hepatic Ketogenesis Induced by Middle Cerebral Artery Occlusion in Mice. In: *Journal of the American Heart Association* 6 (4). DOI: 10.1161/JAHA.117.005556.
- Koizumi, Jin-ichi; Yoshida, Yoji; Nakazawa, Teiji; Ooneda, Genju (1986): Experimental studies of ischemic brain edema. In: *Jpn. J. Stroke* 8 (1), S. 1–8. DOI: 10.3995/jstroke.8.1.
- Kovacic, Peter; Somanathan, Ratnasamy (2010): Clinical physiology and mechanism of dizocilpine (MK-801): electron transfer, radicals, redox metabolites and bioactivity. In: *Oxidative medicine and cellular longevity* 3 (1), S. 13–22. DOI: 10.4161/oxim.3.1.10028.
- Krams, Michael; Lees, Kennedy R.; Hacke, Werner; Grieve, Andrew P.; Orgogozo, Jean-Marc; Ford, Gary A. (2003): Acute Stroke Therapy by Inhibition of Neutrophils (ASTIN): an adaptive dose-response study of UK-279,276 in acute ischemic stroke. In: *Stroke* 34 (11), S. 2543–2548. DOI: 10.1161/01.STR.0000092527.33910.89.
- Kudo, M.; Aoyama, A.; Ichimori, S.; Fukunaga, N. (1982): An animal model of cerebral infarction. Homologous blood clot emboli in rats. In: *Stroke* 13 (4), S. 505–508. DOI: 10.1161/01.str.13.4.505.
- Kuraoka, Mutsuki; Furuta, Takahisa; Matsuwaki, Takashi; Omatsu, Tsutomu; Ishii, Yoshiyuki; Kyuwa, Shigeru; Yoshikawa, Yasuhiro (2009): Direct experimental occlusion of the distal middle cerebral artery induces high reproducibility of brain ischemia in mice. In: *Experimental animals* 58 (1), S. 19–29. DOI: 10.1538/expanim.58.19.
- Kuriakose, Dijji; Xiao, Zhicheng (2020): Pathophysiology and Treatment of Stroke: Present Status and Future Perspectives. In: *International journal of molecular sciences* 21 (20). DOI: 10.3390/ijms21207609.
- Kuroiwa, Toshihiko; Xi, Guohua; Hua, Ya; Nagaraja, Tavarekere N.; Fenstermacher, Joseph D.; Keep, Richard F. (2009): Development of a Rat Model of Photothrombotic Ischemia and Infarction Within the Caudoputamen. In: *Stroke* 40 (1), S. 248–253. DOI: 10.1161/STROKEAHA.108.527853.
- Lai, Ted Weita; Zhang, Shu; Wang, Yu Tian (2014): Excitotoxicity and stroke: identifying novel targets for neuroprotection. In: *Progress in Neurobiology* 115, S. 157–188. DOI: 10.1016/j.pneurobio.2013.11.006.
- Laing, R. J.; Jakubowski, J.; Laing, R. W. (1993): Middle cerebral artery occlusion without craniectomy in rats. Which method works best? In: *Stroke* 24 (2), 294-7; discussion 297-8. DOI: 10.1161/01.STR.24.2.294.
- Lapchak, Paul A.; Zivin, Justin A. (2003): Ebselen, a seleno-organic antioxidant, is neuroprotective after embolic strokes in rabbits: synergism with low-dose tissue plasminogen activator. In: *Stroke* 34 (8), S. 2013–2018. DOI: 10.1161/01.STR.0000081223.74129.04.
- Lee, Jaewon; Bruce-Keller, Annadora J.; Kruman, Yuri; Chan, Sic L.; Mattson, Mark P. (1999): 2-deoxy-d-glucose protects hippocampal neurons against excitotoxic and oxidative injury: Evidence for the involvement of stress proteins. In: *Journal of neuroscience research* 57 (1), S. 48–61. DOI: 10.1002/(SICI)1097-4547(19990701)57:1<48::AID-JNR6>3.0.CO;2-L.
- Lee, Jaewon; Kim, So Jung; Son, Tae Gen; Chan, Sic L.; Mattson, Mark P. (2006): Interferon-gamma is up-regulated in the hippocampus in response to intermittent fasting and protects hippocampal neurons against excitotoxicity. In: *Journal of neuroscience research* 83 (8), S. 1552–1557. DOI: 10.1002/jnr.20831.
- Lees, Kennedy R.; Asplund, Kjell; Carolei, Antonio; Davis, Stephen M.; Diener, Hans-Christoph; Kaste, Markku et al. (2000): Glycine antagonist (gavestinel) in neuroprotection (GAIN International) in patients with acute stroke: a randomised controlled trial. In: *The Lancet* 355 (9219), S. 1949–1954. DOI: 10.1016/S0140-6736(00)02326-6.
- Leist, M.; Nicotera, P. (1998): Apoptosis, excitotoxicity, and neuropathology. In: *Experimental cell research* 239 (2), S. 183–201. DOI: 10.1006/excr.1997.4026.

- Lesage, A. S.; Peeters, L.; Leysen, J. E. (1996): Lubeluzole, a novel long-term neuroprotectant, inhibits the glutamate-activated nitric oxide synthase pathway. In: *The Journal of pharmacology and experimental therapeutics* 279 (2), S. 759–766.
- Li, Ping; Murphy, Timothy H. (2008): Two-photon imaging during prolonged middle cerebral artery occlusion in mice reveals recovery of dendritic structure after reperfusion. In: *J. Neurosci.* 28 (46), S. 11970–11979. DOI: 10.1523/JNEUROSCI.3724-08.2008.
- Li, Yang; Zhang, Xuepeng; Ma, Aijia; Kang, Yan (2021): Rational Application of β -Hydroxybutyrate Attenuates Ischemic Stroke by Suppressing Oxidative Stress and Mitochondrial-Dependent Apoptosis via Activation of the Erk/CREB/eNOS Pathway. In: *ACS chemical neuroscience* 12 (7), S. 1219–1227. DOI: 10.1021/acscchemneuro.1c00046.
- Li, Yuanyuan; Daniel, Michael; Tollefsbol, Trygve O. (2011): Epigenetic regulation of caloric restriction in aging. In: *BMC medicine* 9, S. 98. DOI: 10.1186/1741-7015-9-98.
- Lindfors, Nils; Amberg, Gustav; Ungerstedt, Urban (1989): Intracerebral microdialysis. I. Experimental studies of diffusion kinetics. In: *Journal of Pharmacological Methods* 22 (3), S. 141–156. DOI: 10.1016/0160-5402(89)90011-9.
- Liu, Fudong; McCullough, Louise D. (2011): Middle cerebral artery occlusion model in rodents: methods and potential pitfalls. In: *Journal of biomedicine & biotechnology* 2011, S. 464701. DOI: 10.1155/2011/464701.
- Loddick, S. A.; Rothwell, N. J. (1996): Neuroprotective effects of human recombinant interleukin-1 receptor antagonist in focal cerebral ischaemia in the rat. In: *Journal of cerebral blood flow and metabolism : official journal of the International Society of Cerebral Blood Flow and Metabolism* 16 (5), S. 932–940. DOI: 10.1097/00004647-199609000-00017.
- Longa, E. Z.; Weinstein, P. R.; Carlson, S.; Cummins, R. (1989): Reversible middle cerebral artery occlusion without craniectomy in rats. In: *Stroke* 20 (1), S. 84–91. DOI: 10.1161/01.str.20.1.84.
- Lönnroth, P.; Jansson, P. A.; Fredholm, B. B.; Smith, U. (1989): Microdialysis of intercellular adenosine concentration in subcutaneous tissue in humans. In: *The American journal of physiology* 256 (2 Pt 1), E250-5. DOI: 10.1152/ajpendo.1989.256.2.E250.
- Lönnroth, P.; Jansson, P. A.; Smith, U. (1987): A microdialysis method allowing characterization of intercellular water space in humans. In: *The American journal of physiology* 253 (2 Pt 1), E228-31. DOI: 10.1152/ajpendo.1987.253.2.E228.
- Ludwig, David S. (2020): The Ketogenic Diet: Evidence for Optimism but High-Quality Research Needed. In: *The Journal of nutrition* 150 (6), S. 1354–1359. DOI: 10.1093/jn/nxz308.
- M Tóth, Orsolya; Menyhárt, Ákos; Frank, Rita; Hantosi, Dóra; Farkas, Eszter; Bari, Ferenc (2020): Tissue Acidosis Associated with Ischemic Stroke to Guide Neuroprotective Drug Delivery. In: *Biology* 9 (12). DOI: 10.3390/biology9120460.
- Maalouf, M.; Sullivan, P. G.; Davis, L.; Kim, D. Y.; Rho, J. M. (2007): Ketones inhibit mitochondrial production of reactive oxygen species production following glutamate excitotoxicity by increasing NADH oxidation. In: *Neuroscience* 145 (1), S. 256–264. DOI: 10.1016/j.neuroscience.2006.11.065.
- Manwani, Bharti; Bentivegna, Kathryn; Benashski, Sharon E.; Venna, Venugopal Reddy; Xu, Yan; Arnold, Arthur P.; McCullough, Louise D. (2015): Sex differences in ischemic stroke sensitivity are influenced by gonadal hormones, not by sex chromosome complement. In: *Journal of cerebral blood flow and metabolism : official journal of the International Society of Cerebral Blood Flow and Metabolism* 35 (2), S. 221–229. DOI: 10.1038/jcbfm.2014.186.
- Manzanero, Silvia; Santro, Tomislav; Arumugam, Thiruma V. (2013): Neuronal oxidative stress in acute ischemic stroke: sources and contribution to cell injury. In: *Neurochemistry international* 62 (5), S. 712–718. DOI: 10.1016/j.neuint.2012.11.009.
- Mao, Y.; Yang, G.; Zhou, L. (2000): Temporary and permanent focal cerebral ischemia in the mouse: assessment of cerebral blood flow, brain damage and blood-brain barrier permeability. In: *Chinese medical journal* 113 (4), S. 361–366.

- Marie, C.; Bralet, A. M.; Gueldry, S.; Bralet, J. (1990): Fasting prior to transient cerebral ischemia reduces delayed neuronal necrosis. In: *Metabolic brain disease* 5 (2), S. 65–75. DOI: 10.1007/BF01001047.
- Martin, Kirsty; Jackson, Cerian F.; Levy, Robert G.; Cooper, Paul N. (2016): Ketogenic diet and other dietary treatments for epilepsy. In: *The Cochrane database of systematic reviews* 2, CD001903. DOI: 10.1002/14651858.CD001903.pub3.
- Martin, R. L.; Lloyd, H.G.E.; Cowan, A. I. (1994): The early events of oxygen and glucose deprivation: setting the scene for neuronal death? In: *Trends in Neurosciences* 17 (6), S. 251–257. DOI: 10.1016/0166-2236(94)90008-6.
- Martínez-Reyes, Inmaculada; Chandel, Navdeep S. (2020): Mitochondrial TCA cycle metabolites control physiology and disease. In: *Nature communications* 11 (1), S. 102. DOI: 10.1038/s41467-019-13668-3.
- Massieu, L.; Del Río, P.; Montiel, T. (2001): Neurotoxicity of glutamate uptake inhibition in vivo: correlation with succinate dehydrogenase activity and prevention by energy substrates. In: *Neuroscience* 106 (4), S. 669–677. DOI: 10.1016/s0306-4522(01)00323-2.
- Mayzel-Oreg, Orna; Omae, Tsuyoshi; Kazemi, Mark; Li, Fuhai; Fisher, Marc; Cohen, Yoram; Sotak, Christopher H. (2004): Microsphere-induced embolic stroke: an MRI study. In: *Magnetic resonance in medicine* 51 (6), S. 1232–1238. DOI: 10.1002/mrm.20100.
- McLaughlin, Kelsey L.; Hagen, James T.; Coalson, Hannah S.; Nelson, Margaret A. M.; Kew, Kimberly A.; Wooten, Ashley R.; Fisher-Wellman, Kelsey H. (2020): Novel approach to quantify mitochondrial content and intrinsic bioenergetic efficiency across organs. In: *Scientific reports* 10 (1), S. 17599. DOI: 10.1038/s41598-020-74718-1.
- Mies, G.; Iijima, T.; Hossmann, K. A. (1993): Correlation between peri-infarct DC shifts and ischaemic neuronal damage in rat. In: *Neuroreport* 4 (6), S. 709–711. DOI: 10.1097/00001756-199306000-00027.
- Miller, Daniel J.; Simpson, Jennifer R.; Silver, Brian (2011): Safety of thrombolysis in acute ischemic stroke: a review of complications, risk factors, and newer technologies. In: *The Neurohospitalist* 1 (3), S. 138–147. DOI: 10.1177/1941875211408731.
- Minematsu, K.; Fisher, M.; Li, L.; Davis, M. A.; Knapp, A. G.; Cotter, R. E. et al. (1993): Effects of a novel NMDA antagonist on experimental stroke rapidly and quantitatively assessed by diffusion-weighted MRI. In: *Neurology* 43 (2), S. 397–403. DOI: 10.1212/WNL.43.2.397.
- Moskowitz, Michael A.; Lo, Eng H.; Iadecola, Costantino (2010): The science of stroke: mechanisms in search of treatments. In: *Neuron* 67 (2), S. 181–198. DOI: 10.1016/j.neuron.2010.07.002.
- Musuka, Tapuwa D.; Wilton, Stephen B.; Traboulsi, Mouhieddin; Hill, Michael D. (2015): Diagnosis and management of acute ischemic stroke: speed is critical. In: *CMAJ : Canadian Medical Association journal = journal de l'Association medicale canadienne* 187 (12), S. 887–893. DOI: 10.1503/cmaj.140355.
- Namura, Shobu; Zhu, Jinmin; Fink, Klaus; Endres, Matthias; Srinivasan, Anu; Tomaselli, Kevin J. et al. (1998): Activation and Cleavage of Caspase-3 in Apoptosis Induced by Experimental Cerebral Ischemia. In: *J. Neurosci.* 18 (10), S. 3659–3668. DOI: 10.1523/jneurosci.18-10-03659.1998.
- Navarro-Orozco, Daniel; Sánchez-Manso, Juan Carlos (2022): StatPearls. Neuroanatomy, Middle Cerebral Artery. Treasure Island (FL).
- Nelson, C.; Silverstein, F. S. (1994): Acute disruption of cytochrome oxidase activity in brain in a perinatal rat stroke model. In: *Pediatric research* 36 (1 Pt 1), S. 12–19. DOI: 10.1203/00006450-199407001-00003.
- Newman, John C.; Verdin, Eric (2014): β -hydroxybutyrate: much more than a metabolite. In: *Diabetes research and clinical practice* 106 (2), S. 173–181. DOI: 10.1016/j.diabres.2014.08.009.
- Newman, John C.; Verdin, Eric (2017): β -Hydroxybutyrate: A Signaling Metabolite. In: *Annual review of nutrition* 37, S. 51–76. DOI: 10.1146/annurev-nutr-071816-064916.
- Ng, Yee Sien; Stein, Joel; Ning, Mingming; Black-Schaffer, Randie M. (2007): Comparison of clinical characteristics and functional outcomes of ischemic stroke in different vascular territories. In: *Stroke* 38 (8), S. 2309–2314. DOI: 10.1161/STROKEAHA.106.475483.

- Nicholson, C.; Bruggencate, G. T.; Steinberg, R.; Stöckle, H. (1977): Calcium modulation in brain extracellular microenvironment demonstrated with ion-selective micropipette. In: *Proceedings of the National Academy of Sciences of the United States of America* 74 (3), S. 1287–1290. DOI: 10.1073/pnas.74.3.1287.
- Niessen, Frank; Hilger, Thomas; Hoehn, Mathias; Hossmann, Konstantin-A (2002): Thrombolytic treatment of clot embolism in rat: comparison of intra-arterial and intravenous application of recombinant tissue plasminogen activator. In: *Stroke* 33 (12), S. 2999–3005. DOI: 10.1161/01.STR.0000038096.60932.F4.
- Niessen, Frank; Hilger, Thomas; Hoehn, Mathias; Hossmann, Konstantin-A (2003): Differences in clot preparation determine outcome of recombinant tissue plasminogen activator treatment in experimental thromboembolic stroke. In: *Stroke* 34 (8), S. 2019–2024. DOI: 10.1161/01.STR.0000080941.73934.30.
- Nogawa, Shigeru; Zhang, Fangyi; Ross, M. Elizabeth; Iadecola, Costantino (1997): Cyclo-Oxygenase-2 Gene Expression in Neurons Contributes to Ischemic Brain Damage. In: *J. Neurosci.* 17 (8), S. 2746–2755. DOI: 10.1523/jneurosci.17-08-02746.1997.
- Noh, Hae Sook; Hah, Young-Sool; Nilufar, Rashidova; Han, Jaehee; Bong, Jae-Hwan; Kang, Sang Soo et al. (2006): Acetoacetate protects neuronal cells from oxidative glutamate toxicity. In: *Journal of neuroscience research* 83 (4), S. 702–709. DOI: 10.1002/jnr.20736.
- Noh, Hae Sook; Kang, Sang Soo; Kim, Dong Wook; Kim, Young Hee; Park, Chang Hwan; Han, Jae Yoon et al. (2005a): Ketogenic diet increases calbindin-D28k in the hippocampi of male ICR mice with kainic acid seizures. In: *Epilepsy research* 65 (3), S. 153–159. DOI: 10.1016/j.eplepsyres.2005.05.008.
- Noh, Hae Sook; Kim, Dong Wook; Kang, Sang Soo; Cho, Gyeong Jae; Choi, Wan Sung (2005b): Ketogenic diet prevents clusterin accumulation induced by kainic acid in the hippocampus of male ICR mice. In: *Brain research* 1042 (1), S. 114–118. DOI: 10.1016/j.brainres.2005.01.097.
- Noh, Hae Sook; Kim, Yoon Sook; Lee, Hee Po; Chung, Ki Myung; Kim, Dong Wook; Kang, Sang Soo et al. (2003): The protective effect of a ketogenic diet on kainic acid-induced hippocampal cell death in the male ICR mice. In: *Epilepsy research* 53 (1-2), S. 119–128. DOI: 10.1016/S0920-1211(02)00262-0.
- O'Brien, M. D.; Waltz, A. G. (1973): Transorbital approach for occluding the middle cerebral artery without craniectomy. In: *Stroke* 4 (2), S. 201–206. DOI: 10.1161/01.str.4.2.201.
- O'Donnell, Martin J.; Xavier, Denis; Liu, Lisheng; Zhang, Hongye; Chin, Siu Lim; Rao-Melacini, Purnima et al. (2010): Risk factors for ischaemic and intracerebral haemorrhagic stroke in 22 countries (the INTERSTROKE study): a case-control study. In: *The Lancet* 376 (9735), S. 112–123. DOI: 10.1016/S0140-6736(10)60834-3.
- Offermanns, Stefan; Schwaninger, Markus (2015): Nutritional or pharmacological activation of HCA(2) ameliorates neuroinflammation. In: *Trends in molecular medicine* 21 (4), S. 245–255. DOI: 10.1016/j.molmed.2015.02.002.
- O'Neill, L.A.J.; Kaltschmidt, C. (1997): NF-κB: a crucial transcription factor for glial and neuronal cell function. In: *Trends in Neurosciences* 20 (6), S. 252–258. DOI: 10.1016/S0166-2236(96)01035-1.
- O'Neill, M. J.; Clemens, J. A. (2001): Rodent models of global cerebral ischemia. In: *Current protocols in neuroscience* Chapter 9, Unit9.5. DOI: 10.1002/0471142301.ns0905s12.
- Overgaard, K.; Sereghy, T.; Boysen, G.; Pedersen, H.; Høyer, S.; Diemer, N. H. (1992): A rat model of reproducible cerebral infarction using thrombotic blood clot emboli. In: *Journal of cerebral blood flow and metabolism : official journal of the International Society of Cerebral Blood Flow and Metabolism* 12 (3), S. 484–490. DOI: 10.1038/jcbfm.1992.66.
- Palmblad, J.; Hafström, I.; Ringertz, B. (1991): Antirheumatic effects of fasting. In: *Rheumatic diseases clinics of North America* 17 (2), S. 351–362.
- Pan, Jullie W.; Graaf, Robin A. de; Petersen, Kitt F.; Shulman, Gerald I.; Hetherington, Hoby P.; Rothman, Douglas L. (2002): 2,4-13 C2 -beta-Hydroxybutyrate metabolism in human brain. In: *Journal of cerebral blood flow and metabolism : official journal of the International Society of Cerebral Blood Flow and Metabolism* 22 (7), S. 890–898. DOI: 10.1097/00004647-200207000-00014.
- Park, C. K.; Nehls, D. G.; Teasdale, G. M.; McCulloch, J. (1989): Effect of the NMDA antagonist MK-801 on local cerebral blood flow in focal cerebral ischaemia in the rat. In: *Journal of cerebral blood flow and metabolism :*

- official journal of the International Society of Cerebral Blood Flow and Metabolism* 9 (5), S. 617–622. DOI: 10.1038/jcbfm.1989.88.
- Pierre, Karin; Pellerin, Luc (2005): Monocarboxylate transporters in the central nervous system: distribution, regulation and function. In: *Journal of neurochemistry* 94 (1), S. 1–14. DOI: 10.1111/j.1471-4159.2005.03168.x.
- Praticò, Domenico; Trojanowski, John Q. (2000): Inflammatory hypotheses: novel mechanisms of Alzheimer's neurodegeneration and new therapeutic targets? In: *Neurobiology of Aging* 21 (3), S. 441–445. DOI: 10.1016/s0197-4580(00)00141-x.
- Prins, M. L.; Fujima, L. S.; Hovda, D. A. (2005): Age-dependent reduction of cortical contusion volume by ketones after traumatic brain injury. In: *Journal of neuroscience research* 82 (3), S. 413–420. DOI: 10.1002/jnr.20633.
- Prins, M. L.; Lee, S. M.; Fujima, L. S.; Hovda, D. A. (2004): Increased cerebral uptake and oxidation of exogenous betaHB improves ATP following traumatic brain injury in adult rats. In: *Journal of neurochemistry* 90 (3), S. 666–672. DOI: 10.1111/j.1471-4159.2004.02542.x.
- Rafiki, A.; Boulland, J. L.; Halestrap, A. P.; Ottersen, O. P.; Bergersen, L. (2003): Highly differential expression of the monocarboxylate transporters MCT2 and MCT4 in the developing rat brain. In: *Neuroscience* 122 (3), S. 677–688. DOI: 10.1016/j.neuroscience.2003.08.040.
- Rahman, Mahbubur; Muhammad, Sajjad; Khan, Mahtab A.; Chen, Hui; Ridder, Dirk A.; Müller-Fielitz, Helge et al. (2014): The β -hydroxybutyrate receptor HCA2 activates a neuroprotective subset of macrophages. In: *Nature communications* 5, S. 3944. DOI: 10.1038/ncomms4944.
- Rothwell, Nancy J.; Hopkins, Stephen J. (1995): Cytokines and the nervous system II: actions and mechanisms of action. In: *Trends in Neurosciences* 18 (3), S. 130–136. DOI: 10.1016/0166-2236(95)93890-A.
- Rubiera, Marta; Ribo, Marc; Delgado-Mederos, Raquel; Santamarina, Esteban; Delgado, Pilar; Montaner, Joan et al. (2006): Tandem internal carotid artery/middle cerebral artery occlusion: an independent predictor of poor outcome after systemic thrombolysis. In: *Stroke* 37 (9), S. 2301–2305. DOI: 10.1161/01.STR.0000237070.80133.1d.
- Ruscher, Karsten; Isaev, Nikolaj; Trendelenburg, George; Weih, Markus; Iurato, Linda; Meisel, Andreas; Dirnagl, Ulrich (1998): Induction of hypoxia inducible factor 1 by oxygen glucose deprivation is attenuated by hypoxic preconditioning in rat cultured neurons. In: *Neuroscience letters* 254 (2), S. 117–120. DOI: 10.1016/S0304-3940(98)00688-0.
- Ruskin, David N.; Ross, Jessica L.; Kawamura, Masahito; Ruiz, Tiffany L.; Geiger, Jonathan D.; Masino, Susan A. (2011): A ketogenic diet delays weight loss and does not impair working memory or motor function in the R6/2 1J mouse model of Huntington's disease. In: *Physiology & behavior* 103 (5), S. 501–507. DOI: 10.1016/j.physbeh.2011.04.001.
- Rymer, Marilyn M. (2011): Hemorrhagic stroke: intracerebral hemorrhage. In: *Missouri medicine* 108 (1), S. 50–54.
- Sanderson, Thomas H.; Reynolds, Christian A.; Kumar, Rita; Przyklenk, Karin; Hüttemann, Maik (2013): Molecular mechanisms of ischemia-reperfusion injury in brain: pivotal role of the mitochondrial membrane potential in reactive oxygen species generation. In: *Molecular neurobiology* 47 (1), S. 9–23. DOI: 10.1007/s12035-012-8344-z.
- Saver, Jeffrey L.; Starkman, Sidney; Eckstein, Marc; Stratton, Samuel J.; Pratt, Franklin D.; Hamilton, Scott et al. (2015): Prehospital use of magnesium sulfate as neuroprotection in acute stroke. In: *The New England journal of medicine* 372 (6), S. 528–536. DOI: 10.1056/NEJMoa1408827.
- Schmid-Elsaesser, R.; Zausinger, S.; Hungerhuber, E.; Baethmann, A.; Reulen, H. J. (1998): A critical reevaluation of the intraluminal thread model of focal cerebral ischemia: evidence of inadvertent premature reperfusion and subarachnoid hemorrhage in rats by laser-Doppler flowmetry. In: *Stroke* 29 (10), S. 2162–2170. DOI: 10.1161/01.str.29.10.2162.
- Shimada, N.; Graf, R.; Rosner, G.; Heiss, W. D. (1993): Ischemia-induced accumulation of extracellular amino acids in cerebral cortex, white matter, and cerebrospinal fluid. In: *Journal of neurochemistry* 60 (1), S. 66–71. DOI: 10.1111/j.1471-4159.1993.tb05823.x.

- Shoulson, I. (1998): Where do we stand on neuroprotection? Where do we go from here? In: *Movement disorders : official journal of the Movement Disorder Society* 13 Suppl 1, S. 46–48.
- Sieber, Matthias W.; Claus, Ralf A.; Witte, Otto W.; Frahm, Christiane (2011): Attenuated inflammatory response in aged mice brains following stroke. In: *PLoS one* 6 (10), e26288. DOI: 10.1371/journal.pone.0026288.
- Sims, Neil R.; Muyderman, Hakan (2010): Mitochondria, oxidative metabolism and cell death in stroke. In: *Biochimica et biophysica acta* 1802 (1), S. 80–91. DOI: 10.1016/j.bbadis.2009.09.003.
- Smith, Sharon L.; Heal, David J.; Martin, Keith F. (2005): KTX 0101: a potential metabolic approach to cytoprotection in major surgery and neurological disorders. In: *CNS drug reviews* 11 (2), S. 113–140. DOI: 10.1111/j.1527-3458.2005.tb00265.x.
- Smith, Wade S.; Sung, Gene; Saver, Jeffrey; Budzik, Ronald; Duckwiler, Gary; Liebeskind, David S. et al. (2008): Mechanical thrombectomy for acute ischemic stroke: final results of the Multi MERCI trial. In: *Stroke* 39 (4), S. 1205–1212. DOI: 10.1161/STROKEAHA.107.497115.
- Stamp, Lisa K.; James, Michael J.; Cleland, Leslie G. (2005): Diet and rheumatoid arthritis: a review of the literature. In: *Seminars in arthritis and rheumatism* 35 (2), S. 77–94. DOI: 10.1016/j.semarthrit.2005.05.001.
- Streijger, Femke; Plunet, Ward T.; Lee, Jae H. T.; Liu, Jie; Lam, Clarrie K.; Park, Soeyun et al. (2013): Ketogenic diet improves forelimb motor function after spinal cord injury in rodents. In: *PLoS one* 8 (11), e78765. DOI: 10.1371/journal.pone.0078765.
- Ström, Jakob O.; Ingberg, Edvin; Theodorsson, Annette; Theodorsson, Elvar (2013): Method parameters' impact on mortality and variability in rat stroke experiments: a meta-analysis. In: *BMC neuroscience* 14, S. 41. DOI: 10.1186/1471-2202-14-41.
- Strong, Anthony J.; Anderson, Peter J.; Watts, Helena R.; Virley, David J.; Lloyd, Andrew; Irving, Elaine A. et al. (2007): Peri-infarct depolarizations lead to loss of perfusion in ischaemic gyrencephalic cerebral cortex. In: *Brain : a journal of neurology* 130 (Pt 4), S. 995–1008. DOI: 10.1093/brain/awl392.
- Sullivan, Patrick G.; Rippey, Nancy A.; Dorenbos, Kristina; Concepcion, Rachele C.; Agarwal, Aakash K.; Rho, Jong M. (2004): The ketogenic diet increases mitochondrial uncoupling protein levels and activity. In: *Annals of neurology* 55 (4), S. 576–580. DOI: 10.1002/ana.20062.
- Sumbria, Rachita K.; Klein, Jochen; Bickel, Ulrich (2011): Acute depression of energy metabolism after microdialysis probe implantation is distinct from ischemia-induced changes in mouse brain. In: *Neurochemical research* 36 (1), S. 109–116. DOI: 10.1007/s11064-010-0276-2.
- Suzuki, M.; Sato, K.; Dohi, S.; Sato, T.; Matsuura, A.; Hiraide, A. (2001): Effect of beta-hydroxybutyrate, a cerebral function improving agent, on cerebral hypoxia, anoxia and ischemia in mice and rats. In: *Japanese journal of pharmacology* 77 (2), S. 143–150. DOI: 10.1254/jjp.77.143.
- Suzuki, Motohisa; Suzuki, Mayumi; Kitamura, Yukika; Mori, Saori; Sato, Kazunori; Dohi, Sekiko et al. (2002): Beta-hydroxybutyrate, a cerebral function improving agent, protects rat brain against ischemic damage caused by permanent and transient focal cerebral ischemia. In: *Japanese journal of pharmacology* 78 (1), S. 36–43. DOI: 10.1254/jjp.78.36.
- Tamura, A.; Graham, D. I.; McCulloch, J.; Teasdale, G. M. (1981): Focal cerebral ischaemia in the rat: 1. Description of technique and early neuropathological consequences following middle cerebral artery occlusion. In: *Journal of cerebral blood flow and metabolism : official journal of the International Society of Cerebral Blood Flow and Metabolism* 1 (1), S. 53–60. DOI: 10.1038/jcbfm.1981.6.
- Tieu, Kim; Perier, Celine; Caspersen, Casper; Teismann, Peter; Wu, Du-Chu; Yan, Shi-Du et al. (2003): D-beta-hydroxybutyrate rescues mitochondrial respiration and mitigates features of Parkinson disease. In: *The Journal of clinical investigation* 112 (6), S. 892–901. DOI: 10.1172/JCI18797.
- Toomey, John R.; Valocik, Richard E.; Koster, Paul F.; Gabriel, Melanie A.; McVey, Matt; Hart, Timothy K. et al. (2002): Inhibition of factor IX(a) is protective in a rat model of thromboembolic stroke. In: *Stroke* 33 (2), S. 578–585. DOI: 10.1161/hs0202.102950.
- U Korth (2001): Methodik und Anwendung der Mikrodialyse. Methods and applications in microdialysis. Institut für Anästhesiologie und Operative Intensivmedizin, Universitätsklinikum Mannheim.

- Uesugi, Masafumi; Kasuya, Yoshitoshi; Hayashi, Khoichiro; Goto, Katsutoshi (1998): SB209670, a potent endothelin receptor antagonist, prevents or delays axonal degeneration after spinal cord injury. In: *Brain research* 786 (1-2), S. 235–239. DOI: 10.1016/s0006-8993(97)01431-5.
- Ungerstedt, U. (1971): Stereotaxic mapping of the monoamine pathways in the rat brain. In: *Acta physiologica Scandinavica. Supplementum* 367, S. 1–48. DOI: 10.1111/j.1365-201X.1971.tb10998.x.
- van der Auwera, Ingrid; Wera, Stefaan; van Leuven, Fred; Henderson, Samuel T. (2005): A ketogenic diet reduces amyloid beta 40 and 42 in a mouse model of Alzheimer's disease. In: *Nutrition & metabolism* 2, S. 28. DOI: 10.1186/1743-7075-2-28.
- Vannucci, Susan J.; Simpson, Ian A. (2003): Developmental switch in brain nutrient transporter expression in the rat. In: *American journal of physiology. Endocrinology and metabolism* 285 (5), E1127-34. DOI: 10.1152/ajpendo.00187.2003.
- Veech, R. L.; Chance, B.; Kashiwaya, Y.; Lardy, H. A.; Cahill, G. F. (2001): Ketone bodies, potential therapeutic uses. In: *IUBMB life* 51 (4), S. 241–247. DOI: 10.1080/152165401753311780.
- Veech, Richard L. (2004): The therapeutic implications of ketone bodies: the effects of ketone bodies in pathological conditions: ketosis, ketogenic diet, redox states, insulin resistance, and mitochondrial metabolism. In: *Prostaglandins, leukotrienes, and essential fatty acids* 70 (3), S. 309–319. DOI: 10.1016/j.plefa.2003.09.007.
- Wang, C. X.; Todd, K. G.; Yang, Y.; Gordon, T.; Shuaib, A. (2001): Patency of cerebral microvessels after focal embolic stroke in the rat. In: *Journal of cerebral blood flow and metabolism : official journal of the International Society of Cerebral Blood Flow and Metabolism* 21 (4), S. 413–421. DOI: 10.1097/00004647-200104000-00010.
- Wang, Ray-Yua; Wang, Paulus Shyi-Gang; Yang, Yea-Ru (2003): Effect of age in rats following middle cerebral artery occlusion. In: *Gerontology* 49 (1), S. 27–32. DOI: 10.1159/000066505.
- Watson, B. D.; Dietrich, W. D.; Busto, R.; Wachtel, M. S.; Ginsberg, M. D. (1985): Induction of reproducible brain infarction by photochemically initiated thrombosis. In: *Annals of neurology* 17 (5), S. 497–504. DOI: 10.1002/ana.410170513.
- Weinachter, S. N.; Blavet, N.; O'Donnell, R. A.; MacKenzie, E. T.; Rapin, J. R. (1990): Models of hypoxia and cerebral ischemia. In: *Pharmacopsychiatry* 23 Suppl 2, 94-7; discussion 98. DOI: 10.1055/s-2007-1014542.
- Yakovlev, Alexander G.; Knoblach, Susan M.; Fan, Lei; Fox, Gerard B.; Goodnight, Randyll; Faden, Alan I. (1997): Activation of CPP32-Like Caspases Contributes to Neuronal Apoptosis and Neurological Dysfunction after Traumatic Brain Injury. In: *J. Neurosci.* 17 (19), S. 7415–7424. DOI: 10.1523/jneurosci.17-19-07415.1997.
- Yamada, Kelvin A.; Rensing, Nicholas; Thio, Liu Lin (2005): Ketogenic diet reduces hypoglycemia-induced neuronal death in young rats. In: *Neuroscience letters* 385 (3), S. 210–214. DOI: 10.1016/j.neulet.2005.05.038.
- Yanamoto, Hiroji; Nagata, Izumi; Niitsu, Yoichi; Xue, Jing-Hui; Zhang, Zhiwen; Kikuchi, Haruhiko (2003): Evaluation of MCAO stroke models in normotensive rats: standardized neocortical infarction by the 3VO technique. In: *Experimental neurology* 182 (2), S. 261–274. DOI: 10.1016/s0014-4886(03)00116-x.
- Yin, Junxiang; Han, Pengcheng; Tang, Zhiwei; Liu, Qingwei; Shi, Jiong (2015): Sirtuin 3 mediates neuroprotection of ketones against ischemic stroke. In: *Journal of cerebral blood flow and metabolism : official journal of the International Society of Cerebral Blood Flow and Metabolism* 35 (11), S. 1783–1789. DOI: 10.1038/jcbfm.2015.123.
- Yudkoff, M.; Daikhin, Y.; Nissim, I.; Lazarow, A. (2001): Ketogenic diet, amino acid metabolism, and seizure control. In: *Journal of neuroscience research* 66 (5), S. 931–940. DOI: 10.1002/jnr.10083.
- Zhang, Jing; Yang, Jie; Zhang, Canfei; Jiang, Xiaoqun; Zhou, Hongqing; Liu, Ming (2012): Calcium antagonists for acute ischemic stroke. In: *The Cochrane database of systematic reviews* (5), CD001928. DOI: 10.1002/14651858.CD001928.pub2.
- Zhang, Li; Zhang, Rui Lan; Wang, Ying; Zhang, Chunling; Zhang, Zheng Gang; Meng, He; Chopp, Michael (2005): Functional recovery in aged and young rats after embolic stroke: treatment with a phosphodiesterase type 5 inhibitor. In: *Stroke* 36 (4), S. 847–852. DOI: 10.1161/01.STR.0000158923.19956.73.

Zhang, Rui Lan; Chopp, Michael; Zhang, Zheng G.; Jiang, Quan; Ewing, James R. (1997a): A rat model of focal embolic cerebral ischemia. In: *Brain research* 766 (1-2), S. 83–92. DOI: 10.1016/S0006-8993(97)00580-5.

Zhang, Wen-Hua; Wang, Xin; Narayanan, Malini; Zhang, Yu; Huo, Chunfeng; Reed, John C.; Friedlander, Robert M. (2003): Fundamental role of the Rip2/caspase-1 pathway in hypoxia and ischemia-induced neuronal cell death. In: *Proceedings of the National Academy of Sciences of the United States of America* 100 (26), S. 16012–16017. DOI: 10.1073/pnas.2534856100.

Zhang, Wenting; Zhao, Jingyan; Wang, Rongrong; Jiang, Ming; Ye, Qing; Smith, Amanda D. et al. (2019): Macrophages reprogram after ischemic stroke and promote efferocytosis and inflammation resolution in the mouse brain. In: *CNS neuroscience & therapeutics* 25 (12), S. 1329–1342. DOI: 10.1111/cns.13256.

Zhang, Z.; Zhang, R. L.; Jiang, Q.; Raman, S. B.; Cantwell, L.; Chopp, M. (1997b): A new rat model of thrombotic focal cerebral ischemia. In: *Journal of cerebral blood flow and metabolism : official journal of the International Society of Cerebral Blood Flow and Metabolism* 17 (2), S. 123–135. DOI: 10.1097/00004647-199702000-00001.

Ziegler, Denize R.; Ribeiro, Leticia C.; Hagenn, Martine; Siqueira, Ionara R.; Araújo, Emeli; Torres, Iracy L. S. et al. (2003): Ketogenic diet increases glutathione peroxidase activity in rat hippocampus. In: *Neurochemical research* 28 (12), S. 1793–1797. DOI: 10.1023/a:1026107405399.

Figure index

Figure 1: Cerebral arteries of the human brain.....	8
Figure 2: Illustration of ischemic core and surrounding penumbra.	10
Figure 3: Illustration of pathobiological mechanisms during stroke. Modified from Dirnagl et al. (1999).	10
Figure 4: Chronology of pathobiological processes. Excitotoxicity starts early on and causes further events like peri-infarct depolarizations and neuroinflammation, which exacerbates and accelerates destruction of neuronal tissue. Adopted from Dirnagl et al. (1999).	12
Figure 5: Ramification of the common carotid artery (ACC) in external carotid artery (ACE) and internal carotid artery (ACI). Modified from Schenk & Smith: Dissection Guide & Atlas to the Rat.....	15
Figure 6: Schematic image of middle cerebral artery occlusion. Comparison of occlusion with silicone coated filament (left) and filament with silicone head (right). Figure modified from Tina Schwarzkopf (2015).	16
Figure 7: Acetoacetate, acetone and β -hydroxybutyrate	20
Figure 8: Formation of the three ketone bodies β -hydroxybutyrate, acetoacetate and acetone..	21
Figure 9: Schematic structure of a mitochondrion.....	26
Figure 10: The citric acid cycle and oxidative phosphorylation are closely intertwined. Reactions of the TCA cycle yield NADH and FADH ₂ , which are required to maintain the mitochondrial respiratory chain. Complexes I and II regenerate NAD ⁺ and FAD, which are required for functioning of the TCA cycle with its oxidative properties. Figure adopted from Martínez-Reyes and Chandel (2020).	27
Figure 11: Schematic illustration of a microdialysis probe.....	32
Figure 12: Schematic display of manufacture of microdialysis probes.	33
Figure 13: Implantation region in left striatum. View on mouse skull with coordinates	36
Figure 14: Illustration of microdialysis.	37
Figure 15: Mitochondrial respiratory chain. Figure modified from Tina Schwarzkopf (2015)	46
Figure 16: Respiratory states of mitochondria.	48
Figure 17: Example of a respiratory analysis of isolated mouse mitochondria.	53
Figure 18: First reaction of citric acid cycle. Citrate synthase catalyzes condensation of acetyl-CoA and oxaloacetate to citric acid.....	56
Figure 19: UV spectrophotometrically quantifiable reaction of DTNB and CoA-SH.....	56
Figure 20: Enzymatic reaction of glucose to gluconic acid under release of H ₂ O ₂ . In a second step, enzymatically catalyzed formation of quinonimine, which is detected colorimetrically at 530 nm wavelength. Figure modified from Christian Viel.	59
Figure 21: Enzymatic reaction of lactate to pyruvate under release of H ₂ O ₂ . Second step, enzymatically catalyzed formation of quinonimine, which is detected colorimetrically at 530 nm wavelength. Figure modified from Christian Viel.	60
Figure 22: Enzymatic reaction of pyruvate to H ₂ O ₂ . Second step, enzymatically catalyzed formation of quinone diimine, which is detected colorimetrically at 530 nm wavelength..	61
Figure 23: Transformation of 2,3,5-triphenyltetrazoliumchloride (TTC) to formazane. Electrons are donated by NADH. Reaction is catalysed by succinate dehydrogenase (complex II respiration chain).	62
Figure 24: β -hydroxybutyrate concentrations in microdialysate (mean value \pm S.E.M.) after intraperitoneal injection of β -hydroxybutyrate 30 mg/kg bodyweight.....	65
Figure 25: Glucose concentrations in microdialysate in blue; lactate concentrations in microdialysate in red. .	66
Figure 26: Oxygen consumption measured by respirometry after addition of succinate in concentrations of 1 mM, 3 mM and 10 mM, and pyruvate in concentrations of 1 mM, 3 mM and 10 mM.	67
Figure 27: Oxygen consumption measured by respirometry after addition of BHB in concentrations of 1 mM, 3 mM and 10 mM, and pyruvate in concentrations of 1 mM, 3 mM and 10 mM.....	67
Figure 28: Oxygen consumption measured by respirometry after addition of BHB in concentrations of 1 mM, 3 mM and 10 mM, and BHB and malate in concentrations of 1 mM, 3 mM and 10 mM.	68
Figure 29: Measurement of Laser-Doppler sonography before ischemia, after induction and after reperfusion	69
Figure 30: Oxygen consumption measured by respirometry 60 minutes after transient ischemia..	70
Figure 31: Ratio of mitochondrial respiration 60 minutes after transient ischemia	72
Figure 32: Citrate synthase activity 60 minutes after transient ischemia	73
Figure 33: Oxygen consumption measured by respirometry 60 minutes after transient ischemia with raw data normalized to citrate synthase activity.	73

Figure 34: Oxygen consumption measured by respirometry 24 hours after transient ischemia.	75
Figure 35: Ratio of mitochondrial complex I respiration 24 hours after transient ischemia.....	76
Figure 36: Oxygen consumption measured by respirometry 24 hours after transient ischemia.	76
Figure 37: A) Citrate synthase activity 24 hours after transient ischemia. B) Citrate synthase activity 24 hours after transient ischemia.....	77
Figure 38: Concentrations of A) glucose, B) lactate and C) pyruvate in plasma 24 hours after transient ischemia	79
Figure 39: Effect of β -hydroxybutyrate (BHB) on mouse motoric function. A) Corner Test after 24 hours. B) Chimney Test after 24 hours. C) Rotarod after 24 hours.....	80
Figure 40: Development of mouse weight after undergoing 90-minute transient cerebral ischemia.....	82
Figure 41: Ratio of mitochondrial complex I respiration 24 and 72 hours after transient ischemia.....	82
Figure 42: A) Oxygen consumption of complex I, measured by respirometry 72 hours after transient ischemia	83
Figure 43: A) Oxygen consumption of complex II, measured by respirometry 72 hours after transient ischemia	84
Figure 44: Ratio of mitochondrial respiration 72 hours after transient ischemia	84
Figure 45: Ratio of mitochondrial respiration 72 hours after transient ischemia, normalized to citrate synthase activity.	85
Figure 46: Concentrations of A) glucose, B) lactate and C) pyruvate in plasma 72 hours after transient ischemia	86
Figure 47: Effect of β -hydroxybutyrate (BHB) on mouse motoric function after 24 and 72 hours. A) Corner Test after 24 and 72 hours. B) Chimney Test after 24 and 72 hours. C) Rotarod after 24 and 72 hours.	88
Figure 48: Development of mouse weight throughout one week after undergoing 90-minute transient cerebral ischemia.....	90
Figure 49: Weight loss in percent throughout one week after undergoing 90-minute transient cerebral ischemia.....	91
Figure 50: A) Oxygen consumption of complex I measured by respirometry 7 days after transient ischemia. B): Ratio of mitochondrial respiration of complex I 7 days after transient ischemia.	91
Figure 51: A): Oxygen consumption of complex II measured by respirometry 7 days after transient ischemia.. B) Ratio of mitochondrial respiration of complex II 7 days after transient ischemia	92
Figure 52: Ratio of mitochondrial respiration 7 days after transient ischemia.....	93
Figure 53: Concentrations of A) glucose, B) lactate and C) pyruvate in plasma 7 days after transient cerebral ischemia.....	93
Figure 54: Effect of β -hydroxybutyrate (BHB) on mouse motoric function 7 days after transient cerebral ischemia.....	95
Figure 55: Metabolic pathway of BHB and cellular signaling functions of its metabolites..	108

Table index

Table 1: Composition of diets used in experiments.	30
Table 2: Materials for microdialysis probe manufacture.	31
Table 3: Composition of perfusion solution.	34
Table 4: Standard solution for recovery.	35
Table 5: Coordinates of left striatum from bregma.	36
Table 6: Oxygraph instruments and chemical compounds for the oxygraph.....	44
Table 7: Summary of all substrates, uncouplers and inhibitors, as well as their function.	47
Table 8: Substrates, uncouplers, inhibitors and their solvents for the SUIT protocol of the oxygraph.	49
Table 9: Composition of MRO5 respiratory medium.	50
Table 10: Materials and instruments for TTC staining.	61
Table 11: Composition of PBS buffer.....	61
Table 12: Recovery rates	64

Image index

Image 1: Silicone- covered nylon suture	15
Image 2: Mouse after MCAO.....	40
Image 3: Corner-Test setup.....	41
Image 4: Mice on Rotarod.....	42
Image 5: Chimney-Test setup.....	43
Image 6: Oroboros Oxygraph.....	50
Image 7: BHB and glucose levels.....	77
Image 8: TTC stainings 24 hours after reperfusion.....	80
Image 9: TTC stainings 72 hours after reperfusion.....	88
Image 10: Intraluminal MCAO model with artery ramifications.....	97

Curriculum Vitae

Personal Details

Name	Lehto
First name	Alina Barbara
Date of birth	10/6/1992 in Fairfax County, VA (USA)
Address	Hartmann-Ibach Straße 51 60389 Frankfurt am Main
E-mail address	alinalehto92@icloud.com
Cellphone number	+49-(0)-163-4413931

Education

University

11/1/2018 – now	PhD in pharmacology at Goethe University Frankfurt am Main
07/26/2018	Successful completion of the third state examination
10/2012 – 04/2017	Studies of pharmaceutical sciences at <u>Goethe University Frankfurt am Main</u>
	<u>April 2017:</u> Successful graduation, second part of the pharmaceutical state examination
	<u>March 2015:</u> Successful graduation, first part of the pharmaceutical state examination

School

08/2003 – 05/2012	Leibniz-Gymnasium Östringen
08/1999 – 06/2003	Elementary School in Angelbachtal

Internships / Professional Experience

02/2020- now	Employment at Centrum Apotheke Frankfurt
01/2019- 12/2019	Employment at Titus Apotheke in Frankfurt
06/2018- 12/2018	Employment at the Apfel Apotheke in Frankfurt
12/2017- 05/2018	Practical semester at Lilly Pharma Bad Homburg
06/2017 – 12/2017	Practical semester in the Radilo Pharmacy in Rödelheim
03/2016	Research group internship for 4 weeks at Prof. Dr. Steinhilbers laboratory, Goethe University
08/2015 - today	Pharma- Translations Lehto (self-employed Translation services for pharmaceutical industry)
03/2014 and 03/2013	Internship (Schlossgarten Pharmacy Angelbachtal)

Pharmaceutical Student Association

2013-2016	Part of the pharmaceutical student association, Goethe University Frankfurt am Main as member of the Academic Commission
-----------	--

Languages, further skills and experiences

- Languages
 - German Mother tongue
 - English Mother tongue
 - Italian Basic skills
- Touch typing
- General experience in laboratory procedures (analytics, synthesis, pharmaceutical technology)
- MS-Office Word, Power Point, Excel: very good skills

Participation in trainings:

- Business Administration – Fundamental basics in the pharmacy (June 2014)
- FIP Congress Düsseldorf (October 2015)
- Pharmacon Congress (June 2016)
- Moderation of the Fertigarzneimittelseminar (FAS) and participation in preparing on of the scientific lectures of the FAS (February 2017)
- Felasa-B course (November 2018)

Publications

Parts of the present work have already been published

Lehto, A., Koch, K., Barnstorf-Brandes, J. *et al.* β -Hydroxybutyrate Improves Mitochondrial Function After Transient Ischemia in the Mouse. *Neurochem Res* (2022). <https://doi.org/10.1007/s11064-022-03637-6>

Pending publications

Fedorov, A., **Lehto, A.**, Klein J. Preliminary title: Inhibition of mitochondrial respiration by general anaesthetic drugs.

Publications that are not discussed in this dissertation

Thinnes A, Westenberger M, Piechotta C, **Lehto A**, Wirth F, Lau H, Klein J. Cholinergic and metabolic effects of metformin in mouse brain. *Brain Res Bull.* 2021 May;170:211-217. doi: 10.1016/j.brainresbull.2021.02.018. Epub 2021 Feb 19. PMID: 33617923.

Viel C, Brandtner AT, Weißhaar A, Lehto A, Fuchs M, Klein J. Effects of Magnesium Orotate, Benfotiamine and a Combination of Vitamins on Mitochondrial and Cholinergic Function in the TgF344-AD Rat Model of Alzheimer's Disease. *Pharmaceuticals (Basel)*. 2021;14(12):1218. Published 2021 Nov 24. doi:10.3390/ph14121218

Acknowledgments

First, I would like to thank Prof. Klein, who made this thesis possible and who was always there to give scientific advice and input throughout the last years. Thank you for always having an open door and a moment of time to discuss any sort of question, no matter if it was lab-related or personal. The lunch breaks with interesting and funny conversations will be missed in the future and I will make sure to keep them in good memory.

I want to thank Christian Viel for being the inspiring, kind, and curious friend that you have become. Without you, everyday business at the office would have been just half as fun, and especially the last two years would have been far more joyless. I am beyond grateful for every scientific and non-scientific discussion we had throughout the years, for all the laughter and smart advice, in the office or in private. Your curiosity is something I will always look up to.

Thank you, Helene Lau, Marius Fuchs, and Constantin Kondak for always having an open ear, for the often funny lunch conversations, and for every advice in scientific questions.

A heartfelt thank you goes to my master's students Anton Fedorov and Katja Jarosch, who both worked the oxygraph so tirelessly and were always great company in the lab.

Thank you to all the other university friends for advice when needed. Special thanks to Robin Brunn, Caro Möller, Larissa Pokos, Marcel Walther and Carole Savin for picking up the phone many times for spontaneous calls!

Also, I want to thank my wonderful friend Pia Vestweber for being my confidante and companion through ups and downs ever since we met. Your support, your advice and all the quality-time we have had together are invaluable to me.

Finally, I want to thank my parents Conny and Mike, and my brother John for their unconditional love, support, and kindness.

Thank you for always encouraging and supporting John and me to go the extra mile, and never once doubting the decisions we have made. Thank you for always being there and always having an open door. Thank you for every nice word, every pizza night, every phone call, and every vacation. I am lucky to have such an amazing family and I admire you for your patience, generosity, and selflessness.